Detection of Specific Biological Antigens using AC Electrochemical Impedance Spectroscopy

Darrel Angelo Mazzari
Marquette University

DETECTION OF SPECIFIC BIOLOGICAL ANTIGENS USING AC ELECTROCHEMICAL IMPEDANCE SPECTROSCOPY

by

Darrel A. Mazzari, B.S.E.E., M.S., P.E.

A Dissertation submitted to the Faculty of the Graduate School,
Marquette University,
in Partial Fulfillment of the Requirements for
the Degree of Doctor of Philosophy

Milwaukee, Wisconsin

August 2011

ABSTRACT
DETECTION OF SPECIFIC BIOLOGICAL ANTIGENS USING AC ELECTROCHEMICAL IMPEDANCE SPECTROSCOPY

Darrel A. Mazzari, B.S.E.E., M.S., P.E.

Marquette University, 2011

When certain antigens are present in our environment, a rapid, on-site, accurate, selective, and repeatable detection method can be invaluable in preventing illness or saving lives. Rapid detection of these antigens is important to avert spreading infections.

Currently, capturing a sample and sending it to a laboratory can take weeks to get results, which can be much too long. Conventional sensing methodologies include various electrical measurements as capacitive, potentiometric, piezoelectric, surface plasmon resonance (SPR), and quartz crystal microbalance (QCM). Of particular power and interest is Alternating Current (AC) Electrochemical Impedance Spectroscopy (EIS) which provides for the characterization of the electrical properties of many biological interfaces without biological destruction or interference.

The application of unique detection techniques of the latter, in this dissertation, resulted in high selectivity and sensitivity even with the presence of non-specific contaminants. Prior to this work, the measurement media was a liquid. However, a particularly formidable task has remained of detection of unlabeled antigens in air. EIS, a powerful technique for identifying electrode surface molecular reactions by measuring the electrical characteristics of the resultants over a frequency spectrum, was employed to detect impedance changes at the formation of an antibody-antigen conjugate. A new gel was developed capable of keeping antibodies active for extended periods of time, and also capturing antigens from the air. Another development was attaching the self-assembling monolayer, 3-MPTS (3-mercaptopropyl)trimethoxysilane, onto gold nanoparticles to create a unique active electrode.

The primary purpose of this dissertation work was to prove the concept of being able to capture a specific (to the antibody) antigen in the air, conjugate it with a specially coated non-dry electrode, and rapidly characterize the reaction with EIS. This work was the first to successfully accomplish this detection task utilizing a novel colloidal gold nanoparticle electrode, an active antibody, IgG, and a novel modified hydrogel.

ACKNOWLEDGEMENTS

Darrel A. Mazzari, B.S.E.E., M.S., P.E.

I wish to heartily thank all my friends and relatives who provided encouragement to me to complete my studies and the work of this degree.

I want to thank all of my PhD committee members for their time spent advising me and reviewing my work. It is deeply appreciated. Special thanks to Dr. Martin Seitz, who provided much appreciated guidance, and moral and financial support. I want to thank Dr. Dean Jeutter for his mentoring, patience, and use of his laboratory. I want to thank Dr. James Courtright for his knowledgeable assistance in biological experiment design and measurements. I want to thank Dr. Charles Koehler for his assistance and advice in Material Science, FTIR, and EIS. I want to thank Dr. Daniel Sem and Tim Jonera of the Marquette University Chemistry Department for their consultation, assistance, and use of equipment.

Finally, I want to especially thank my wife, Jacqueline, for all her encouragement, patience, and beautiful support over the years.

TABLE OF CONTENTS

LIST OF FIGURES

GLOSSARY OF TERMS AND SYMBOLS

ANOVA	analysis of variance
AuNP	gold nanoparticle
BSA	Bovine Serum Albumin
C	capacitance, F or μF
C	concentration, M or mM
C_o	concentration of the oxidized form
C_R	concentration of the reduced form
C_{dl}	double layer capacitance, F or F
$C_{dl.ave}$	average double layer capacitance
CMA	Colloidal gold / MPTS / Antibody (layers of functionalization)
CMI	Colloidal gold / MPTS / IgGab (a specific CMA)
CPE	constant phase element
CPE-Θ	angle of rotation of a CPE
CG	Colloidal Gold or Gold Nanoparticles
CV	Cyclic voltammetry
collagen gel	gelatin
D	diffusion coefficient, cm2/s
D_O	diffusion coefficient of the oxidized form, cm2/s
D_R	diffusion coefficient of the reduced form cm2/s
e	ac voltage or potential phasor, V
ε_r	the relative static permittivity (sometimes called the dielectric constant) of the material between the plates, (vacuum =1)

ε_0	the permittivity of free space (8.854×10^{-12} F/m)
E	amplitude of ac voltage, V
E_R	potential drop across a resistor, V
E_C	potential drop across a capacitor, V
E_R	equivalent potential, V or mV
$E_{½}$	half-wave potential, V or mV
F	the Faraday constant; charge on one mole of electrons
FDU	The FDU (Facilitating Detection Unit) is the unit of the sensor that is utilized to detect and determine if the object of interest is present at the location of interest. aka sensor head
FDC	The FDC (Facilitating Detection Component) is based upon electrochemical properties and reactions that produce unique and detectable outputs
FDE	The FDE (Facilitating Detection Element) comprises the precise methodology used to detect the antigen.
GLYGEL	glycerol /agarose modified hydrogel
GHA	Glycerol / H_2O / Agarose modified hydrogel
GNP	Gold NanoParticles or Colloidal Gold
I	current, A
i	ac current phasor, A
IgG	Human IgG, Purified Immunoglobulin
IgGab	Anti-Human IgG FITC antibody produced in goat
IgM	Human IgM, Purified Immunoglobulin

IgMab	Anti-Human IgM FITC antibody produced in goat
j	√-1
K_a	Association constant
K_d	Dissociation constant
MPTS	a sol-gel molecule that forms a Self-Assembling Monolayer (SAM)
	3-MPTS (3-mercaptopropyl)trimethoxysilane
n	stoichiometric # of electrons involved in an electrode reaction
O	oxidized form of the standard system 0+ ne R
PBS	Phosphate Buffered Saline
T	time, S
R	resistance, Ω
	gas constant. J mol-l K-1
	reduced form of the standard system 0÷ ne ↔R
R_S	solution phase resistance, µF /cm^2
R_S	charge transfer resistance, µF /cm^2
redox	oxidation-reduction reactions (oxidation is loss of electrons, reduction is gain of electrons)
s	seconds
SAM	Self-Assembling Monolayer
q	charge, C
T	absolute temperature, K
X_C	capacitance resistance. Ω
W	Warburg impedance, µF •cm^{-2}•$s^{0.5}$

W_0	Warburg impedance of the oxidized form, $\mu F \cdot cm^{-2} \cdot s^{0.5}$
W_R	Warburg impedance of the reduced form. $\mu F \cdot cm^{-2} \cdot s^{0.5}$
Z	impedance, Ω/cm^2
Z_{Re}	real impedance, Ω/cm^2
Z_{img}	imaginary impedance, Ω/cm^2
Z_f	faradic impedance in Randles equivalent circuit, Ω/cm^2
α	transfer coefficient
φ	phase angle of an AC voltage or current
ω	angular frequency

CHAPTER 1

RATIONALE AND SPECIFIC AIMS

Introduction and Rationale

The purpose of the studies described in this dissertation was to develop an in-depth understanding of the reactionary performance of an electrochemical biosensor to detect dangerous concentrations of antigens in our environment or other venues. The importance of this research can be illustrated by some examples.

Mycobacterium tuberculosis (TB) is normally spread through the air when a person with untreated pulmonary TB coughs or sneezes, coughs, sneezes, talks, spits or just simply breathes into the air, and then another person becomes infected when he or she inhales minute particles of infected sputum from that air [56]. Usually, prolonged exposure to a person with untreated TB is necessary for the infection to occur.

Anthrax is an acute infectious disease caused by the spore-forming bacterium *Bacillus anthracis* which is normally present, at low levels of concentration, in the soil. Anthrax most commonly occurs in wild and domestic livestock (such as cattle, sheep, and goats). Infections can occur in humans when he or she comes in contact with infected animals or their hides. Infections cannot occur from human to human. In the fall of 2001, an outbreak of cutaneous and inhalation anthrax occurred on the United States East coast and Florida which resulted from a still unsolved act of bioterrorism involving letters intentionally contaminated with anthrax spores [57].

A large outbreak of Shiga toxin-producing *Escherichia coli* (*E. coli*) O104:H4 (STEC O104:H4) infections took place in Germany in 2011. The responsible strain caused hemolytic uremic syndrome (HUS)-a type of kidney failure that is associated with Shiga toxin-producing *E .coli*. In 2010, *E. coli* O145 infections were linked to shredded

romaine lettuce from a single processing facility. Investigators used pulsed-field gel electrophoresis (PFGE) to identify the DNA involved. Most *E. coli* strains are harmless, but some serotypes can cause serious food poisoning in humans, mainly through fecal-oral transmission, and can lead to product recalls. Hand washing can remove most *E. coli* on them and is usually effective to prevent contamination of food. The harmless strains of *E. coli* are part of the normal flora of the gut, and can benefit their hosts by preventing the growth of pathogenic bacteria within the intestine [58].

The bioimmunosensors of this study rely on single or multiple specific antibodies to be available. Once the pathogens have been identified and specific antibodies produced, our bioimmunosensors can be utilized to identify contaminated areas or products. An organism, such as a human can withstand a certain amount of infection, depending on the state of its immune system. Nearly any foreign substance, in small amounts, can be tolerated, as long as the antigen invader can be eliminated by one or more operations of the immune system (assuming there is no runaway auto immune response.) Therefore, the absolute lower limit of detection of the bioimmunosensors need not be of ultimate concern as long as the value is below the non-tolerable concentration of the pathogens. The lower limit of detection is the minimum input of physical parameter that will create a detectable output change. The sensitivity of the bioimmunosensor is defined as the slope of the output vs. input curve, in the range of a linear characteristic (or linear to some simple mathematical function of the measurement such as logarithmic), and determines the accuracy of the output value reading.

Electrochemical sensors are a subsection of chemical sensors, which are sensors that use chemical processes in the recognition and transduction procedures [50]. The term biosensor is applied to devices either used to monitor living systems, or incorporating biotic elements such as cells, protein, nucleic acid, or biomimetic polymers. Biosensors are used in, and connection with, pharmaceutical companies, personal health care, environmental pollutants, and the food industry [1]. Blood glucose biosensors for diabetes sufferers are by far the most pervasive with nearly 87% of the market [2]. When detrimental biological agents (antigens) e.g., mold, anthrax, or other viruses, bacteria or parasites, are present in air or water, we may have violent immunological, possibly lethal, reactions if contact is made with our bodies. However, capturing a sample and sending it to a laboratory can take weeks to get results, which is much too long in the general case.

The application of unique detection techniques can affect high selectivity and sensitivity. Conventional sensing methodologies include various electrical measurements as capacitive [3], potentiometric [4], piezoelectric [5], surface plasmon resonance (SPR) [6], and quartz crystal microbalance (QCM) [7]. Of particular power and interest is electrochemical impedance spectroscopy (EIS) which provides for the characterization of the electrical properties of many biological interfaces without biological destruction or interference [8].

Electrochemical impedance spectroscopy (EIS) is one of the most powerful and sensitive technologies, today, for examining the surface electrical properties of an electrode and its coatings.

Electrochemical cells consisting of two and three electrodes were constructed to perform experiments to examine alterations of the interfacial electron transfer features occurring at the electrode surface. The adsorption and desorption of insulating materials on conducting materials, i.e., electrodes, enables the property of capacitance that can be measured quite accurately by EIS [9].

Because EIS involves the measurement of inherent electrical properties of the sample involved, EIS does not require chemical labels. In addition, since low voltages and currents generally are used, the technique is also non-destructive, which is especially important in measurements of biological materials [26]. With EIS, a small-signal electrical excitation across a broad range of AC frequencies is applied through an electrode surface interface, in this case a biological complex, and the resulting electrical properties, e.g., numerically complex (real and imaginary) capacitances, are measured quite precisely [11].

Capacitance deals with time and time constants of polarization of molecules. There are several ways to polarize them, and EIS analyzes different effects based on frequency, which is, of course, based on time – the time to polarize before an electrical excitation reverses [13]. To cause polarization there must be some movement. The high frequencies, 100 kHz and above are used to measure bulk effects due to lattice movement (back and forth), and with dipolar movement. Intermediate frequencies down to 10 hertz or so, are used for the long range motion, and subHertz reveals space charge stacking.

Various styles and compositions of electrodes are used in biomedical applications for making measurements of bioelectric events. Low current density and small size are important in order to introduce only a miniscule amount of perturbation that does not

significantly alter the operation of the process to be measured. Biological functions often show electric activity in the form of a constant DC field, a constant current, or time-varying currents [15]. A biomedical electrode is a transducer which provides communication between the biological system and an electronic device, so that the events can be measured or controlled externally. Since the currents in biological systems are transmitted in the form of ions [16], the electrode is a transducer converting ionic to electrical currents.

Previous antibody-based immunosensors required long incubation times to get a stable indication (8 minutes to 20 days)[41][49], mainly because the electrode was in a liquid and some distance from the introduction of the antigen. Systems with mixers can reduce the times to the lower end of the reaction time, above, but they increase the complexity of the immunosensor.

The overall aim of this research is to construct a unique, reproducible bioelectrode that can rapidly detect, using EIS, specific antigens with antibodies, and operate in liquid media or air with the presence of non-specific antigens.

Specific Aims

The following is a roadmap for the research performed to reach the overall aim, above. Explicitly, the objectives of this dissertation are organized in two specific experimental aims:

Aim 1: To develop a novel label-free immunosensor in a non-liquid environment using parallel paths.

Aim 2: To develop a novel label-free immunosensor for specific antigen detection using immobilized antibodies on a self-assembled monolayer on gold nanoparticles in a non-liquid modified hydrogel environment with a linear/serial configuration.

Overall goal: To present a novel sensor technology that can rapidly detect specific antigens in air using antibodies.

Significance

These studies significantly advance our knowledge through the understanding of the ways the conjunction of specific macromolecules can be detected utilizing electrochemical impedance spectroscopy with a novel antibody coated bioelectrode operating in a novel hydrogel medium.

Challenges

A primary challenge to developing a sensor for biological macromolecule electrical detection is instigating a specific change in electrical characteristics that can be readily detected without destroying the biological activity [17]. That being done, another challenge is the environment of the reaction of interest. Contamination which is present can interfere with the desired biological process. In addition, detection in the air presents the challenge of encapsulating the target macromolecules because, in their native state, cannot easily, if at all, be volatized.

Organization of This Document

This dissertation is divided into five chapters:

Chapter 1 presents the motivations, rationale, and specific aims of the work.

Chapter 2 presents an explanation of biosensor components.

Chapter 3 addresses experimental Aim 1 to develop novel non-liquid medium for a parallel biosensor.

Chapter 4 addresses experimental Aim 2 to develop novel a serial biosensor for antigens in air and/or liquid utilizing a novel modified hydrogel.

Chapter 5 summarizes conclusions and suggests directions for future work.

This study addresses a unique topic in the area of EIS immunosensors – a bioelectrode capable of detection of antigens from a liquid and from the air. The immobilization of the targets of biological conjugates is crucial to the detection sensitivity, repeatability, and reusability of electrodes. Gold electrodes, and/or self-assembled monolayers with colloidal gold, provide platforms for the attachment of proteins and permit adsorption of protein molecules, resulting in a matrix for the immobilization of macromolecules, while retaining the bioactivity of antibodies and antigens [24] [25]. Signal amplification of the immunoconjugates is also a key factor to provide a signal that is significantly greater than the background noise in order to be measured reliably.

Current technologies of Biosensors with Gold Nanoparticles

Type of Biosensor	Principle of Detection	Functions of GNP's	Properties Used	Sensor Advantages	Typical Examples
Optical biosensor	Changes in optical properties	Enhancement of refractive index changes	Large dielectric constant, high density, high molecular weight	Improved sensitivity	DNA sensor with GNPs responses 1000 times more sensitive than without [69].
		Enhancement of electron transfer	Conductivity, quantum dimension	Improved sensitivity	Electron transfer rate of 5000 per second with GNP's, while 700 per second without NP's[68]
Piezoelectric biosensor	Changes in mass	Biomolecule Immobilization, amplification of mass change	Biocompatibility, high density, Large surface-to-volume ratio	Improved sensitivity	DNA sensor using GNPs as amplification tags with detection limit of 10^{-16}mol/L [70]
Electrochemical biosensor	Changes in electrical characteristics	Immobilization platform	Biocompatibility, large surface area	Improved sensitivity and stability	Glucose biosensor with GNPs achieves detection limit of 0.18 μM [71].
	Changes in electrical characteristics	High catalytic action	Biocompatibility, large surface area	Improved sensitivity and stability	GNP-modified indium tin oxide by seeding sensor for H_2O_2 [74]
	Catalysis of reactions	High surface energy, interface-dominated properties	Improved sensitivity and selectivity	Improved sensitivity and selectivity	NADH sensor based on GNPs shows 780 mV overpotential decrease without any electron transfer mediators [72].

Figure 1: Table of Current technologies of Biosensors with Gold Nanoparticles (GNP's) modified[64].

Experimental Paradigm

Our experimental framework involves a step-by-step analysis of the electrochemical reactions occurring at the working electrode modified surface. The results of one experiment were used as the starting point, or controls, for the next. This

paradigm was very efficient, because it was not necessary to design separate experiments for control experiments; the previous experiment *was* the control. These reactions shaped the impedance spectrum recorded when a small electrical signal (5-10 mvac) was applied to the interface. By tracking the data before and after a binding event (in this case the union of an antibody and its associated specific antigen) a pattern, like a fingerprint, was defined and used to identify a similar event occurrence of this same type. Electrodes were used in biomedical applications for both making measurements of biological events and also to deliver current to biological entities [18][19]. Measurement, for the sake of accuracy and pseudo-linearity, needed to involve low current density in order to introduce the least amount of perturbation, due to ohmic heating, which could alter the operation of the process to be measured.

The 3-probe EIS measurement system cell was utilized containing a platinum wire counter electrode, a Ag-AgCl reference electrode, and a working electrode with a modified Au base for initial experiments. Nyquist, Bode, and cyclic voltammetry plots provided the informative output. Previous studies have detected carcinomic antigens [27], DNA hybridizations [28], and antibody–antigen reactions [29]. A 2-probe system (eliminating the working electrode) was used in advanced experiments since it is more practical if the medium characteristics are also to be contributing to the measurements, or are negligible and can be ignored. A novel 2-probe system was developed and utilized with a uniquely formulated hydrogel for measurement with both the parallel and serial configurations.

Objectives and Significance

A unique implementation of a 2-probe EIS system is the subject of our research. Results with previous non-specific, combined with specific, antibody reactions have not been easily interpretable. *To date, studies of EIS bioimmunosensors have made measurements under controlled liquid antigen environments, lacking non-specific antigens to avoid poor characterizations.* In this dissertation, specific and non-specific reactions were differentiated and a novel bioimmunosensor was developed with variable stringency control. In addition, monitoring antibody/antigen reactions with antigens from air has been largely problematic due to the challenges of keeping the antibodies active in an air atmosphere. This formidable challenge was overcome by the application of a novel modified hydrogel medium to bring the antigens from the air to the antibodies in a biocompatible environment.

CHAPTER 2

THE BIOSENSOR

Components of a biosensor

The **FDU (Facilitating Detection Unit)** is the part of the sensor that is utilized to detect and determine if the object of interest is present at the location of interest of the FDU. In our case, the object of interest was a molecular biological antigen, IgG. Other examples include, but not limited to, a protein, bacterium, virus, toxin, or an active, or potentially active, molecular complex, capable of conjugating with an anti substance, e.g. an antibody. The place of interest is the medium surrounding the FDU, in our case, especially, but not limited to, environmental air. The output of the FDU is the raw data signal or information.

The FDU raw output is then fed into the **FDD (Facilitating Detection Device)** that contains the associated electronics and signal, or other, processors that are used to display of the results in a user-friendly fashion.[28]. Typically, the results are stored in a database.

The FDU is composed of **FDC('s) (Facilitating Detection Component(s)**.) This dissertation's final FDC's were colloidal gold particles, each coated with a self assembling monolayer to which antibodies of the antigen of interest were attached. The FDC's were based upon electrochemical properties and reactions that produced unique and detectable outputs and conditions. These were captured and identified through direct measurement, combined into a coherent signal at the FDU, and, then, sent to the FDD where the raw data was analyzed with instrumentation, signal processing, and data mining.

The FDC contained one or more **FDE (Facilitating Detection Element(s)**) (aka the biological recognition element(s).) The FDE comprised the precise methodology

used to detect the antigen [21]. In this dissertation's case, it was the covalent bonding of the "lock and key" association of the antigen and its associated antibody. This is a well known and well studied phenomenon in chemical and biological science.

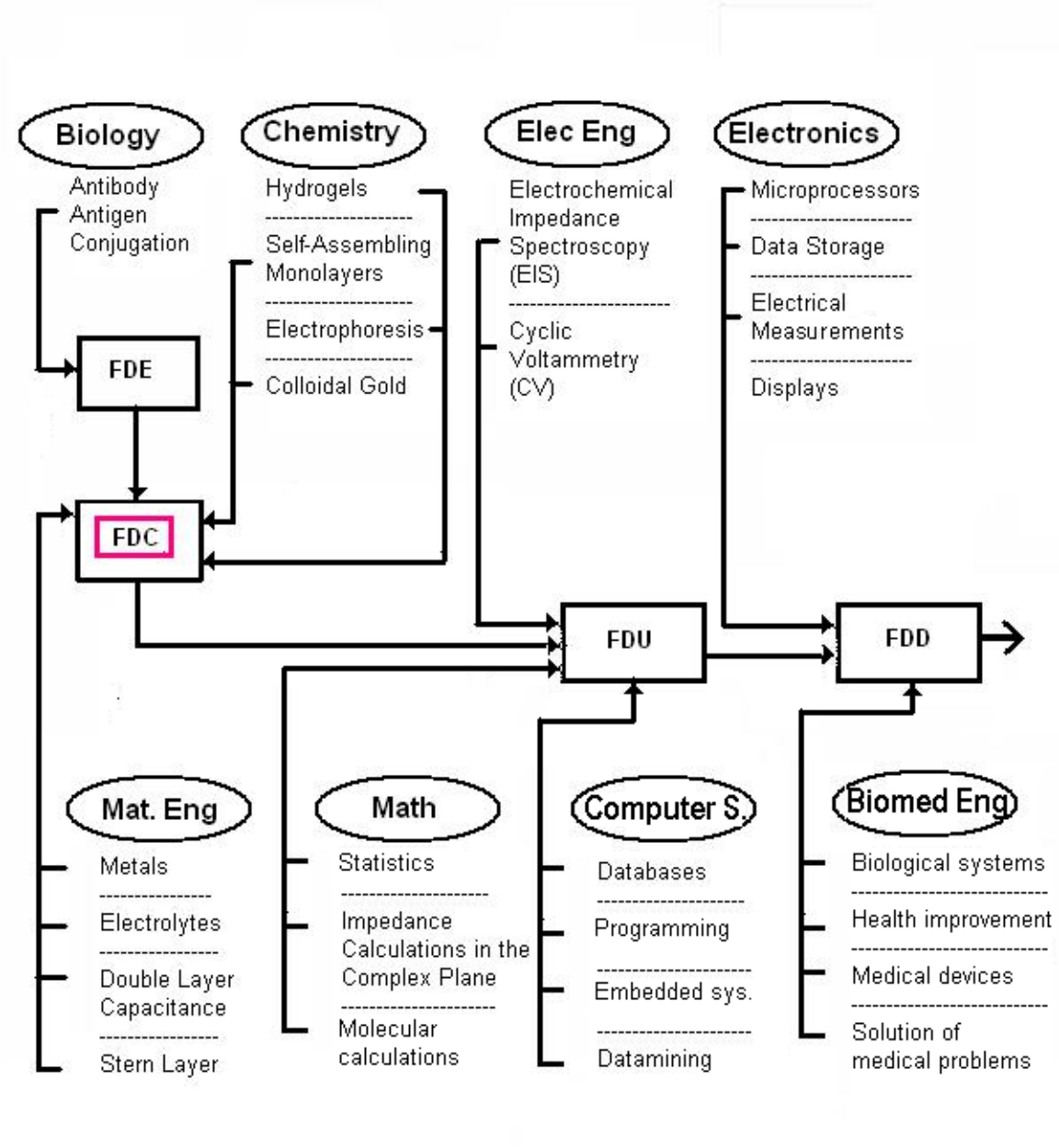

Figure 2: **The integration of disciplines utilized to create the novel FDC used to construct the FDD.**

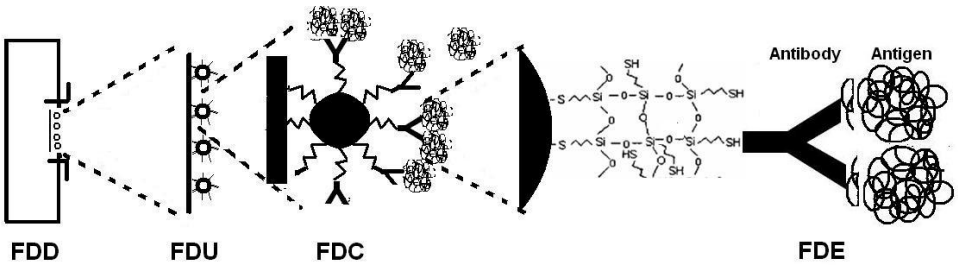

Figure 3: **Exploded view of linear (serial) FDD (Facilitating Detection Device).**

The construction of the unique biosensor developed here (Figure 3) involves many disciplines of science. This is illustrated in Figure 2.

Examples of biosensors

Electrochemical sensors are a subsection of chemical sensors, which are sensors that use chemical processes in the recognition and transduction procedures. The basic difference is the FDE. If the FDE monitors a chemical, nonorganic, reaction, the sensor is electrochemical. An example is a Geiger counter which is a particle detector that measures ionizing nuclear radiation such as alpha particles, beta particles or gamma rays. A particle or photon of radiation reacts with an inert, low pressure gas (usually helium, neon or argon with halogens added) and makes the gas briefly, electrically, conductive. This is the FDE or Facilitating Detection Element. A cascading effect of many photons causes an electrical current in the gas. This is the FDC or Facilitating Detection Component. The inert gas is contained in a closed chamber, forming the FDU or Facilitating Detection Unit. The output current of the tube is then amplified and displayed by the FDD or Facilitating Detection Device as in Figure 3.

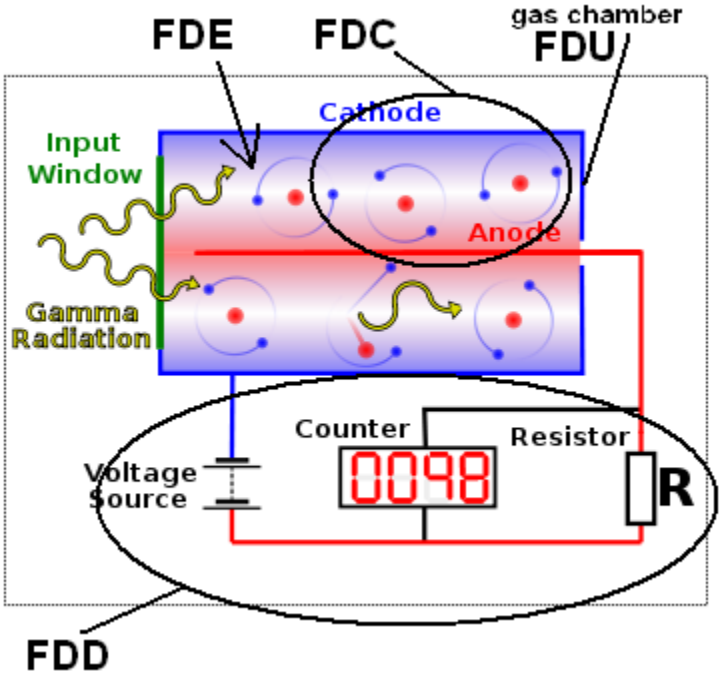

Figure 4: **A Geiger counter diagram [23].**

The term biosensor is applied to devices either used to monitor living systems, or incorporating biotic elements for the FDE's. An example of a typical biosensor is a plant moisture meter. A water ion reacts with the metal spike (electrode) when there is moisture in the soil. This is the FDE. Two electrodes in close proximity will conduct an ionic electric current in the presence of moisture. This is the FDC. There is a connection between one or more FDC's with appropriate wires and electrical parts (resistors, diodes, capacitors, etc.) and this becomes the FDU. Then, the output from this arrangement is connected to an amplifier and meter (the FDD) and the result is a plant moisture meter as shown in Figure 4.

Another example of a biosensor is a glucose tester which is used by diabetics all over the world.

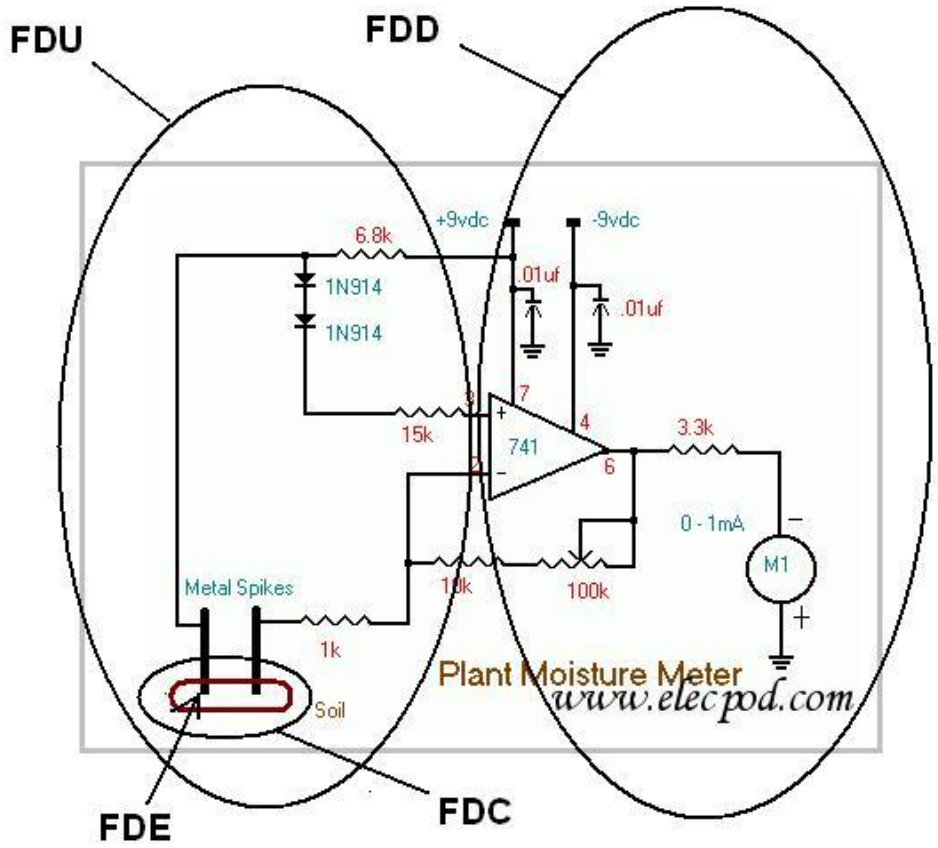

Figure 5: **Typical plant moisture meter diagram.**

Antibodies

Antibodies can be polyclonal or monoclonal. If an antigen is introduced into a vertebrate, polyclonal antibodies are formed as a result of the reaction of some of the animal immune system's B-lymphocyte cells turning into plasma cells and producing antibodies that bind to that antigen. However, though each B-cell produces one antibody for a binding site on the antigen, the antibodies produced by different B-cells can be for different binding sites on the same antigen. Monoclonal antibodies are produced by derived or cloned from one parental cell, and thusly, are targeted for only one epitope or

binding site on the antigen. Georges Köhler and César Milstein at the University of Cambridge, in 1975, came up with a way to make monoclonal antibodies in the laboratory, and they received the 1984 Nobel Prize in Medicine. Monoclonal antibodies can be produced in vitro or in vivo. They can be then used to detect an antigen in a solution with a Western blot test or to detect an antigen in a whole cell with an immunofluorescence test.

Why a gel?

The "lock and key" interaction between molecules in order to form ionically bonded conjugates relies on the shape of the epitopes of each molecule. In order for antibodies to conjugate with antigens specific to them, they must be in a medium that allows movement of their paratopes to align with the epitopes and move together, thus to insert the "key" in the "lock." In addition, the medium must not alter the shape of the molecules by breaking or bending any bonds that substantially contribute to the epitope's shape.

The prerequisites above are innate in certain fluids; however, this does not include dry air. Some liquids can fulfill these requirements; however, we do not want them to dry out too rapidly. Therefore, a gel was chosen as the antibody medium. A gel is a colloidal suspension of a solid dispersed in a liquid or a semi-rigid solid which exhibits no flow when in the steady-state. Though gels are mostly liquid by weight, they behave like solids due to a three-dimensional cross-linked network within the liquid. The internal network structure results from physical or chemical bonds, crystallites or other junctions that remains intact within the extending liquid. The antigens that come in

contact with the surface of the gel are captured ("stick") at that point, become hydrated (if dry), and, then, diffuse down into the gel. First, we had to determine the electrical characteristics of the gel to be used and the corresponding concentrations of the optimal ingredients that also allow the antibodies to retain their bioactivity.

Prior biosensors have been shown to detect specific antigens using electrode immobilized antibodies in liquids [31][49] [73], but have not been effective in air because of the inability to keep antibodies bioactive in dry air.

The parallel embodiment of our FDC is constructed with four parts:

1. A gold surfaced electrode
2. A self-assembled monolayer (SAM) of MPTS covalently attached to the gold (Figure 13)
3. Colloidal gold nanoparticles covalently attached to the ends of the SAM (Figure 15)
4. Antibodies (as capture molecules) covalently attached to the colloidal gold nanoparticles (Figure 23)

Self Assembled Monolayers (SAM)

The self-assembly monolayer (SAM) technique is a highly topical and powerful field of research in nanotechnology. We are all self-assemblers. The cells in our bodies form organs, bones, fingers, eyes, etc. without external forces directing the assembly. The process of structures formed by molecules selectively binding to a molecular site without external influence is not fully understood, but it promises to give rise to a wide variety of applications [28], and since the SAM phenomena (Figure 5) is more a physical principle than a quantifiable property, as applied in physics, chemistry, and biochemistry, and thusly is interdisciplinary [38].

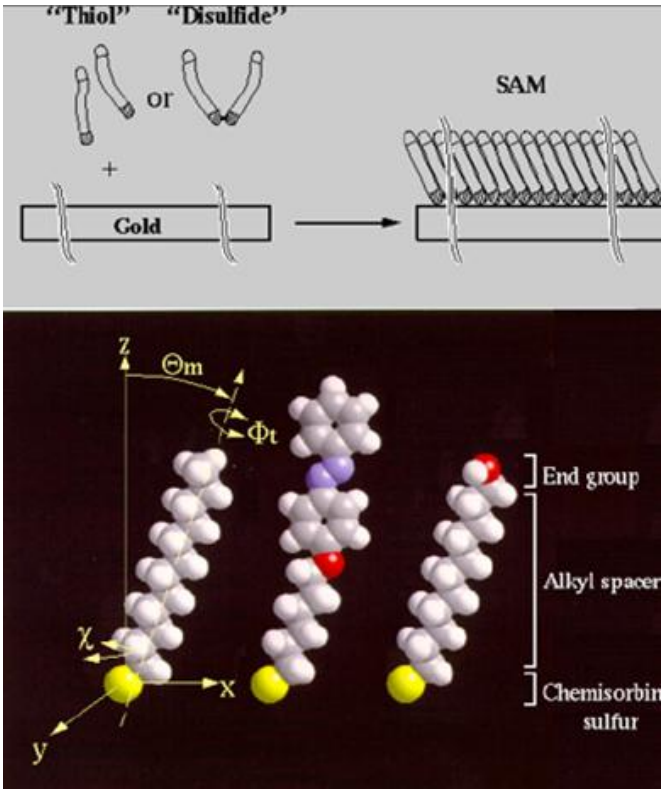

Figure 6: **The Assembly of Monolayers [32].**

SAM's also permit reliable control over the environment layout, and enable a high packing density of an immobilized recognition center, or multiple centers, at a substrate surface. Many systems undergo the process of self-assembly. Organosulfur-based species self-assemble at a noble metal species [30]. Organosilane-based species self-assemble on hydroxylated surfaces such as silicon and glass.

This dissertation's research capitalized on the stability and physicochemical properties of sulfur-containing compounds, e.g. MPTS, which had a strong affinity for gold surfaces. In the case of alkanethiols, the mechanism of binding is considered to be

the oxidative addition of the S–H bond followed by reductive eliminated hydrogen, resulting in the formation of a thiolate species.

SAM's have a common general structure (see Figure 5). At the head end, there is a thiol or disulfide base. This attaches to the substrate. Then, there is an alkyl spacer. Finally, there is an end group which can be of a wide variety of functional groups, allowing the group to be attached to even biological entities such as antibodies. One should think of this, not as a coating of the substrate, but as a surface "converter". A biomaterial surface such as a metal can be converted by the SAM into a biological surface.

Functionalization attributes desired with SAM's include that they be ionic, zwitterionic, homogenous, and have a high packing density. The spontaneous adsorption of thiols and disulfides onto gold has been investigated. This allowed many functional groups to be attached to the highly ordered monolayer surface with a fairly easy preparation [37].

Sol-gel materials

Sol-gel-derived inorganic materials exhibit a number of advantages. They operate at low temperatures for encapsulation of biorecognition elements [46]. The porosity can be adjusted by mixture concentrations. They react little with other chemicals, have high thermal stability, and exhibit negligible aqueous swelling [14].

FTIR technology

Our research incorporates Fourier Transform InfraRed spectroscopy (FTIR) measurement technology that permits the classification of a broad range of organic compounds and some inorganic pigments based upon the absorption of infrared energy. A spectrum can be plotted, and molecules predicted.

Cyclic voltammetry

Cyclic voltammetry measurements involve linearly sweep stepping a voltage excitation on an analyte sample from, typically, a negative value to a positive value and then reversing the steps back to the starting value, while recording the resulting current. The current vs. voltage is plotted on a graph in the range of a redox reaction. The current increases with voltage (potential) until it reaches the reduction (or oxidation) potential of the analyte, where it falls off as the concentration of the analyte depletes near the electrode surface. As the applied voltage is reversed, reoxidation is performed and a current of reverse polarity is generated [59]. If the electron transfer is rapid and the current is limited by diffusion, the current peak will be related to the square root of the voltage scan rate.

Hysteresis is often displayed between the reduction peak (Epc) and oxidation peak (Epa) due to polarization overpotential due to analyte diffusion rates and barriers of transferring electrons from the metal electrode and the analyte. This can be characterized by the Butler-Volmer equation and Cottrell equation reduced to:

$$| E_{pc} - E_{pa} | = \frac{57mV}{n} \qquad \text{(Eq. 2.1)}$$

for an *n* electron process [67].

EIS technology

Another measurement technology that our research incorporates is Electrochemical Impedance Spectroscopy (EIS). EIS involves the application of a small sinusoidal electrochemical perturbation, voltage or current, over a wide spectrum of frequencies. This multi-frequency excitation allows the measurement of the capacitance of the electrode, and the measurement of several electrochemical reactions that take place at very different rates. The instrument utilized for EIS measurements was the EG&G (Princeton Research) 283 Potentiostat, which consists of a potentiostat plus special hardware to apply and measure the AC sinusoidal signals. In depth analysis will follow in subsequent chapters of this dissertation.

Resistance and Impedance

When current flows through a non-superconducting straight wire, the molecules of the wire tend to interfere and slow down the electron (current) flow, the action of which absorbs energy and generally converts it to heat. This is known as resistance and ordinarily is measured in units called ohms. Georg Simon Ohm (1787-1854) developed the equations relating voltage, current, and resistance as follows:

The current in a circuit is directly proportional to the applied voltage and inversely proportional to the resistance of the circuit (Ohm's Law). That is,

$$R = \frac{E}{I} \qquad \text{(Eq. 2.2)}$$

where R is the resistance
E is the electromotive force (voltage)
I is the current

However, this only applies to an ideal resistor having the properties of

a.) obeying Ohm's Law at all current and voltage levels

b.) having a resistance value that is independent of frequency

c.) having AC current and voltage signals that it are in phase with each other.

In practice, ideal resistors do not exist, and the resistance is more complex. Therefore, the term impedance is used to include all of the other factors and terms involved in the concept. Impedance encompasses all the exceptions to the attributes of the ideal resistor mentioned above. The handling of the impedance of an AC circuit with multiple components can be tedious if only sine's and cosine's are used to represent the voltages and currents. A mathematical construct which makes this easier is the use of complex exponential functions.

Conductivity is closely related to diffusion in a concentration gradient; impedance spectroscopy can be used to determine diffusion coefficients in a variety of electrochemical systems, including membranes. Their impedance can be measured by applying an AC voltage to an electrochemical cell, and measuring the resulting current. This sinusoidal voltage generates an AC current signal of the same frequency and its harmonics. This current signal is the sum of sinusoidal functions or a Fourier series [11].

In order for the response to be pseudo-linear, electrochemical impedance is normally measured using a small excitation signal. In a linear system, the current resulting from a sinusoidal voltage will be a phase shifted sinusoid at the same frequency.

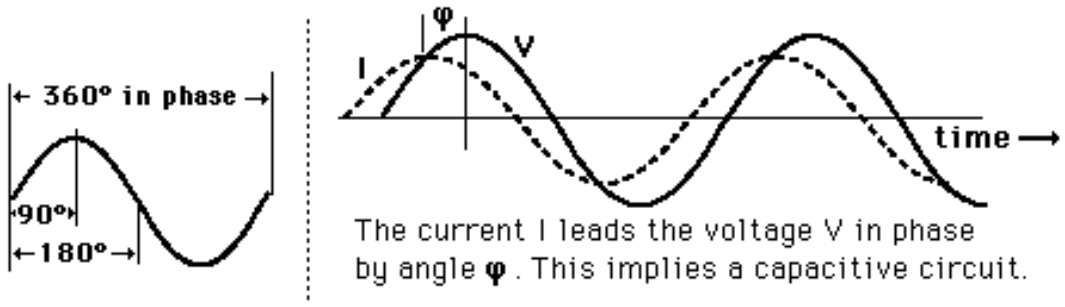

Figure 7: The phase relationship of current and voltage.

The excitation signal, expressed as a function of time in Figure 6, has the form:

$$E(t) = E_0 \cos(\omega t) \qquad \text{(Eq. 2.2)}$$

where E(t) is the potential at time t_r
E_0 is the amplitude of the signal
ω is the radial frequency.

The relationship of radial frequency ω (radians/second) and frequency f(hertz) is:

$$\omega = 2\pi f \qquad \text{(Eq. 2.3)}$$

In a linear system, I_t, is shifted in phase Φ and has amplitude, I_0:

$$I(t) = I_0 \cos(\omega t - \phi) \qquad \text{(Eq. 2.4)}$$

Applying an expression like Ohm's Law the impedance of the system is:

$$z = \frac{E(t)}{I(t)} = \frac{E_0 \cos(\omega t)}{I_0 \cos(\omega t - \phi)} = Z_0 \frac{\cos(\omega t)}{\cos(\omega t - \phi)} \qquad \text{(Eq. 2.5)}$$

Impedance is therefore expressed in terms of a magnitude, Z_0, and a phase shift Φ.

According to Euler's relationship,

$$\exp(j\phi) = \cos\phi + j\sin\phi \qquad \text{(Eq. 2.6)}$$

To express the impedance as a complex function, the voltage would be

$$E(t) = E_0 \exp(j\omega t) \qquad \text{(Eq. 2.7)}$$

and the current response is

$$I(t) = I_0 \exp(j\omega t - j\phi) \qquad \text{(Eq. 2.8)}$$

As a complex number, the impedance is

$$Z = \frac{E}{I} = Z_0 \exp(j\phi) = Z_0(\cos\phi + j\sin\phi) \qquad \text{(Eq. 2.9)}$$

Therefore, Z(ω) is composed of a real and an imaginary part.

The Randles equivalent circuit is the most common circuit model of electrochemical impedance [11][34]. It includes:

a. the solution resistance
b. a double layer capacitor
c. a charge transfer or polarization resistance

The equivalent circuit for the Randles cell is shown in Figure 7. The double layer charge transfer reaction is in parallel with the impedance and is made up of the charge transfer resistance, which is inversely proportional to the rate of electron transfer, and the Warburg impedance, Z_w, which grows from mass transfer limitations [65].

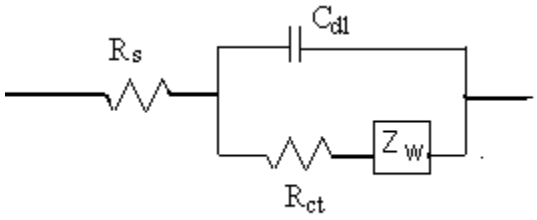

Figure 8: **The equivalent circuit diagram of the double layer capacity effect (Randles cell).**

Plotting the real part of Z on the x-axis and the imaginary part of Z on the y-axis of a chart is called a Nyquist plot (also called the Cole-Cole plot or Complex Impedance

Plane plot.) In this plot, the y-axis is negative and each point on the Nyquist plot is the impedance at one frequency.

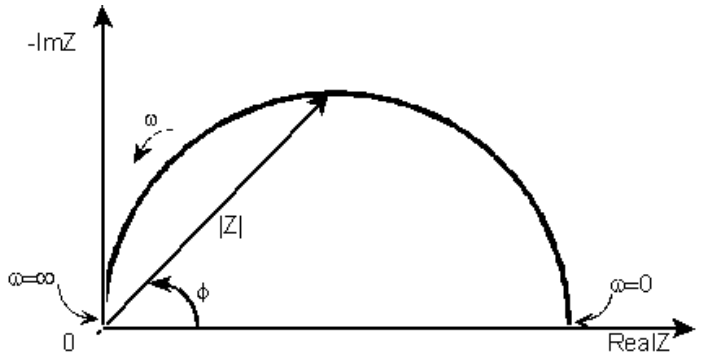

Figure 9: **A Nyquist plot of impedance over a frequency spectrum from 0 hertz to infinity.**

Higher frequency information is on the left of the plot and the low frequency is on the right. This is true for EIS data when impedance falls as frequency rises. The Nyquist plot (Figure 8) traces the impedance as a vector of the absolute value of |Z|, at an angle Φ with the x-axis. The Nyquist plot for a Randles cell is a semicircle. The resistance is the value along the real axis value at the high frequency intercept (near the origin). However, for any data point on the Nyquist plot, the frequency that was used to record any particular point cannot be determined. The value on the real Z axis at the low frequency intercept is the bulk resistance plus the polarization resistance. Therefore, the diameter of the semicircle would leave the polarization resistance as in Figure 9.

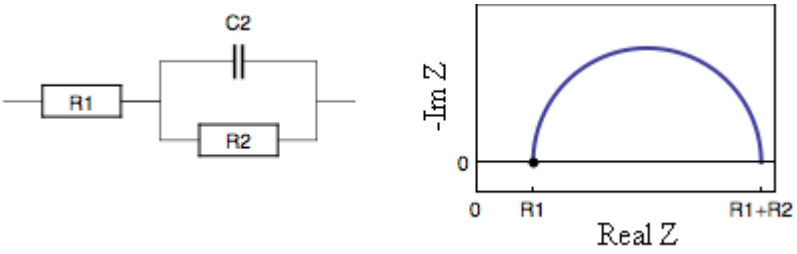

Figure 10: **This circuit diagram represents the Nyquist plot.**

The semicircle represents a single time constant, though impedance plots can contain more than one time constant.

A Bode plot (Figure 10) has the impedance plotted against the log of the frequency on the x-axis, and both the absolute value of the impedance (|Z| =Z0) and phase-shift on the y-axis.

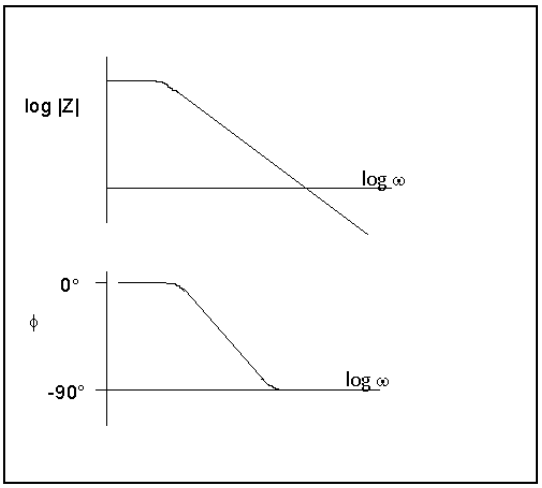

Figure 11: **The Bode plot. Unlike the Nyquist plot, the Bode plot does not explicitly show frequency information.**

Metallic electrodes and the double layer

When an electrolyte comes in contact with a metallic electrode, there is an ion-electron exchange. The term "double layer" refers to the displacement of electrical charges associated with the electrode surface exposed to aqueous solution. There is a tendency for ions in the solution to combine with the metallic electrode and also for the metallic ions to enter the solution [40]. The basic type of charge distribution was proposed by Helmholtz (1879) who postulated that there exists a layer of charge of one sign tightly bound to the electrode and a layer of charge of the opposite sign in the

electrolyte [36]. This separation is called the electrical double layer and is measured in ionic dimensions. As illustrated in Figures 11 & 12, in the Stern layer, also called the condensed layer, the ions are aligned against the surface. The Gouy layer is a diffuse atmosphere past the Stern layer [33]. In this layer, the density of ions is given by the Poisson-Boltzmann relationship:

$$c_{St,i}(i) = c_L(i) \cdot exp\left\{ -\frac{z(i) \cdot F}{R \cdot T} \cdot \psi_{St,i} \right\} \qquad \text{(Eq. 2.10)}$$

where

$C_{St,i}(i)$	Stern layer concentration of species i (mmol/L)
$C_L(i)$	concentration in the liquid phase of species i (mmol/L)
z(i)	valency number of species i (eq/mol)
F	Faraday constant (C/mol)
R	Boltzmann constant (1.38x10-23 J/K mol)
T	temperature (K)
$\psi_{St,i}$	electric potential of i th Stern layer (V)

and the Debye length equation:

$$\lambda_D = \sqrt{\frac{\varepsilon RT}{F^2 \frac{1}{2} \sum_i c_i z_i^2}} \qquad \text{(Eq. 2.11)}$$

where

F	electron charge ($1.6x10^{-19}$ C)

ε relative dielectric constant for water at 25 C times the permittivity in vacuum (8.854×10^{-12} C/V-m)

n_i ion concentration (ions/m^3)

The double layer effect extends about 10 nm from electrodes, where beyond there is usually an equal density of positive and negative ions.

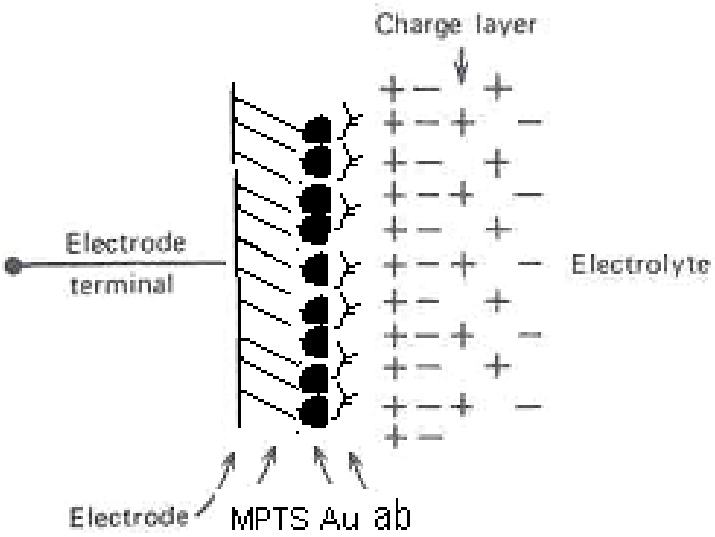

Figure 12: Electrode surface functionalization and charges

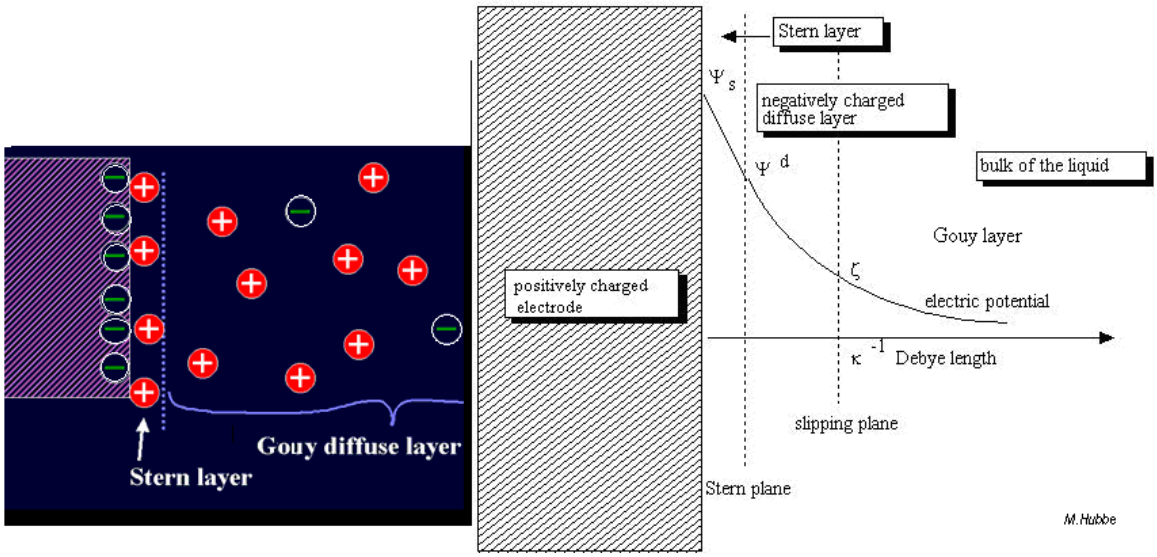

Figure 13: Electrode-Electrolyte Interface - Charge distribution-double layer interface [2].

Electrode Models

The computational study of electrodes often is analyzed by developing an equivalent electrical circuit diagram as an analogy to the electrochemical process. With that diagram having been defined, standard mathematical analysis of that electric circuit can be used to model the electrode interface.

An essential issue to be addressed is how the physical parameters of the SAM, attached to the working electrode surface, affect the impedance measurements. The surface area of the monolayer perpendicular to the current flow, through the SAM of interest, is a critical factor contributing to the capacitance component of the impedance. The surface of the SAM is not solid. Rather, it is the assemblage of the ends of molecular chains oriented in the same direction. The density, and thusly the number of chains per area, determines the relative static permittivity or dielectric constant of the SAM, which allows the same charge to be stored with a smaller voltage or electric field [10]. At the saturation point of the SAM, the dielectric constant will level off at some value. This phenomenon is the key to the reproducibility in the construction of a biosensor [21].

The capacitance is calculated using the geometry of the conductors and the dielectric properties of the insulator between the conductors. Capacitance is directly proportional to the surface area of the conductor plates and inversely proportional to the separation between them. The capacitance of a parallel-plate capacitor with plate area *A* separated by a distance *d* is closely equal to:

$$C = \varepsilon_r \varepsilon_0 \frac{A}{d} \text{ (in SI units)} \qquad \text{(Eq. 2.12)}$$

where

C is the capacitance in farads, F

A is the area of overlap of the two plates measured in square meters.

ε_r is the relative static permittivity of the material between the plates,

(vacuum =1) --also called the dielectric constant

ε_0 is the permittivity of free space (8.854×10^{-12} F/m)

d is the separation between the plates, measured in meters.

The total impedance of the electrode interface has several components.

1. The double-layer impedance at the surface of the electrode-electrolyte, including the Stern layer.
2. The impedance of the SAM [36].
3. The impedance formed by the attachment of the antibody and by the antibody-antigen conjunction.
4. The bulk impedance of the electrolyte through the Gouy layer [33].

The latter is ignored through the 3-probe EIS arrangement.

The total capacitance is the reciprocal of the sum of the reciprocals of 1-4.

A bare gold electrode has been reported in literature to have a surface capacitance of 15 - 33.5 $\mu F/cm^2$ [44][45]. When the bare gold electrode is exposed to very diluted solution (2%) of 3-MPTS (3-mercaptopropyl)trimethoxysilane, the MPTS forms an ordered monolayer. A low concentration prevents multilayer formation. Sulfide groups are adsorbed at the solid-liquid interface by a strong chemisorption of the head group (Si) to form a highly ordered structure. After the SAM has formed, another exposure to MPTS will, indeed, form another SAM over the previous one.

Gold nanoparticles are attached to the Si-O-Si ends of the MPTS. The bifunctional molecule, MPTS, contains both -SH and $-OCH_3$ groups, forms covalent

bonds with gold substrates through its thiol groups on one end and gold nanoparticles on the -OCH_3 ends. The behavior of MPTS on gold surface and its organizational structure are influenced by following forces [43]:

a. interactions between thiol head groups and the Au lattice,
b. interactions between the alkyl chains, and
c. interactions between the end groups of the thiols.

These determine the final molecular organization and specific topography. The hydrophilic "head groups" form clumps or assemblies on the surface of the substrate, while the hydrophobic "tail groups" assemble away from the substrate. Islands of tightly packed molecules nucleate and grow until the surface of the substrate becomes covered in a single monolayer. The contact angle is determined by the thermodynamic equilibrium of the liquid and solid phase of the head and tail groups and the surface free energy of the electrode substrate.

The Au nanoparticles can attach antibodies without having them lose their bioactive properties. Ellipsometric measurements (at 632.8 nm and 70° angle incidence) yield an average film thickness of 8 Å following a 6 h assembly of the thiol-containing gel [44]. The maximum dimension size of MPTS molecule is 0.6–0.7 nm [43]. Aswal used ellipsometry to show the thickness of the MPTS SAM, using, was 0.8±0.1 nm, which is close to the theoretical value of the length of MPTS molecule (0.77 nm) [47]. A calculation of the capacitance of the monolayer with the colloidal gold attached is as follows:

[45] MPTS+CG+Ab electrode R (Eq. 2.13)

(20mF/cm^2 *(.8nm+20nm+.1nm)/ (8.85400e-12 * (PI*(4mm ** 2)) = 9.392 × 10^{11} mF

The biosensor of this dissertation worked on the principle of restriction. Electricity flows through a wire by means of the movement of electrons; electricity flows through a liquid by means of the movement of ions; in this case, with 0.1 M $K_3[Fe(CN)_6]$/ $K_4[Fe(CN)_6]$ as the redox couple or with functionalized colloidal gold nanoparticles in our linear/serial configuration. The conjugation of the immobilized antibodies and the antigens impedes the flow of ions. However, our goal was to have 95% to 97% of the path for the flow of ions to the Au electrode closed off with the monolayer and antibody matrix. In this arrangement, the antigen conjugation had the greatest effect on the change in capacitance. As an analogy, if one takes a drink from a fire hose, there will be little effect on the water flow. If, on the other hand, one drinks from a water fountain, there is a very discernable change in water flow. That is the principle of restriction.

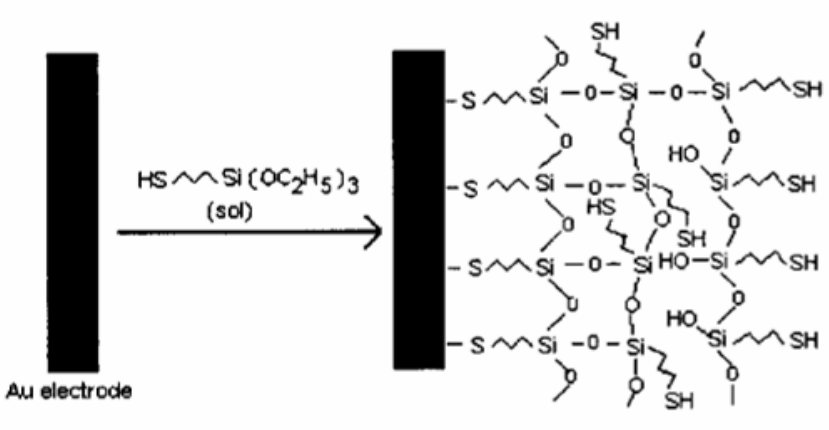

Figure 14: **The MPTS self-assembling monolayer is applied to the gold electrode as described[14]. Thiol groups extend out.**

Discussion

Because of DTNB's specificity for -SH groups at neutral pH, Ellman's Reagent is useful as a sulfhydryl assay reagent (see Figure 14). It also has a high molar extinction coefficient (also known as molar absorbtivity) and short reaction time. The resulting

NTB (“yellow colored” species) produced in this reaction has a high molar extinction coefficient in the visible range to be measured by a spectrophotometer.

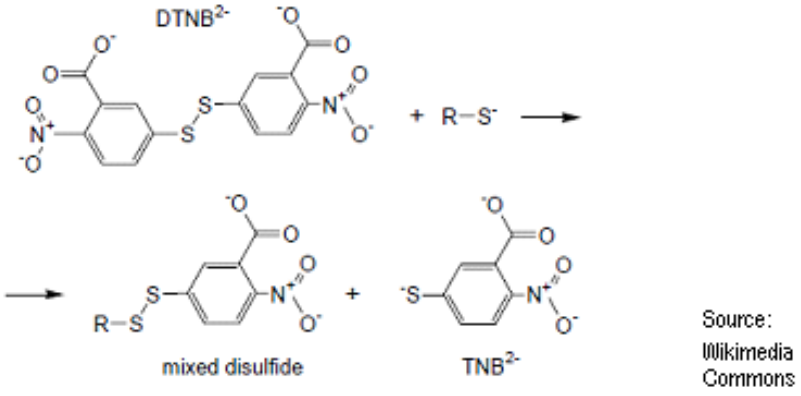

Figure 15: **DTNB attacks the disulfide bond to yield a mixed disulfide and 2-nitro-5-thiobenzoic acid (NTB)**

While the understanding of a single SAM has been facilitated [14], the structure and properties of multiple layers is less understood (see Figure 15). An experimental paradigm ideally suited for the purposes of this study is to determine the optimal length of the dielectric SAM to provide the best observable impedance change in the presence of the anti-body/antigen conjugate.

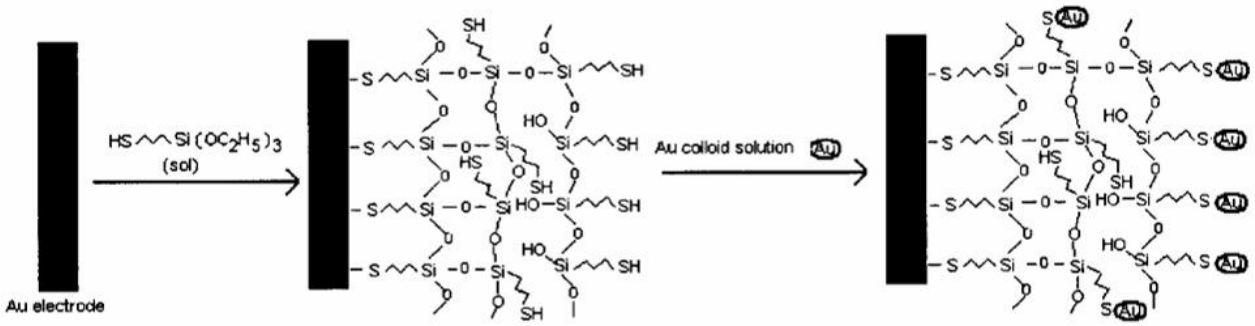

Figure 16a: **Colloidal gold nanoparticles are attached to the ends of each SAM.**

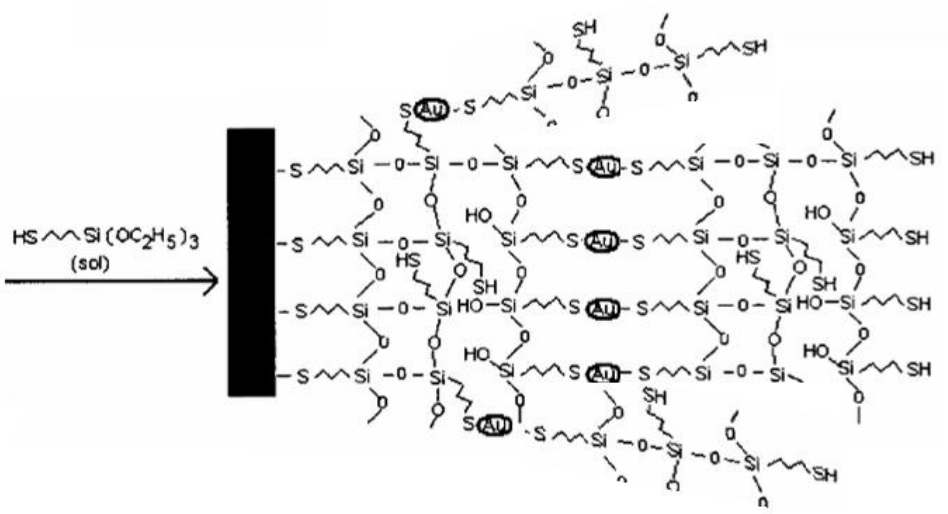

Figure 17b: **Colloidal gold nanoparticles are attached to the ends of each SAM before another SAM is extended onto the previous.**

As the length of the chains of the SAM extend, the permittivity of the dielectric remained constant, but the separation of the "plates" of the capacitor increased and the impedance was inversely proportional to the distance of separation.

Determination of saturation MPTS monolayer coverage of colloidal gold

Colloidal gold with 20 nm diameters serves a dual purpose in the electrical property contribution of impedance. First, it is a source of ions for the conduction process. Gold nanoparticles were produced in a liquid by reduction of chloroauric acid ($H[AuCl_4]$). The Au^{3+} ions to be reduced to neutral gold atoms were negatively charged. Colloidal gold, consistent with the Turkevich [48] method, formed because sodium citrate (or Trisodium 2-hydroxypropane-1,2,3-tricarboxylate) ($Na_3C_6H_5O_7$) was added as a reducing agent and its ions prevented the gold from sticking together.

Colloidal gold also provided an attachment platform for the MPTS monolayer base as did the fixed gold substrate in Figure 13, which, in turn, attached the antibodies at their other ends. This structure alters the dielectric constant of the complex, which changes the capacitance and, therefore, the impedance spectrum. This will change further when the antigen specific to the antibody attached to the monolayer conjoins with the antibody, facilitating the detection of the antigen.

Results

Sensitivity is the amount of sensor output change per measured quantity changes. An ideal sensor has a linear output, and therefore the sensitivity is defined as the ratio between output signal and measured quantity. In practice, a sensor typically approaches linearity in its rated range, which will be determined by this experiment. Literature reports a linear calibration in the range of 8.3–2128 ng/ml and detection limits of 3.3 ng/ml plotted against the logarithm of the antigen concentration [14]. This dissertation's research is concerned with detecting the higher levels of concentration that would be dangerous in our environment..

Discussion

The saturation point was the antigen concentration that does not produce any more significant results than the previous (lower) concentration. This was the point where the formation of new conjugates would cease to increase appreciably [41] (see Figure 16).

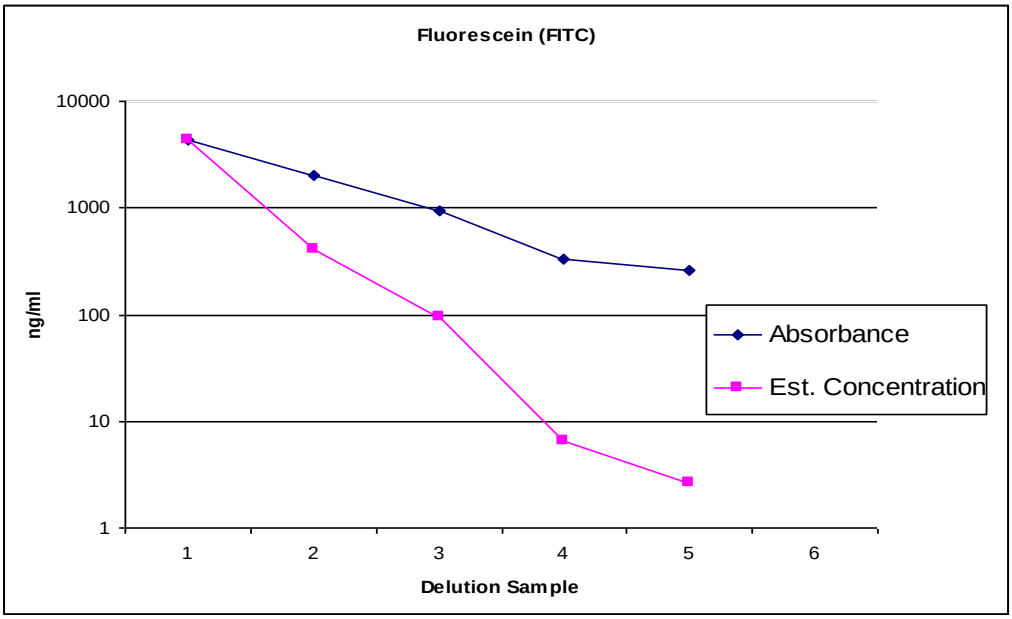

Figure 18: **The antibody concentration determination by fluorescence of Fluorescein (FITC).**

Indications were that approximately 300 data points spread over 8-10 frequencies would be sufficient to characterize the impedance/admittance profile [42]. The selectivity was determined by comparing the specific antibody-antigen interactions with non-specific interactions [39]. EIS was used to measure the impedance at the range of frequencies from 0.1 Hz to 100 kHz as impedance was dominant at the antigen-antibody junction at those frequencies.

The DC bias voltage can also alter the EIS response (see Figure 17).

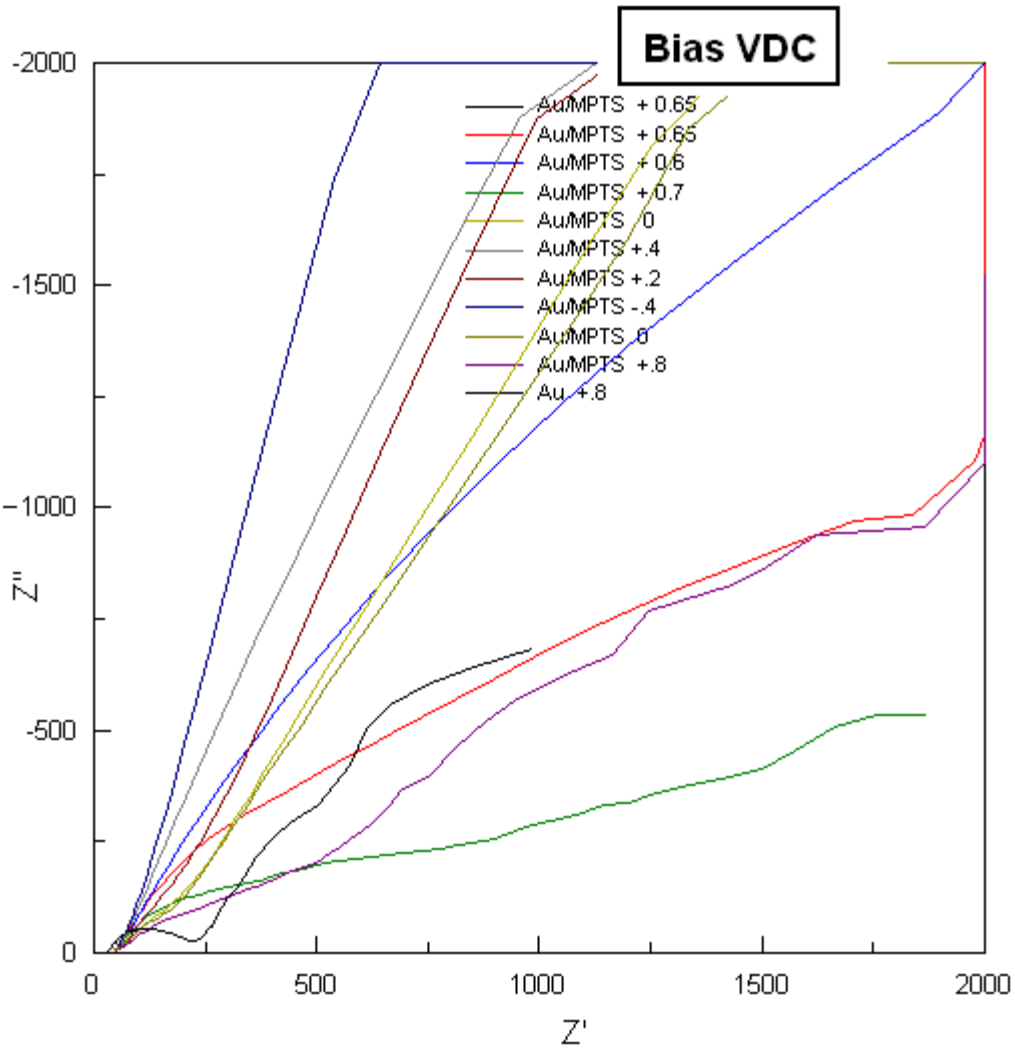

Figure 19: **EIS plots for Au / MPTS (one monolayer) with various DC biases.**

CHAPTER 3

AIM 1: TO DEVELOP A NOVEL LABEL-FREE IMMUNOSENSOR IN A NON-LIQUID ENVIRONMENT USING PARALLEL PATHS

AIM 1: TO DEVELOP A NOVEL LABEL-FREE IMMUNOSENSOR IN A NON-LIQUID ENVIRONMENT USING PARALLEL PATHS

Introduction

While antibody-antigen biosensors have been studied in solution, either with simple buffers or a redox couple, use with antibodies-antigens in air has not been successful because the antibodies and antigens need the conformation ability enabled by a solution to conjugate and the solution dries out rapidly when exposed to air. To overcome this challenge, we used a novel hydrogel media with glycerol, which stays intact for an extended period of time. The purpose of Aim 1 was to demonstrate the ability to detect a specific antigen, through EIS measurements of the antibody/antigen conjugation, using a functionalized gold substrate electrode, .in a *non-liquid (gel)* media.

Research Experimental Strategy

This study requires an integration of several areas of scientific research. In order to prove the validity of the results, a step-by-step matrix of experiments was identified and implemented as illustrated in Figure 18. The results build upon each other and also demonstrate the contributions of each component to the final immunosensor.

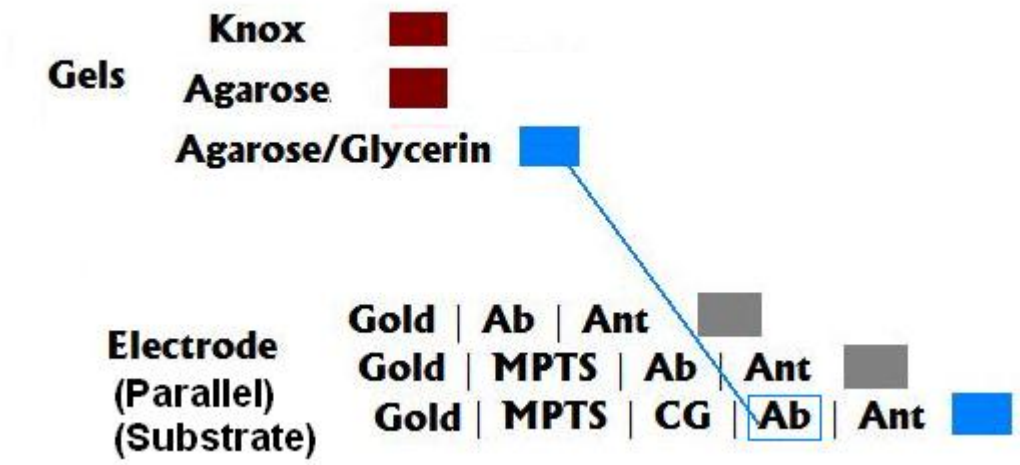

Figure 20: **Progression of experiments leading to the Agarose/Glycerol Gel**

The reason for hydrogels

In order to allow the conjugation of antibodies and antigens, a certain amount of conformation of the protein molecules must occur at the combining, or binding, sites. Referred to as the "lock and key" concept, the "lock" must be typically unblocked to permit the "key" portion of the antigen to insert or slide into the cleft-shaped "lock" site of the antibody. This ability is called activity. The "lock" is located in the Fab portion of the antibody and is formed from the hypervariable regions of the heavy and light chains (see Figure 19). Multiple types of bonds are utilized to secure the antigen at the binding site of the antibody, including hydrogen bonds, Van der Waals forces, electrostatic bonds, and attractive hydrophobic bonds due to the close positioning of non-hydrophilic portions of the two molecules. The combination of the attractive and repulsive forces operating between the antigenic determinant and the binding site of the antibody is the equilibrium constant called affinity. Affinity becomes quite high as the distance between the atoms becomes small; the forces are inversely proportional to the square of this distance. Even

a distance of an atom or two can make a significant difference of affinity [53]. None of these bonds are covalent, however, and no new molecules are formed. This makes the antigen-antibody conjugation a reversible reaction, as caused by chemical, electrical, or thermal denaturing.

Figure 21: **Antibody-Antigen binding [55]**

Hydrogels consist of solid three-dimensional networks that span the volume of a liquid medium. Surface tension effects give hydrogels their solid characteristic polymer chains, which are hydrophilic. Many gels are thixotropic as they become fluid when agitated, but resolidify when resting. This aids in the "lock and key" operation on a molecular level. An example of a thixotropic fluid is the synovial fluid found in joints between some bones.

Prior biosensors have been shown to detect specific antigens using electrode immobilized antibodies in liquids [49], but have not been effective in air because of the inability to keep antibodies bioactive in air. In order for the antibodies to remain active and conjugate with their specific antigens, the antibodies need to be in a fluid type

medium, because the epitopes need to conform slightly to form an exact "lock and key" joining. A gaseous environment will not work, because the antibody proteins will dry out and become stiff. A solid media is out of the question to have any movement at all. A liquid is ordinarily used, but has the drawbacks of:

1.) the need to be agitated or mixed, in order for the antigens to come in contact with the antibodies, or the antigen movement will have to rely on slow Brownian motion, or have an electrical charge force migration through the liquid.
2.) if exposed to air, the liquid will dry out.
3.) the liquid based immunosensor cannot be used in any orientation when depending on gravity to contain the liquid.

Our novel approach was a gel media. This, too, allowed motion of molecule, but did not have all the drawbacks of a liquid.

The value of electrical conductivity (conductance) and the specific electrical resistance (resistivity) is temperature dependent.

$$\rho = (R \cdot A) / l \qquad \text{(Eq. 3.1)}$$

where

R = resistance Ω

ρ = specific resistance Ω·m

l = length of the conductor m

A = cross section m^2

In a limited temperature range resistivity is approximately linear:

$$\rho(T) = \rho(T_0) \cdot (1 + \alpha \cdot (T - T_0)) \qquad \text{(Eq. 3.2)}$$

where

α = temperature coefficient (A ratio of increased conductor resistance per degree Celsius rise in temperature.)

T = temperature

T_0 = any temperature at which the electrical resistivity ρ (T_0) is known

(such as T_0 = 295.95 K = 22.8°C room temperature)

A number of experiments were performed to determine the ultimate components of the biosensor. The step-by-step experiment paradigm dictated that each step be concluded with a successful experiment in order to proceed to the next step. Therefore, if an experiment was unsuccessful, it would be modified or replaced with another, until satisfactory results were obtained.

Materials

The IgG was Human IgG, Purified Immunoglobulin, Reagent Grade, (Sigma-Aldrich) I4506.

The IgM was Human IgM, Purified Immunoglobulin, (Sigma-Aldrich) I8260.

The IgGab was Anti-Human IgG FITC antibody produced in goat - affinity isolated antibody, buffered aqueous solution (Sigma-Aldrich) F9512

The IgMab was Anti-Human IgM FITC antibody produced in goat - affinity isolated antibody, buffered aqueous solution (Sigma-Aldrich) F5384

Commercial collagen (Knox) was purchased in a local grocery store.

The hydrogel was Agarose - Type VI, High Gelling Temperature (Sigma-Aldrich) A3893

The thread used for the linear/serial immunosensor was cotton covered, polyester

The sol-gel 3-MPTS (3-mercaptopropyl)trimethoxysilane was purchased from Fluka (#63797).

Methods

For purposes of this research, all experiments were performed at room temperature. Initial experiments were conducted with a 3-probe arrangement for EIS measurements as in Figure 20.

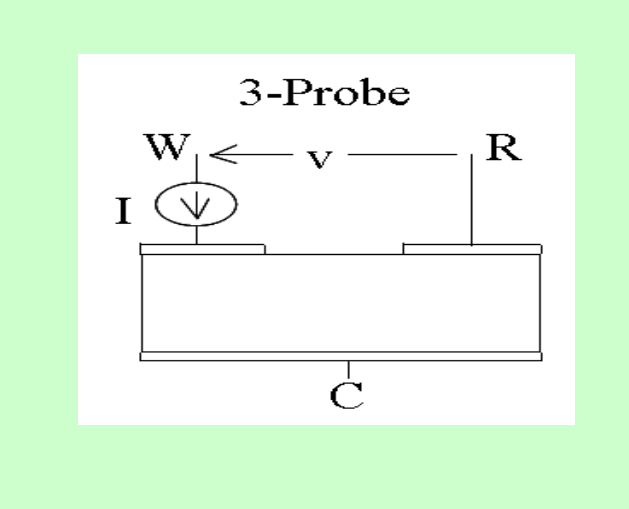

Figure 22: **A 3-probe implementation was utilized here as it canceled out the bulk effects of the medium.**

Experiment Equipment

The impedance and cyclic voltammetry measurements were performed using a Solartron 1260 frequency response analyzer coupled to an EG&G 283 Potentiostat /Galvanometer (EG&G, New Jersey, USA). An IEEE 488 GPIB bus interface connected

them to a personal computer running Windows XP (Figure 21). The combination coped with ultra low current less than 100µA and capacitance levels less than 1 pF. Measurements were made of absolute values of impedance and phase shift while sweeping frequencies between 1 Hz and 10 Mhz. Specially designed software packages Z-plot/Z-View for impedance and Corrware for cyclic voltammetry (Scribner Associates, Southern Pines, NC, USA) were used to gather and plot data. A Garmin microcell (Figure 22) was used to contain the electrodes and measurement media in initial experiments. Custom built fixtures were then developed to accommodate the novel arrangements of the specially developed hydrogel and functionalized electrodes.

All glassware in all experiments was cleaned with 50% strength HNO_3 (diluted with water) for at least 12 hours, rinsed thoroughly with distilled water, and dried prior to use.

Figure 23: **The Potentiostat /Galvanometer**

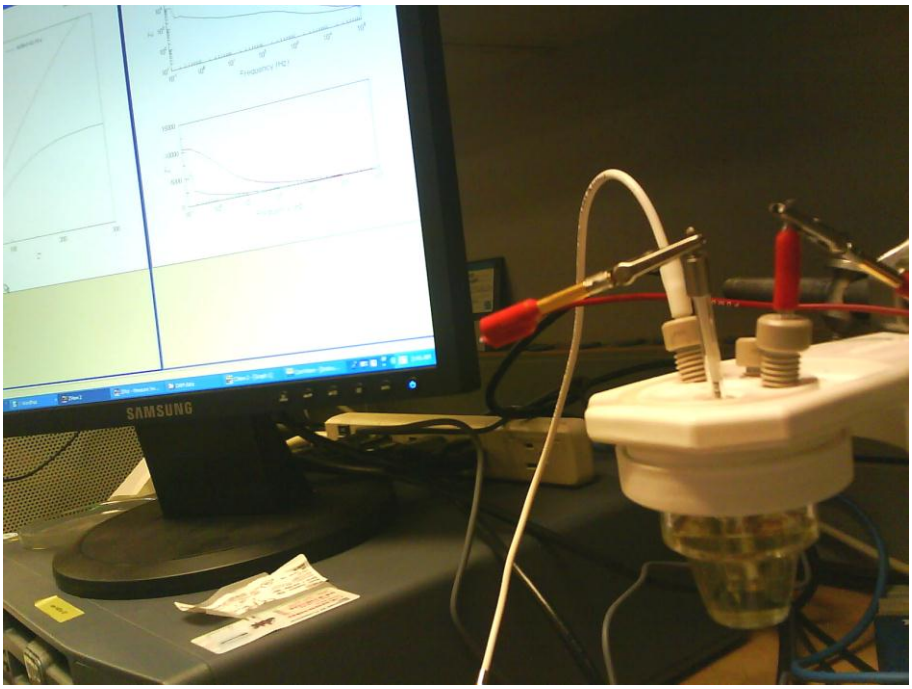

Figure 24: **The microcell and PC with custom interface to the Potentiostat /Galvanometer.**

Several gels were evaluated:

a. Collagen gel was prepared as directed by the manufacturer. It did evaporate slowly, but, more significantly, unfortunately, it had mold growing on it in a few days. Adding a preservative to the gel was rejected due to the possible detrimental side effects it might have on the bioimmunosensor and antigens.

b. Standard 2% agarose hydrogel, as used in electrophoresis, did not grow mold, but was totally dried out in a matter of days.

c. A novel mixture hydrogel was developed. Glycerol was tested as a moistening agent for the hydrogel. Equal parts of glycerol and distilled water were mixed and 2%-4% agarose power

(derived from seaweed) was added. The mixture was heated in a microwave oven until boiling; then the oven was turned off. When boiling stopped, the mixture was again brought to boiling by the microwave oven. This procedure was repeated several times, until a clear product was produced, and then the hydrogel was allowed to cool. This novel hydrogel could be poured into a fixture and over electrodes as required by the design of the immunosensor. This hydrogel does not dry out for months and holds its shape well. It can also be remelted and reused, if not contaminated; it can also be stored indefinitely in a closed container.

The electrical impedance characteristics of this last hydrogel were acceptable for use in the immunosensor in that the gel was conductive, but has an impedance value of almost one megohm per square centimeter.

The parallel embodiment of our FDC was constructed with four parts:

5. A gold surfaced electrode
6. A self-assembled monolayer (SAM) of MPTS covalently attached to the gold
7. Colloidal gold nanoparticles covalently attached to the ends of the SAM
8. Antibodies (as capture molecules) covalently attached to the colloidal gold nanoparticles

In this parallel arrangement, colloidal gold nanoparticles were utilized to amplify the response of detection by providing a spherical attachment on the ends of the SAM, opposite the end attached to the gold base electrode. This allowed many more antibodies to attach at the end of each molecule of the SAM.

Preparation protocol of Colloidal Gold Nanoparticle Suspension

The desired nanoparticle size was approximately 20-40nm [ref]. The protocol to prepare the capture molecules, colloidal gold consisting of 20 nm diameter gold nanoparticles, was as follows:

1.) Mix 200 ml of H_2O and 1.00 ml of 1% $HAuCl_4$

2.) Add 1.50 ml of 0.075% $NaBH_4$/1% trisodium citrate and 0.55 ml of 1% trisodium citrate

3.) Stir continuously for 6 hours at room temperature (It can be stored at 4^oC if for future use.)

Preparation protocol of MPTS Self-Assembled Monolayer Solution

1.) In a separate container, mix 200ml of the sol-gel MPTS with absolute ethanol and aqueous acid (0.1M HCl) at a molar ratio of 1:4:3.5 and sonicate for at least 1 hour until it is a homogenous solution.

Attaching a solgel monolayer to the gold substrate.

MPTS ((3-mercaptopropyl) trimethoxysilane) is a bifunctional molecule that contains both thiol and silane functional groups. The thiol groups are the binding moieties for the covalent attachment of MPTS (as prepared in Step 4 above) to gold surfaces. The sulfur-gold bond has advantages and was, therefore, the first bond tested in this thesis.

The sulfur-gold bond is a strong covalent bond with a high bond enthalpy of 418±25kJ/mol [53] and this well known bond has been measured at a force of 1.4±0.3nN at loading-rates of 10nN/sec [54]. Bonds between biomolecules are generally weaker as they are usually formed by Van der Waals forces which cause physisorption.

In this parallel embodiment, the gold electrode surface is covalently attached with a theoretical MPTS molecule length of 0.77 nm [47] to the gold base electrode as in Figure 13. The hydrophilic head groups of the MPTS point toward and are covalently attached to the gold substrate, lowering the gold surface free energy. This can take up to 2 hours. Once the assembly is stopped via washing with distilled water and methanol as previously described, and after an exposure of colloidal gold nanoparticles, an additional SAM can be applied over the first as in Figure 15. The gold milliprobe (Princeton Applied Research (formerly EGG) G0227), presents a round surface area 2 mm ± 0.2mm in diameter (0.0314 cm^2). The gold milliprobe was meticulously polished with alumina suspensions (1.0μ, 0.1μ, 0.05μ), then rinsed with distilled water. The gold surface was then carefully cleaned in piranha solution (3:1 sulfuric acid (H_2SO_4) and 30% hydrogen peroxide (H_2O_2)), which cleans off organic residues. [This is highly reactive -- use with caution.] Since the piranha solution is a strong oxidizer, it will remove organic matter, and it will also hydroxylate most surfaces (add OH groups), making them extremely hydrophilic.

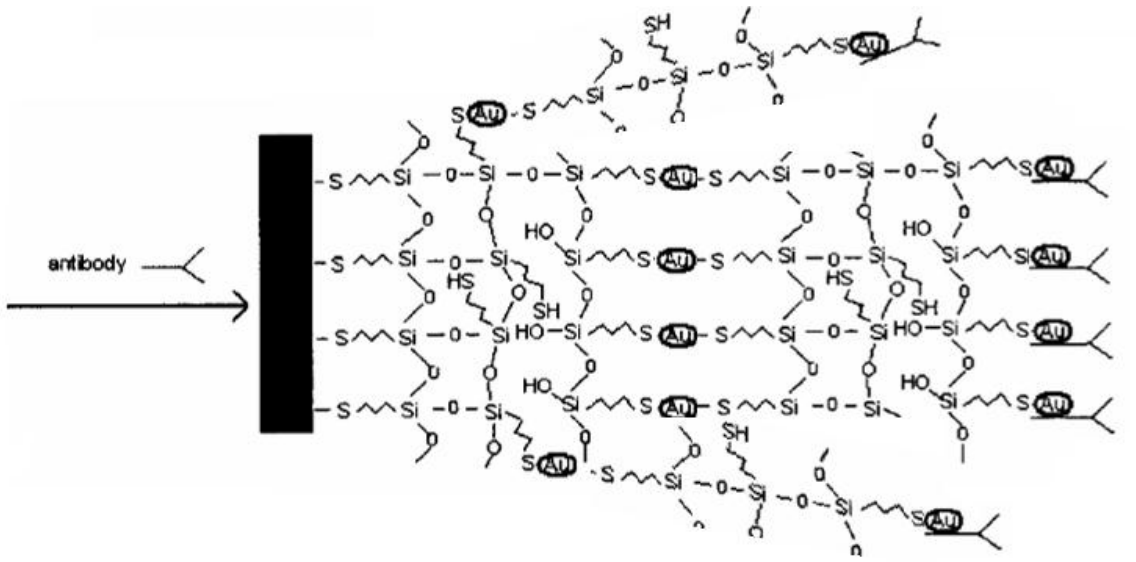

Figure 25: **The Antibodies are attached to the ends of the extended SAM's after a last exposure of colloidal gold nanoparticles.**

Experiment A1-1: Comparison of gels needed to keep antibodies active

Multiple gels were compared for their various properties. Collagen gel was one candidate. Also, the hydrogel, agarose, was tested in various mixtures. Finally, in a novel mixture, glycerol was added to the gel in order to prevent drying out too rapidly, and to keep the antibodies active. This hydrogel lasted the longest time (months) without drying out. The glycerol-H_2O-agarose (GHA) was mixed in a ratio of 1:1:.02 and prepared as previously described for a hydrogel. EIS measurements were performed with a DC bias of essentially zero and an AC amplitude of 10 mV. The frequencies were swept from 100 KHz down to a frequency where the data was not longer significant (10 to 0.1 Hz), as the time for measurements rapidly increases at very lower frequencies.

1.) Once the gel reaches a gelatin ous state, it cannot be readily mixed, but the antigens can still migrate to the antibodies through Brownian motion or move with electromotive force. However, the time to migrate was reduced by placing the functionalized electrode close to the surface of the media, so that the path, after capture and entry, was minimized, as long as the electrode remained immersed. Of course, this can be accomplished in a liquid by placing the electrode near the exposed surface of the media, but there would have to be some sort of mechanism to lower the electrode as evaporation occurs (to prevent drying out) and still maintain electrical contact with the measurement circuit.
2.) The novel hydrogel did not dry out appreciably, when exposed to air (even after months of exposure).
3.) The hydrogel is not too fluid, so it could be used in any orientation.

Therefore, the optimum properties of the hydrogel were characterized. The hydrogel held its shape and only dried out over an extended period of time (approximately 5 months).

The next portion of the experiment involved using a gel formed by mixing 75 ml of PBS and 7.6 g of collagen. The mixture was heated in a 1000 W microwave oven for 12 seconds. A platinum electrode and a bare gold electrode were used for measurements of the gel as shown in Figure 24.

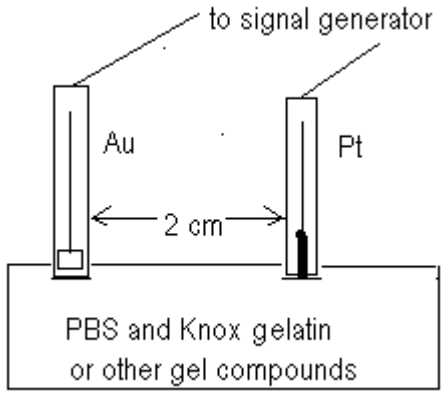

Figure 26: **EIS plots for glycerol and Collagen gel -- 2-probe.**

The purpose of this portion of the experiment was to observe the contributions of the various components of the electrode medium to the sigmoidal cyclic voltammetry and EIS spectra. The voltage in the CV was cycled from -1 to +1 vdc.

Test 1: Collagen gel

a. At an ambient temperature of 22.8 ^{o}C, 75 ml of 10 mM PBS (Phosphate-Buffered Saline) (pH 7.4) was added to 1 packet of Collagen gel (7.6 g). The solution was heated in a 1000W microwave for 20 seconds and allowed to gel in a Petri dish. A 2 probe EIS arrangement was used for measurements. The gold milliprobe and a Ag/AgCl reference electrode (PAR K0265) was positioned into the gelatin , 2 cm apart. EIS and Cyclic Voltammetry were measured.

b. To the collagen gel , the redox couple, 5 mM $K_3[FeCN)_6]/K_4[Fe(CN)_6$ (redox I and redox II) was introduced and remelted by 40 seconds in the microwave oven. EIS and Cyclic Voltammetry were measured.

c. To the Collagen gel of Test 1a, 5 ml of glycerol was added and remelted by 40 seconds in the microwave oven. EIS and Cyclic Voltammetry were measured.

d. Finally, the redox couple above (redox I and redox II) was introduced to the collagen gel /Glycerol and EIS and Cyclic Voltammetry were remeasured.

Test 2: Collagen gel and Colloidal Gold

a. A solution of collagen gel was prepared as in Test 1a above, to which 1 ml (as described above) of hydrotetrachloroaurate (colloidal gold) in dilute HCl was added, heated for 40 seconds in a 1000W microwave oven, and stirred continuously until near gelled, and allow to gel. EIS and CV were measured.

Test 3: Agarose Hydrogel plus Glycerol with Colloidal Gold

a. Test 1b was repeated, except using 0.2 g agarose instead of Collagen gel and 4 ml glycerol (the agarose did not dissolve completely, even after heating 40 seconds in a 1000W microwave oven, the agarose solution can only reach 2% to 3% saturation.) EIS and CV were measured.

b. Colloidal gold was added to Test 3a as in Test 2a. EIS and CV were measured.

Experiment A1-2: To compare successive building of the antibody sensor FDC parts, in order to determine the contribution of the electrical characteristics of the various coatings of the antibody immobilization.

The hydrogel, colloidal gold, and colloidal gold with an MPTS monolayer were applied to the electrode.

For Aim 1

a. A bare Au electrode was cleaned and measured with EIS and cyclic voltammetry in the presence of $K_3[Fe(CN)_6]$/ $K_4[Fe(CN)_6]$ as a redox probe at room temperature.

The gold electrode was polished with alumina slurries, cleaned through sonication in distilled water for at least 30 minutes, immersed in piranha solution (a 2:1 mixture of sulfuric acid (H_2SO4) with hydrogen peroxide (H_2O_2)) for 5 minutes, and rinsed with absolute ethanol. All electrochemical measurements were conducted in the presence of ($K_4Fe(CN)_6$•3H2O), $K_3[Fe(CN)_6]$/$K_4[Fe(CN)_6]$ (1:1, 5 mM) (salts potassium ferricyanide/ferrocyanide) (aka potassium hexacyanoferrate(III)/hexacyanoferrate(II) ion) (aka Prussian red /yellow prussiate of potash) in 20mM PBS (containing 0.1M KCl, pH 7.4) as a redox probe for electron transfer. Impedance measurements were performed sweeping the frequency range from 100,000 Hz to 0.1 Hz., with 10 steps per logarithmic decade, and an amplitude of 5 ma.

b. The electrode was coated with MPTS (3-mercaptopropyl)-trimethoxysilane in ethanol at concentration 10^{-4} mol/L for formation of a SAM as illustrated in Figure 13, by immersing in the MPTS sol-gel for 8 h at 22^{O}C room temperature, and then rinsed with water and absolute ethanol for 0.5 h to remove the physically adsorbed molecules.

The MPTS modified electrode was placed in the FTIR to verify the presence of the SEM by analyzing the surface compounds [14]. The Au nanoparticles can attach antibodies to them without having them lose their bioactive properties. Silica sol for the self-assembly was prepared by dissolving MPTS, methanol, and 0.15M HCl in the molar ratio 1:3:3. After stirring for 0.5 hr., 5 ml of methanol was added.

c. The molecular components of the SAM were determined with the FTIR.

d. The SAM was measured with EIS and cyclic voltammetry.

e. The solution was titrated with DTNB (5,5'-Dithio-*bis*-(2-nitrobenzoic acid), (Ellman's reagent -molecular weight: 396.35) and the results were assessed. This indicated the number of thiols at the surface of the SAM.

A preparation was used of 50 ml Ellman's reagent (5, 5'-dithiobis-(2-nitrobenzoic acid) or DTNB) (a chemical used for measuring the amount of thiol groups) and 2.5 ml of a reaction buffer of 0.1 M sodium phosphate, pH 8.0, containing 1 mM EDTA (Ethylenediaminetetraacetic acid) a crystalline acid chelator which binds to, and makes unavailable, metal ions in a solution, and forms a sodium salt [44].

f. Area and density were calculated.

g. The time of exposure was increased to MPTS by one hour.

h. The sequence from step c was repeated until the density did not increase from previous iteration.

The MPTS sol-gel SAM was attached to the Au electrode as previously described. At the end of the incubation period, non-specifically bound chains were flushed out with distilled water. A colloid gold solution of nanoparticles was prepared and administered as described previously [14].

Using the electrode of Aim 1, at the saturation point, more layers were assembled with MPTS and measured with DTNB and EIS. The colloidal gold nanoparticles served as subsequent targets of a new SAM extension layer of MPTS. The quantity of free mercapto groups remained relatively constant as the monolayer chains were each being extended, since they were on the end of the chains.

a. The electrode was saturated as in Aim 1.

b. Colloidal gold nanoparticles were introduced to the ends of the self-assembled monolayers of MPTS.

c. The electrode was exposed to another MPTS self-assembled layer as above.

d. The coated electrode was measured with DTNB and EIS.

c. Go to step b.

Many factors affect the antibody/antigen conjugate formation. These include concentration, pH, temperature, electrical potential, non-specific blockage, etc. By keeping as many of these constant and controlled as possible, the concentration can be made the measured dominant factor.

Experiment A1-3: Effects of diffusion time on gel covered gold disk electrode characteristics

An electrode made of stainless steel mesh was placed on the top surface of the previously described GHA hydrogel mixture. An MPTS/IgGab coated gold electrode was positioned 2 cm below the top electrode under a layer of hydrogel. The specific antigen was introduced on the top of the stainless steel mesh electrode. EIS measurements were made between the electrodes for 30 minutes as the antigen diffused through the hydrogel toward the bottom gold electrode and became positively detectable.

For Aim 1, a plastic eyedropper was cut off at the top and bottom as a container for the gel based sensor. An electrode made of stainless steel mesh was placed on the top surface of the previously described hydrogel mixture. This was a mesoporous/ macroporous hydrogel. In this instance, agarose 2% mixed with glycerol (the mixture referred to as GHA) was used.

An MPTS/IgGab coated, EG&G Princeton M0227 milli-probe with a 2 mm in diameter gold pellet on the end, was positioned 2 cm below the top electrode under a layer of gel (see Figure 25). The specific antigen was introduced on the top, near the stainless steel mesh electrode. EIS measurements were made between the electrodes for 30 minutes as the antigen diffused through the hydrogel toward the bottom gold electrode and became positively detectable.

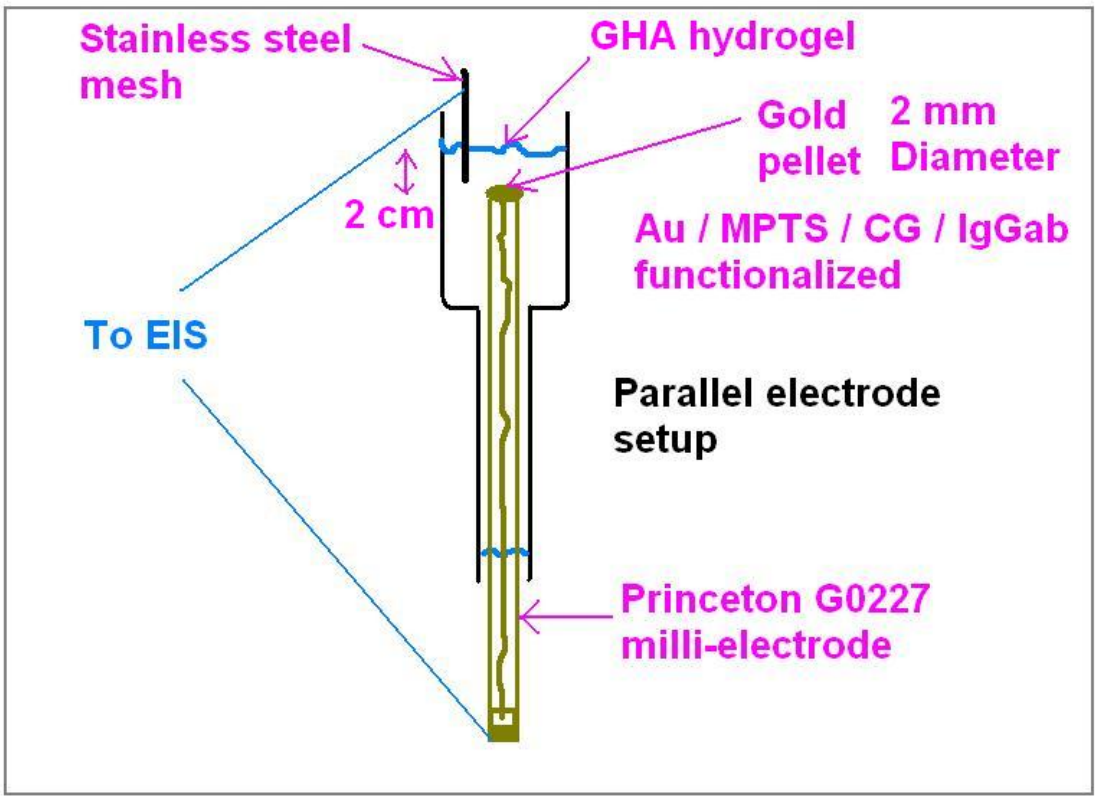

Figure 27: **Experimental setup for testing the parallel mode electrode.**

In this procedure, GHA gel was used to isolate the MPTS/antibody solution from air, and still allow antigens to pass through by diffusion and attach as in Figure 26.

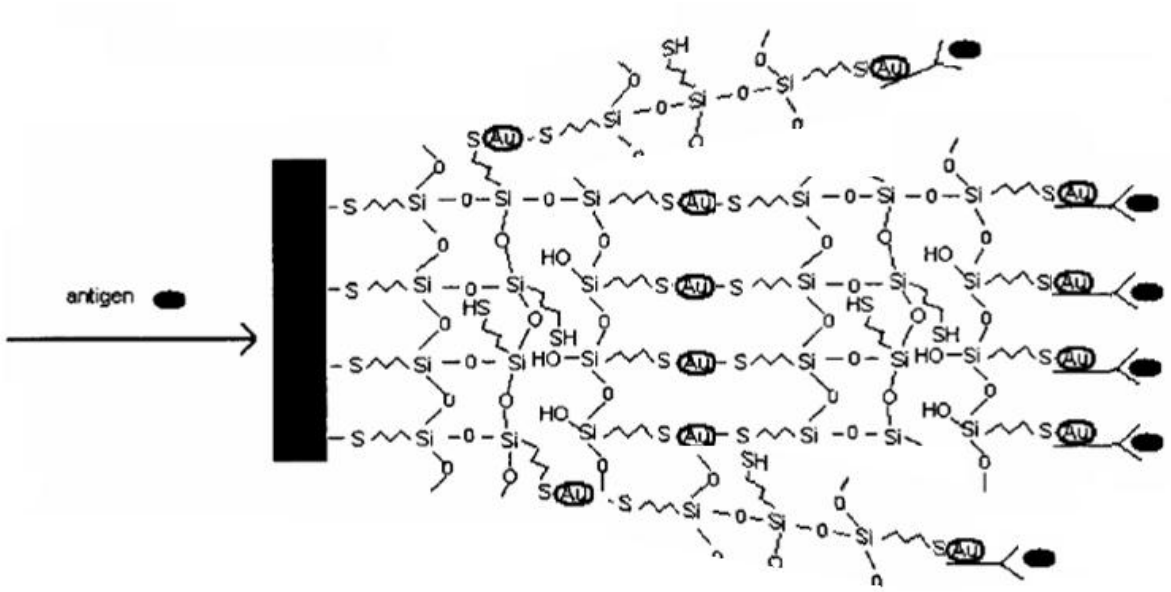

Figure 28: **Antigens for conjugates on the specific antibodies.**

Experimental Strategy for Aim 2

The research of this dissertation requires the integration of a number of areas of science as explained in Chapter 2. In order to prove the validity of the results, a step-by-step sequence of experiments was identified and implemented. The results build upon each other and also demonstrate the contributions of each component of the final bioimmunosensor. As illustrated in Figure 18, the step-by-step experiments of Chapter 3 resulted in the development of the uniquely formulated hydrogel medium for the functionalized parallel gold substrate electrode [51]. When the novel hydrogel (GHA) identified and developed, it could be utilized is Aim 2 to develop a novel

bioimmunosensor (Figure 27). In this chapter, that knowledge was extended upon, and Aim 2 utilized same unique hydrogel by use with a new, novel type of electrode - the linear/serial electrode. Experiments were designed and performed to measure each individual component's contribution to the overall measurement, including significant combinational contributions. Experimental results were used from the literature if there was a similar experiment previously documented.

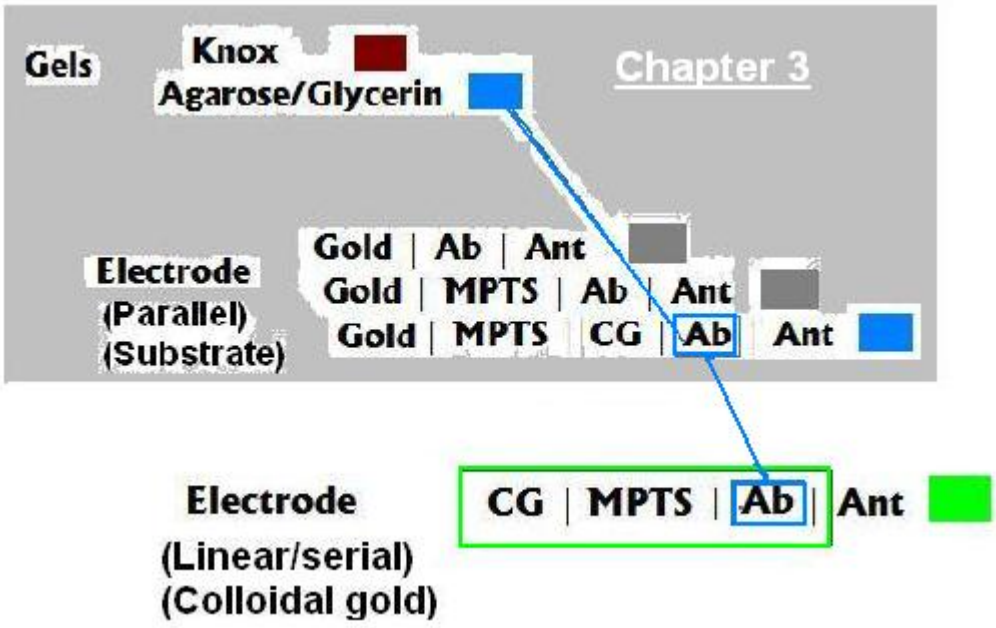

Figure 29: **Progression of experiments leading to the novel Linear/serial Electrode**

Aim 2 Experiment Equipment

The equipment used for EIS and CV measurements was the same as used in Chapter 3. All glassware in all experiments was cleaned with 50% strength HNO_3 (diluted with water) for at least 12 hours, rinsed thoroughly with distilled water, and dried prior to use.

Aim 2 Materials and Methods

In the first step of the linear/serial embodiment, colloidal gold nanoparticles were formed to provide a base of attachment and also act, in place of a redox couple, to conduct ionic current.

The linear/serial embodiment of the FDC was constructed with four steps:

1. Colloidal gold nanoparticles are formed as the bases.
2. A self-assembled monolayer (SAM) of MPTS surrounds and covalently attaches to the gold nanoparticles.
3. Antibodies (as capture molecules) are covalently attached to the ends of the SAM[20].
4. The FDC is then implemented along a confining apparatus, in a hydrogel, as described in Chapter 3.

Preparation protocol of Colloidal Gold Nanoparticle Suspension

The desired colloidal gold nanoparticle size is approximately 20-40nm. The preparation of the capture molecules, colloidal gold with 20 nm diameter gold nanoparticles [51], was performed as in Chapter 3.

Preparation protocol of MPTS Coated Colloidal Gold Nanoparticle Suspension

The preparation protocol of the MPTS covered colloidal gold was as follows:

1.) In a separate container, mix 20ml of the sol-gel MPTS, absolute ethanol, and aqueous acid (0.1M HCl) at a molar ratio of 1:4:3.5 and sonicate for 1 hour until it is a homogenous solution.

2.) Mix 10ml of the solution (suspension) of colloidal 20 nm gold nanoparticles, above, with 20ml of the solution from Step 1 of this protocol, at room temperature, stirring gently for 10 seconds, and then set in darkness for 12 hours. (Do not sonicate or disturb.) This will attach the self-assembling monolayer (SAM) to the gold nanoparticles. Each colloidal gold nanoparticle is covered with a covalently attached, self-assembled monolayer of solgel MPTS, as one might imagine toothbrush bristles on a basketball.

Preparation of Colloidal gold/MPTS/Antibody (CMA)

3.) Add 10ml of the antibody (IgGab 0.54 mg/ml) and gently rock for 4 hours.

5.) The results of Step 3 will be added to the confining entity after construction of the bioimmunosensor.

The optical properties (reflection, diffusion, scattering, etc) of colloidal gold cause a suspension of such to appear to be different colors depending upon the size of the gold nanoparticles. The color of our colloidal gold was consistent with the color of a suspension of 20 nm diameter gold nanoparticles (Figure 28).

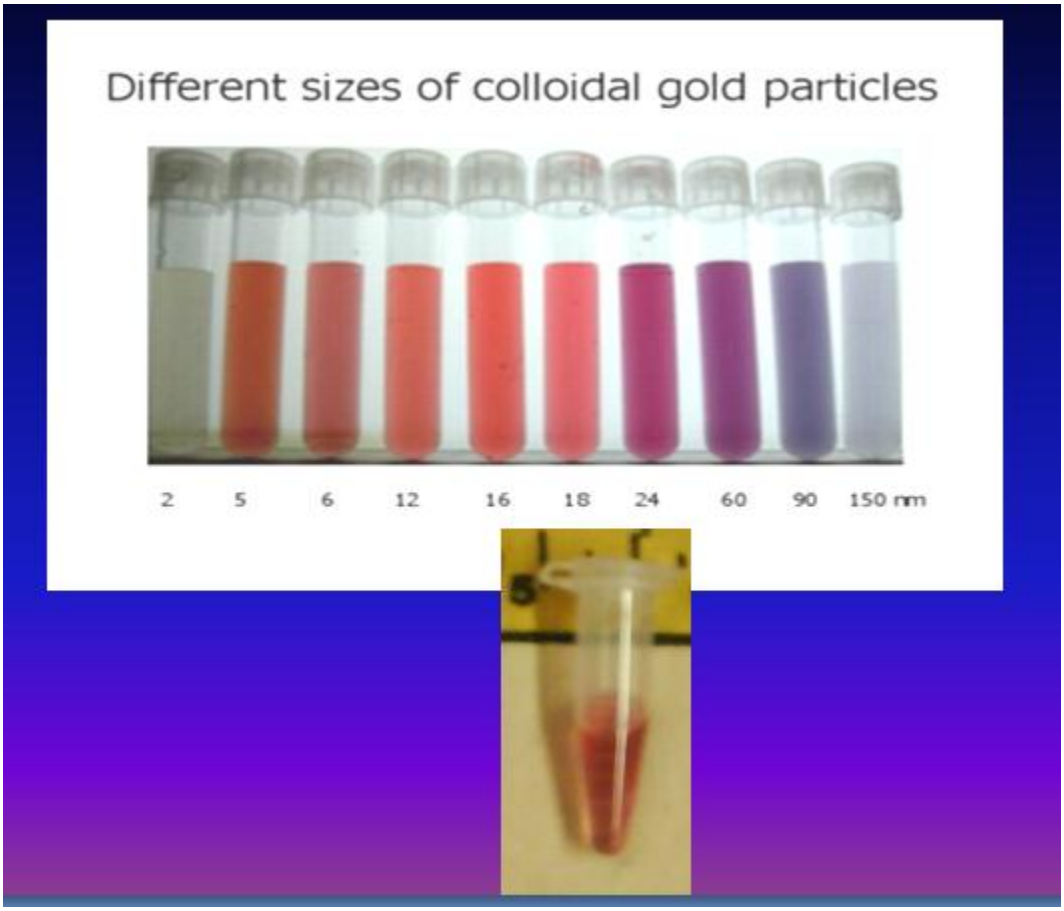

Figure 30: (Above) Colloidal Gold color vs. sizes (Source: nanoopticalmaterials.com) (Below) Colloidal Gold produced by preparation protocol [51]

Experiment A2-1: Verification of the conformation of our FDC's on gold leaf for imaging with an AFM (Atomic Force Microscope)

An AFM (Atomic Force Microscope) (Veeco Instruments Innova AFM, bought by Bruker AXS) (Figure 29) scan indicated the small conformation of the colloidal gold particles which had been coated with an MPTS self-assembling monolayer. They were placed upon a gold substrate and allowed to dry, forming a strong bond: nanoparticle gold—MPTS—gold substrate.

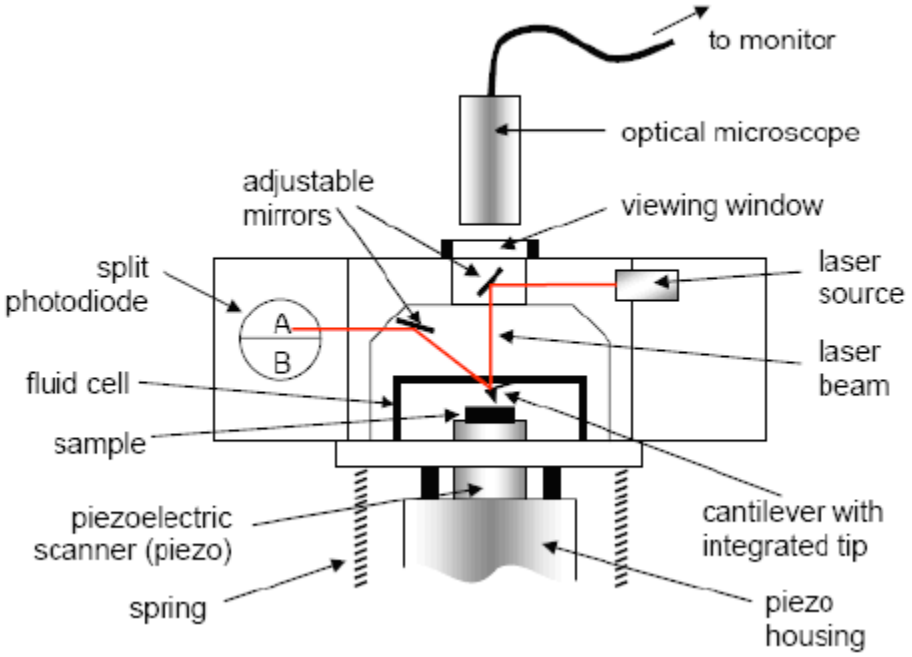

Figure 31: **Schematic diagram of the main features of a Veeco Instruments multimode Atomic Force Microscope.**

The force acting on the tip for the Atomic Force Microscope was kept constant by adjusting the z-position of the piezo scanner. This operation was called the constant force AFM mode. It gave a topographic image. The topographical data reflected the corrugation height of the sample surface, corresponding to the change in the movement of the Z piezoelectric scanner in the constant force mode, while the lateral force was the derivative of the cantilever torsion as the tip scanned obliquely, corresponding to the friction characteristics of the surface. A laser beam reflected off the tip and a photcell then measured the deflection of the tip. Feedback that was supplied to the piezoelectric scanner that kept the force (cantilever deflection) constant. The AFM was used to scan colloidal gold coated with MPTS sol-gel as represented by the center objects in Figure 30.

By applying AC-voltage to the piezo scanner attached to the other end of the cantilever, the AFM could be operated in the tapping mode.

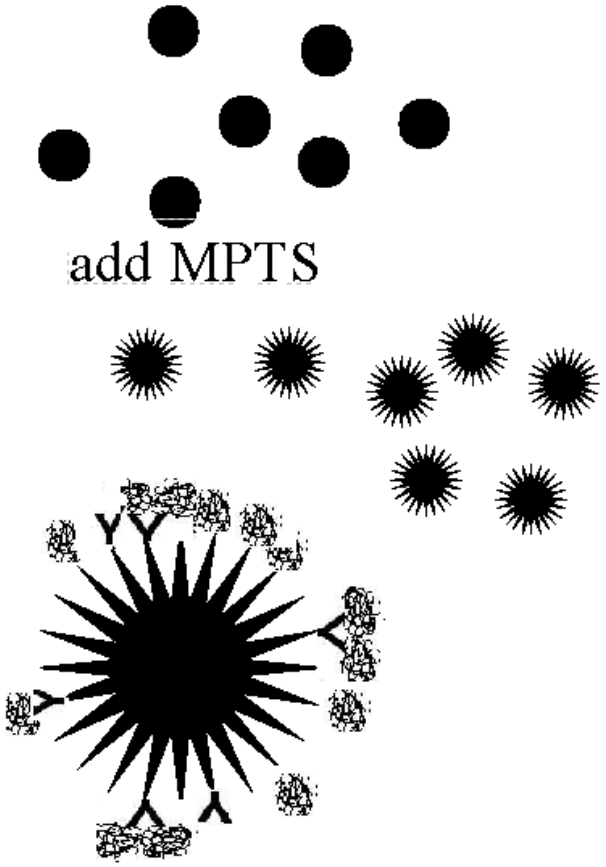

Figure 32: Conceptual colloidal gold coated with MPTS sol-gel and antibody/antigens. (not to scale)

Experiment A2-2: To compare conductivity of gel, colloidal gold, and colloidal gold with an MPTS monolayer

A solution (suspension) of colloidal gold and colloidal gold with an MPTS monolayer was tested electrically, as well as the gel alone, for a baseline or control.

Experiment A2-3: To determine the charge and mobility of the colloidal gold nanoparticles, with, and without a MPTS monolayer coating

An electrophoresis of the colloidal gold was performed. This determined the charge (e.g. if the nanoparticle moved toward, away, or neither (did not move) relative to the positive and negative electrodes of the electrophoresis chamber) and mobility of the nanoparticles as their speed of travel is observed.

Electrophoresis was performed as follows:

> A gel was prepared mixing 0.3 g of agarose (type VI hi temp Sigma A3893) with 20 ml of TBE x1 buffer. After thorough mixing the solution was heated for 30 seconds in a 1000W microwave oven, then poured into the EPU chamber. Lane 1 was loaded with colloidal gold (20nm diameter). Lane 2 was loaded with the same colloidal gold coated with MPTS. (see Figure 31)

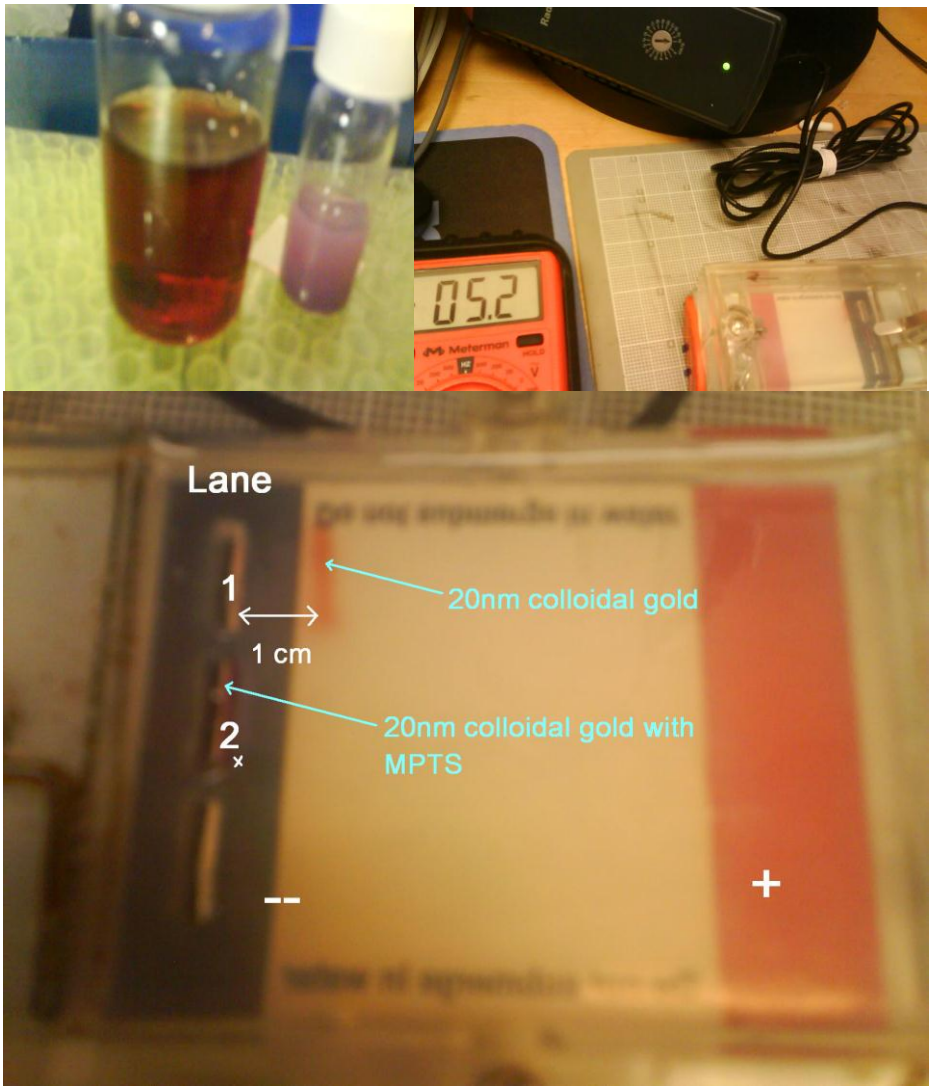

Figure 33: **Electrophoresis: Top left – Colloidal gold in larger bottle, CG with MPTS in smaller, Top right-experiment setup, Bottom-Lane 1 (upper) CG, Lane 2 (middle) CG/MPTS**

MATLAB and the software language *R* were utilized in the computation of statistics. Microsoft EXCEL was utilized in the preparation of the graphs, along with the EIS software CORRWARE.

Results of Aim 1 Experiments

Experiment A1-1: Comparison of gels needed to keep antibodies active

Test 1: Collagen gel

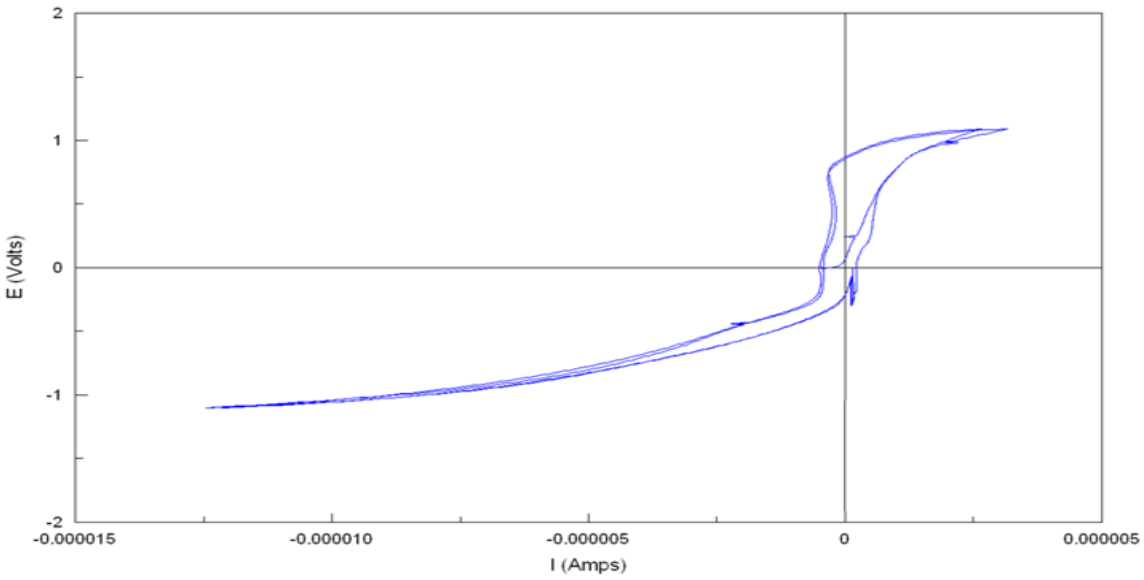

Figure 34: Cyclic voltammetry plot for Collagen gel in PBS

Cyclic voltammetry revealed a negligible amount of polarization in Figure 32.

Figures 33 & 34 show the Nyquist, Bode, and CV plots for collagen gel. The 45^{o} Nyquist plot trace indicates that the collagen gel was fairly conductive. This would not be the best choice for the medium for the research as it would tend to "short out" or overwhelm the capacitance change measurements of interest.

Figures 35 - 37 show similar results for addition of PBS and glycerol to the gels. Figure 38 indicates that the addition of a redox couple (trace *c*) was not necessary for obtaining EIS results, and therefore, because the redox couple could affect the conjugation process, it was eliminated from the system.

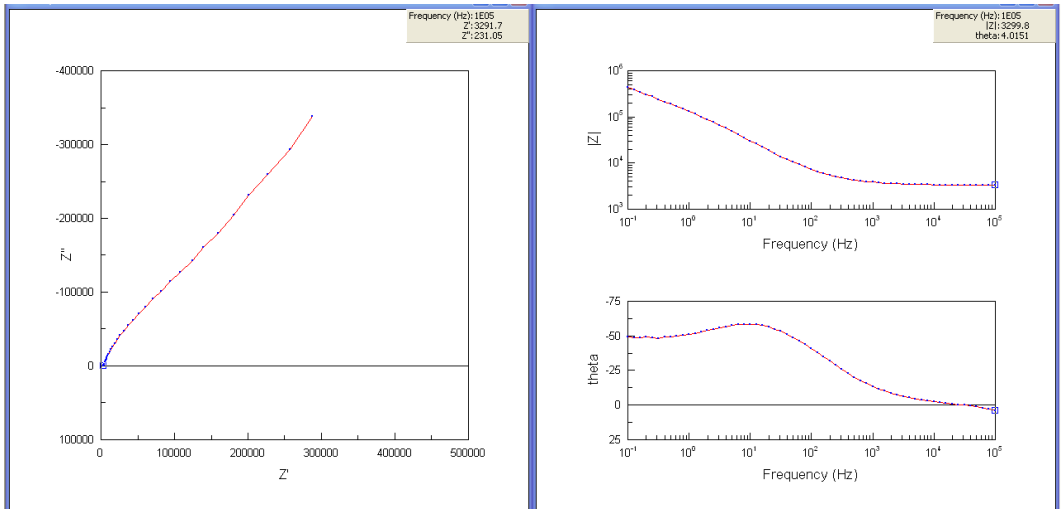

Figure 35: EIS plots for collagen gel in PBS

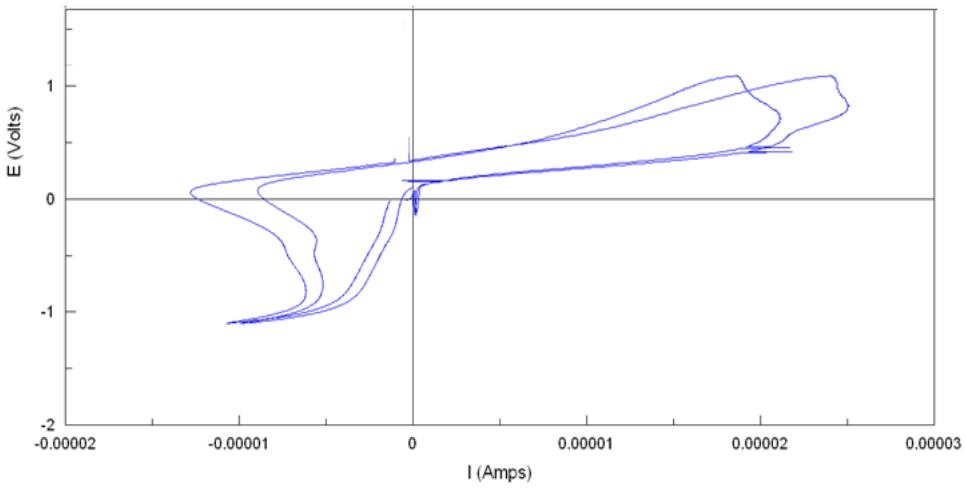

Figure 36: Cyclic voltammetry plot for PBS/Collagen and redox probe

The cyclic voltammetry sweeps of the PBS/Collagen and redox probe differ slightly because the oxidation and reduction reactions of the PBS/Collagen at the electrode surface did reverse completely [52]. The microcell used for this experiment did not allow for mixing of the contents, which would produce nearly identical sweeps.

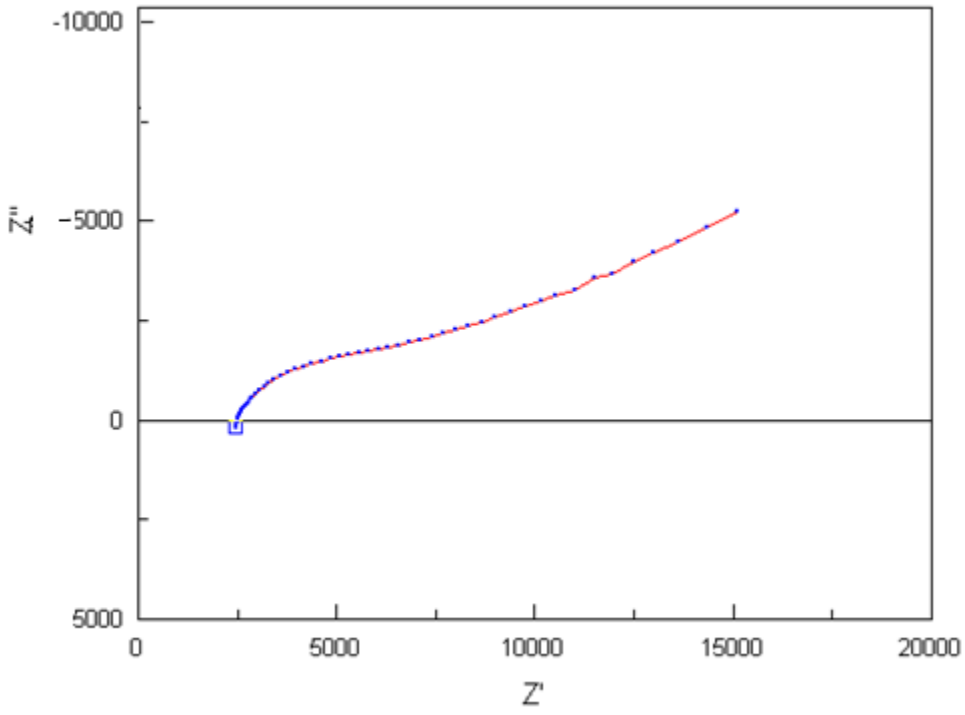

Figure 37: EIS plot for PBS/Collagen gel with a redox probe couple

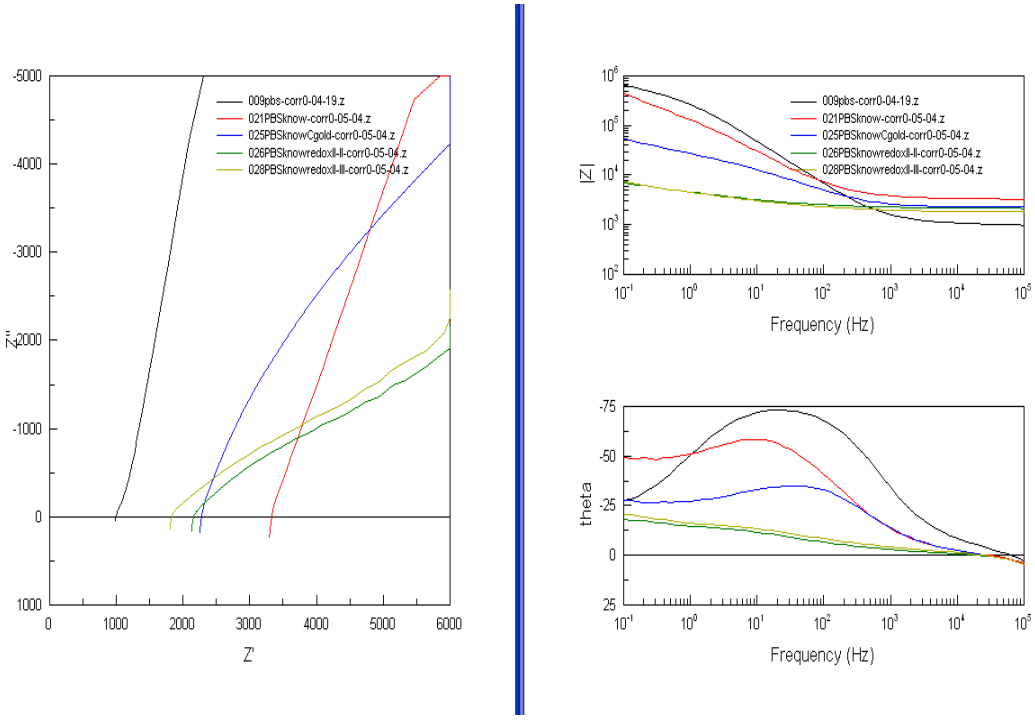

Figure 38: **EIS plots for glycerol and Collagen gel-- 2-probe.**

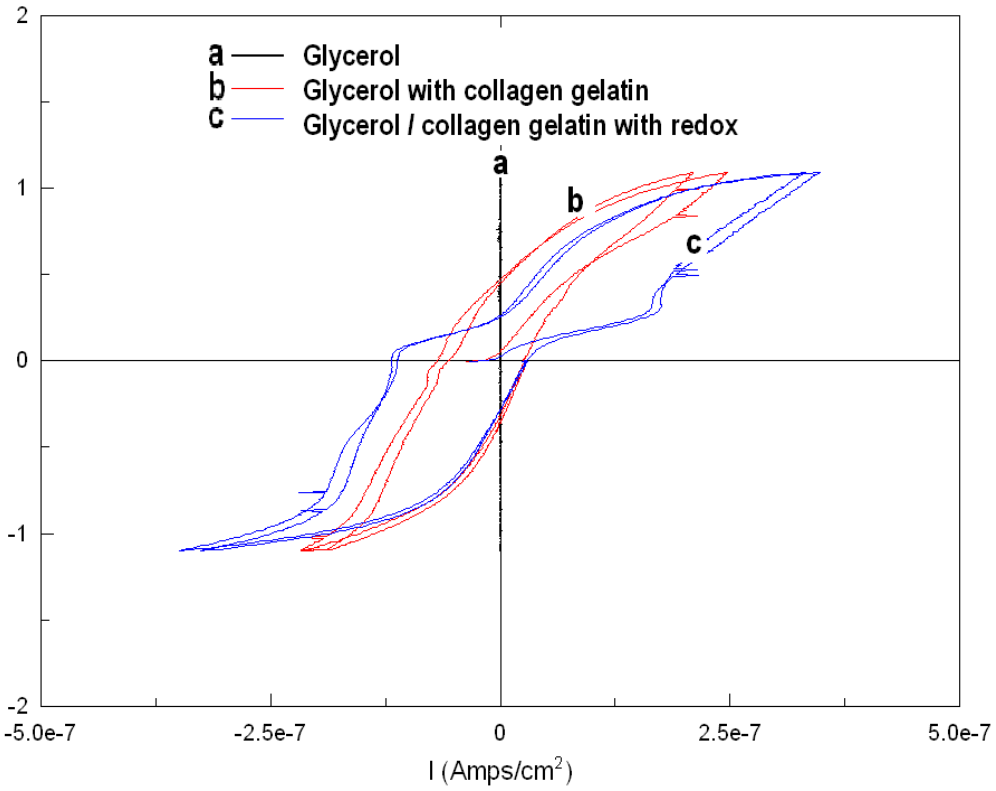

Figure 39: Cyclic voltammetry plot for a-Glycerol (vertical line through 0,0), b-Collagen gel, c-with redox I and redox II

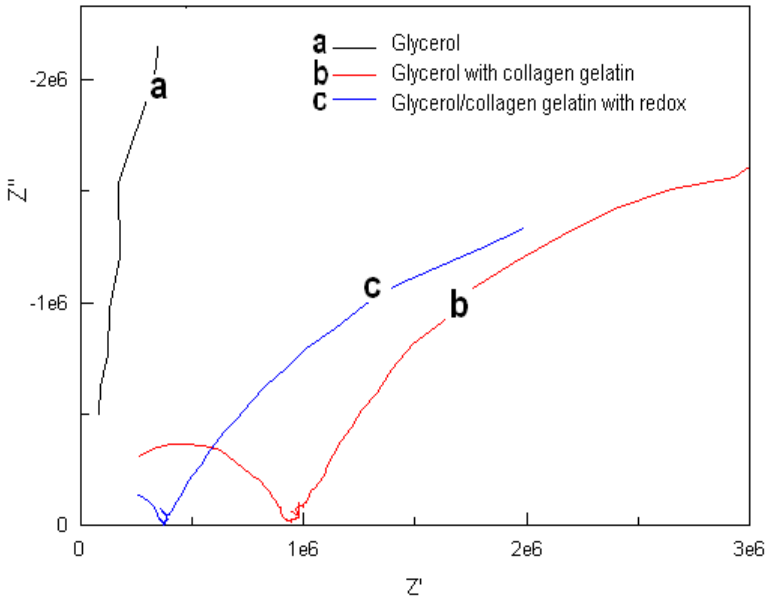

Figure 40: EIS plot for a-Glycerol, b-w/collagen gel, and c- w/collagen gel with redox I and redox II

Test 2: Collagen gel and Colloidal Gold

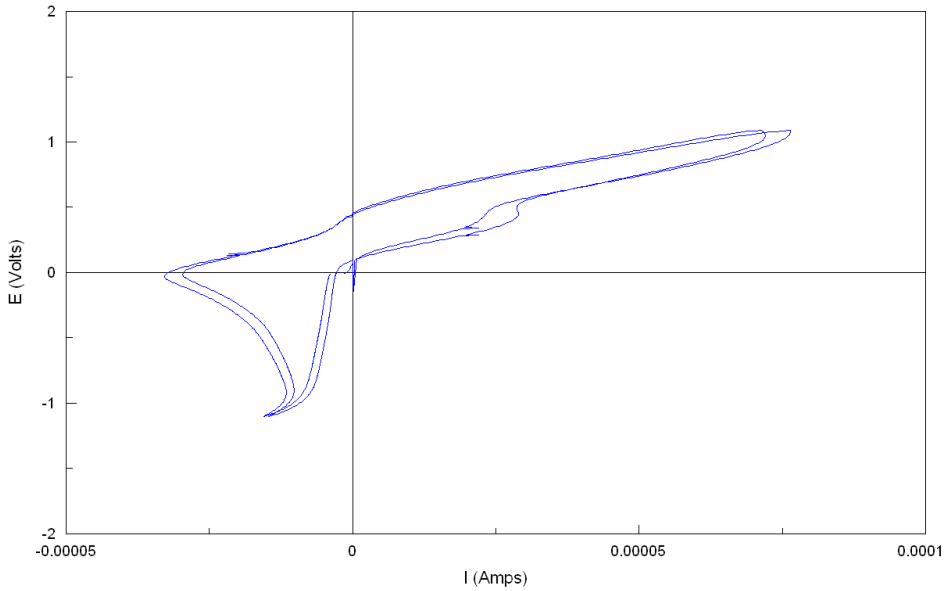

Figure 41: CV plot for PBS/ collagen gel, and colloidal gold

PBS was substituted for distilled water in the collagen gel to see if there was a beneficial effect for the gelatin electrical characteristics. As can be seen in Figures 39 & 40, the substitution did not make a significant difference.

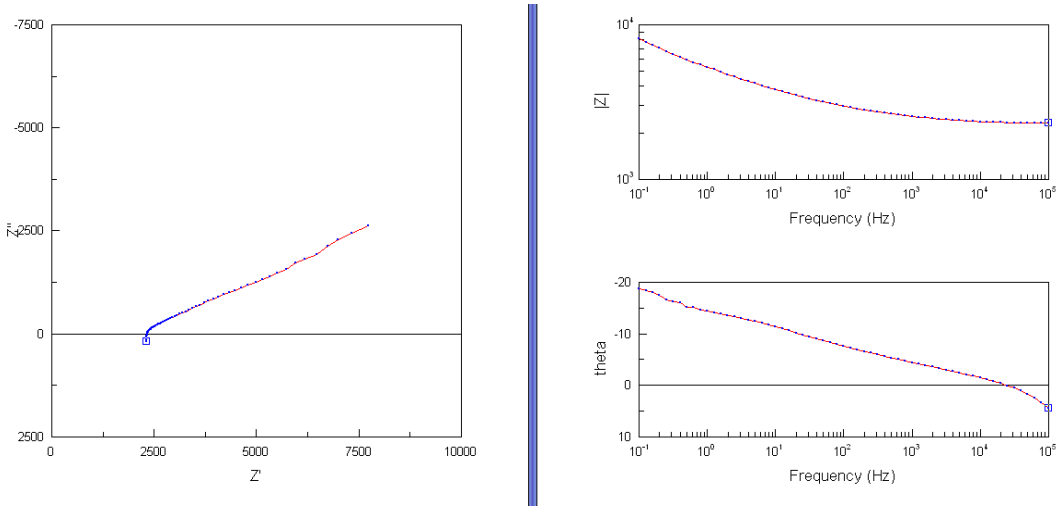

Figure 42: EIS plots for PBS/ collagen gel, and colloidal gold

Test 3: Agarose Hydrogel plus Glycerol with Colloidal Gold

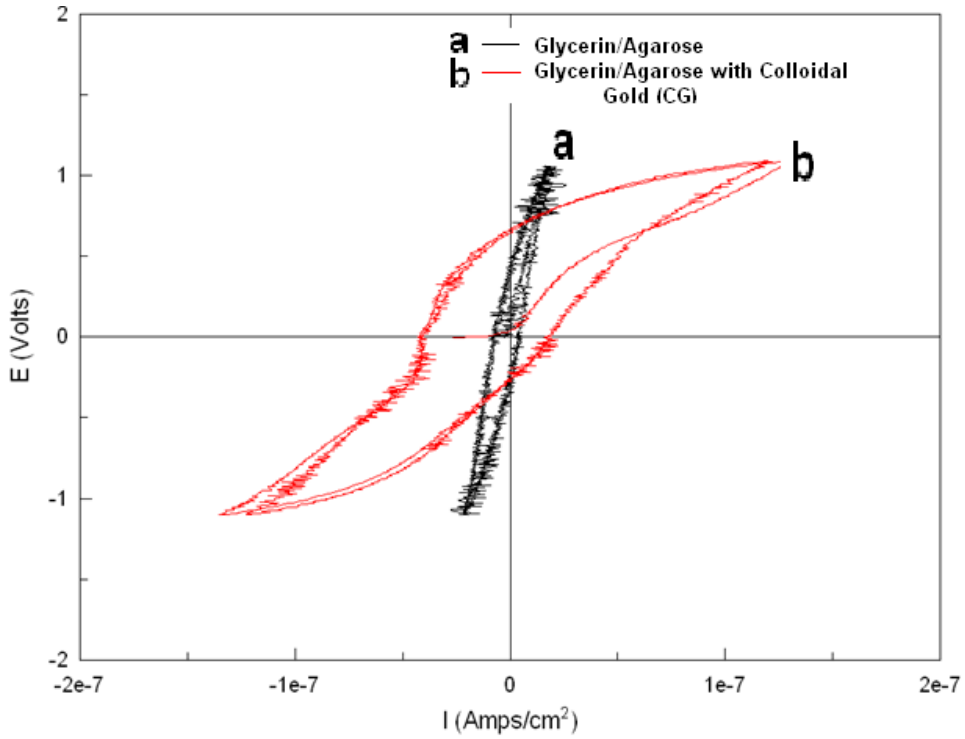

Figure 43: CV plot for Agarose/Glycerol, and colloidal gold

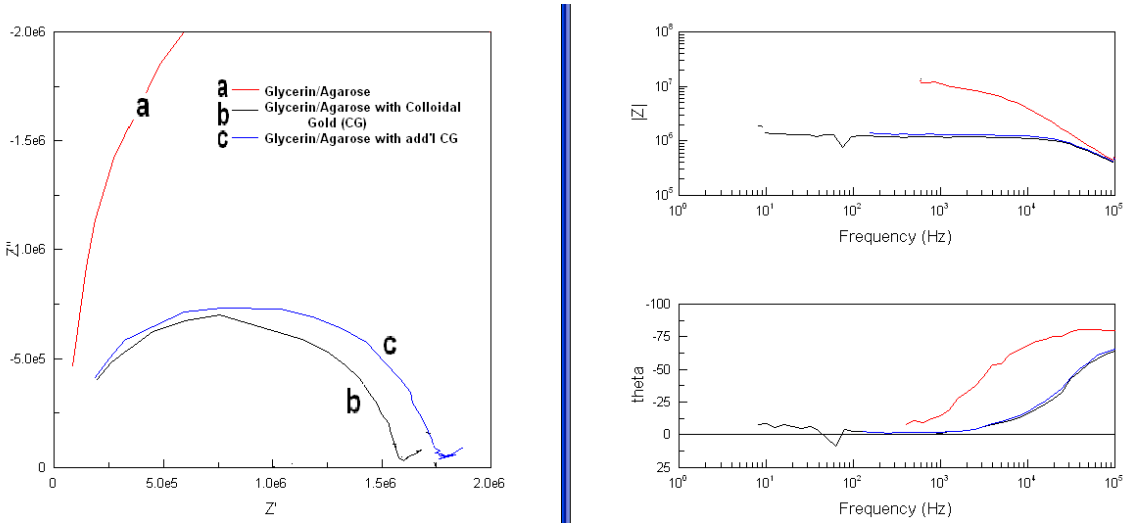

Figure 44: EIS plots for Glycerol/Agarose, and colloidal gold

Figures 41 & 42 show that the Glycerol/Agarose with colloidal gold produced the best results without a redox couple necessary because the Z" zero intercept was easily discernible.

Experiment A1-2: To compare successive building of the antibody sensor FDC parts, in order to determine the contribution of the electrical characteristics of the various coatings of the antibody immobilization.

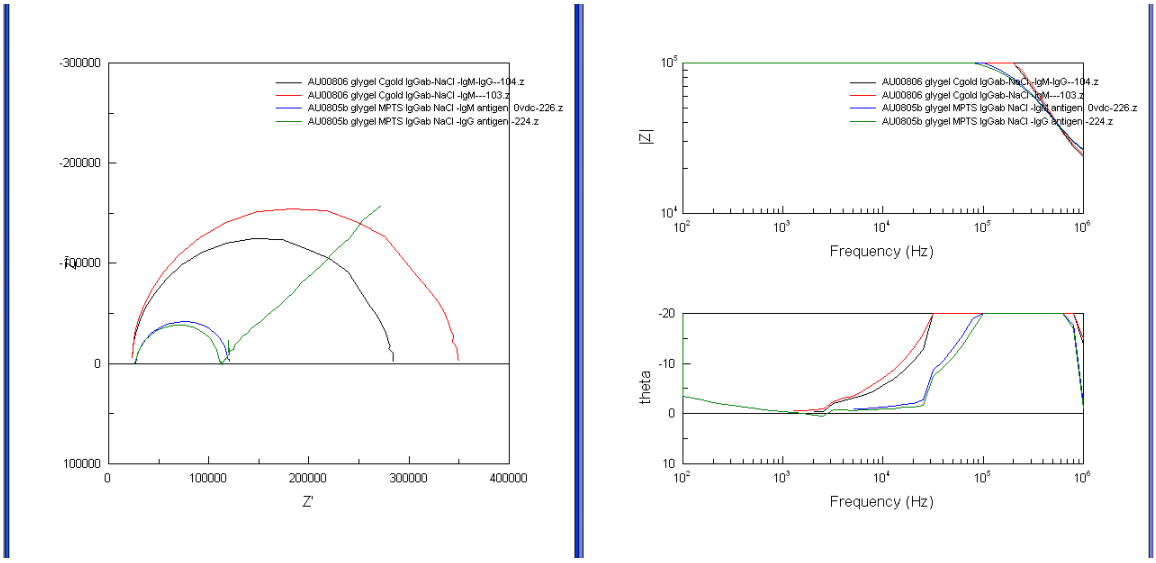

Figure 45 EIS colloidal gold coated (with/without MPTS) / IgGab antibody / IgG antigen and IgGab/IgM non-specific antigen

Figures 43 & 44 show how successive layers of the biosensor affect the EIS readings and how antigens lowered impedance in initial experiments with specific antigens having the greatest changes.

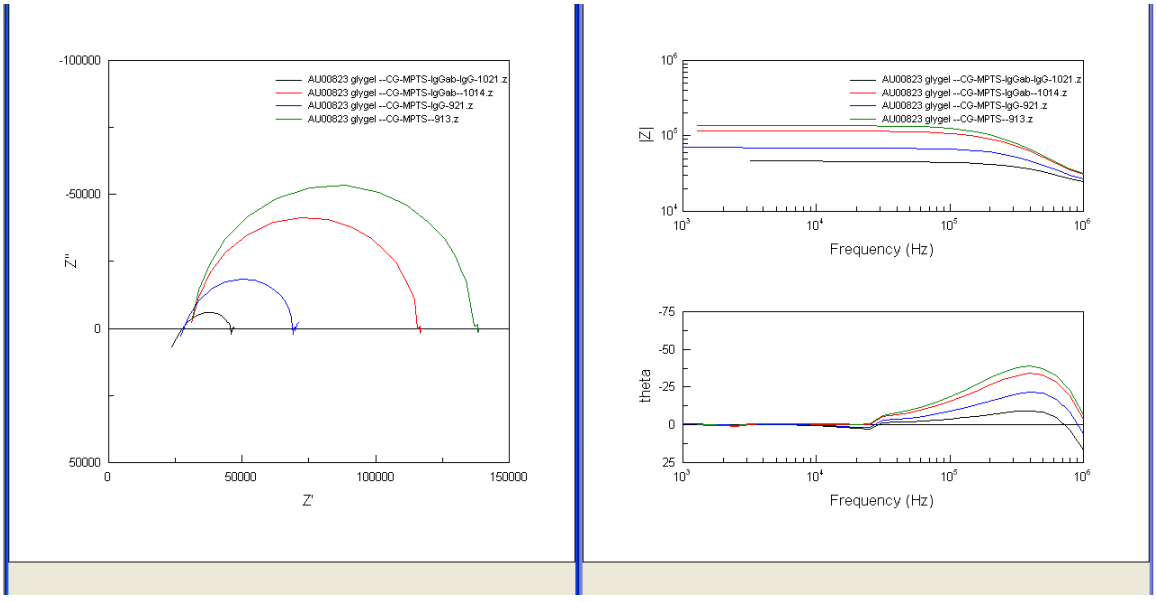

Figure 46 Colloidal gold coated with MPTS / IgGab antibody / IgG antigen

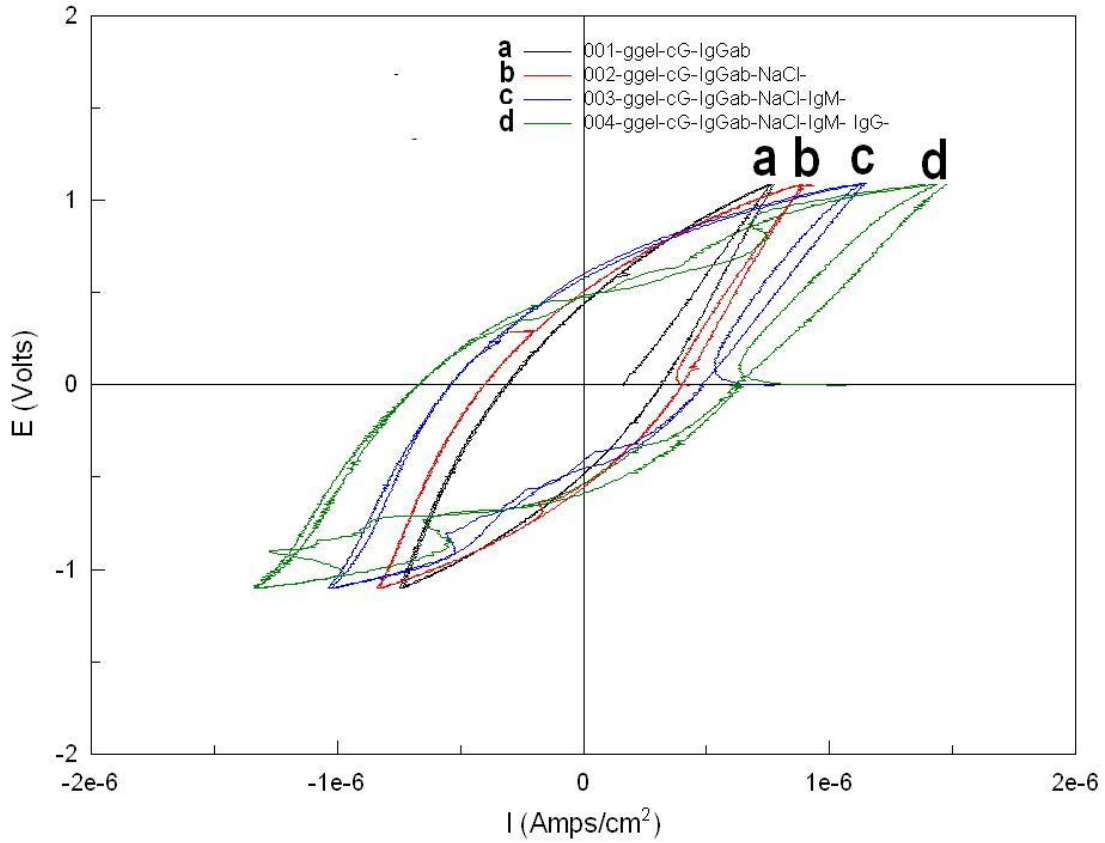

Figure 47: **Cyclic Voltammetry plots of progressive layer of functionalization of an electrode.**

The cyclic voltammetry measurements showed a progressive effect of the addition of layers to the electrode as hydrogel, colloidal gold, and colloidal gold with an MPTS monolayer, and antigen, were applied.

The previously described results shown, verified that a MPTS self-assembled monolayer could be applied to the gold electrode and quantified by FTIR and visible spectrophotomer. In a further test, the preparation of DTNB was scanned with a visible light spectrophotometer to provide a baseline or blank. The MPTS-coated Au foil then was put into the solution of DTNB. Ellman's Reagent is useful as a sulfhydryl assay reagent because of its specificity for -SH groups at neutral pH and short reaction time.

At various intervals, the DTNB solution was rescanned on the spectrophotometer (see Figures 46 & 47).

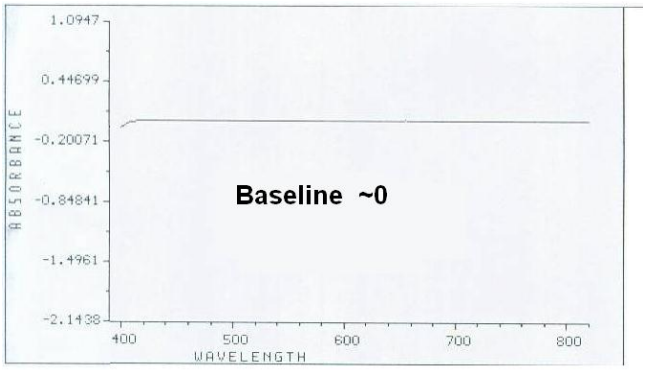

Figure 48: Spectrophotometer baseline or blank reading.

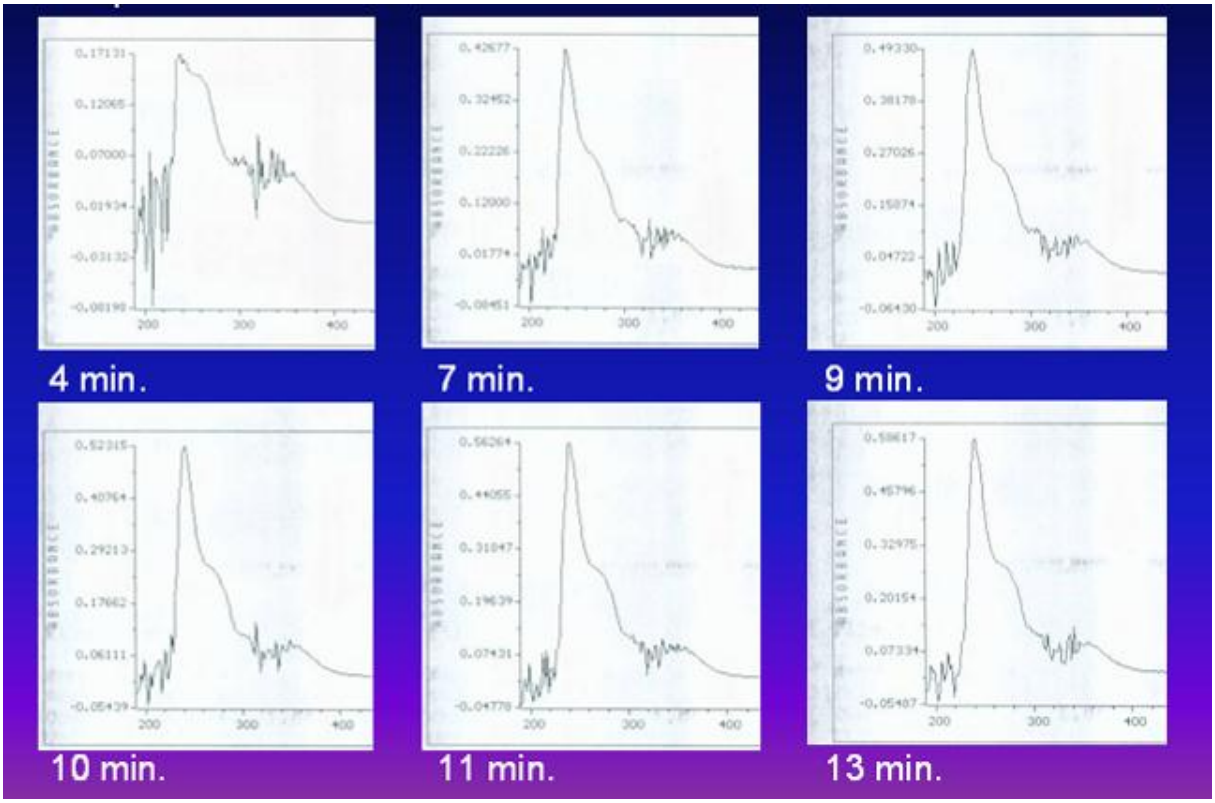

Figure 49: **The preparation of DTNB was scanned with a visible light spectrophotometer to provide a baseline or blank. At various intervals, the DTNB solution was rescanned on the spectrophotometer.**

The MPTS/DTNB coated Au foil was also scanned with the FTIR with the results shown in Figure 48. The important information to observe in the plots are traces b & d. Trace b shows the FTIR spectrum for the coating applied to the gold electrode after the MPTS exposure. Trace d is a standard trace of MPTS. The similarity of the spectrums show that the coating applied to the gold electrode is consistent with MPTS.

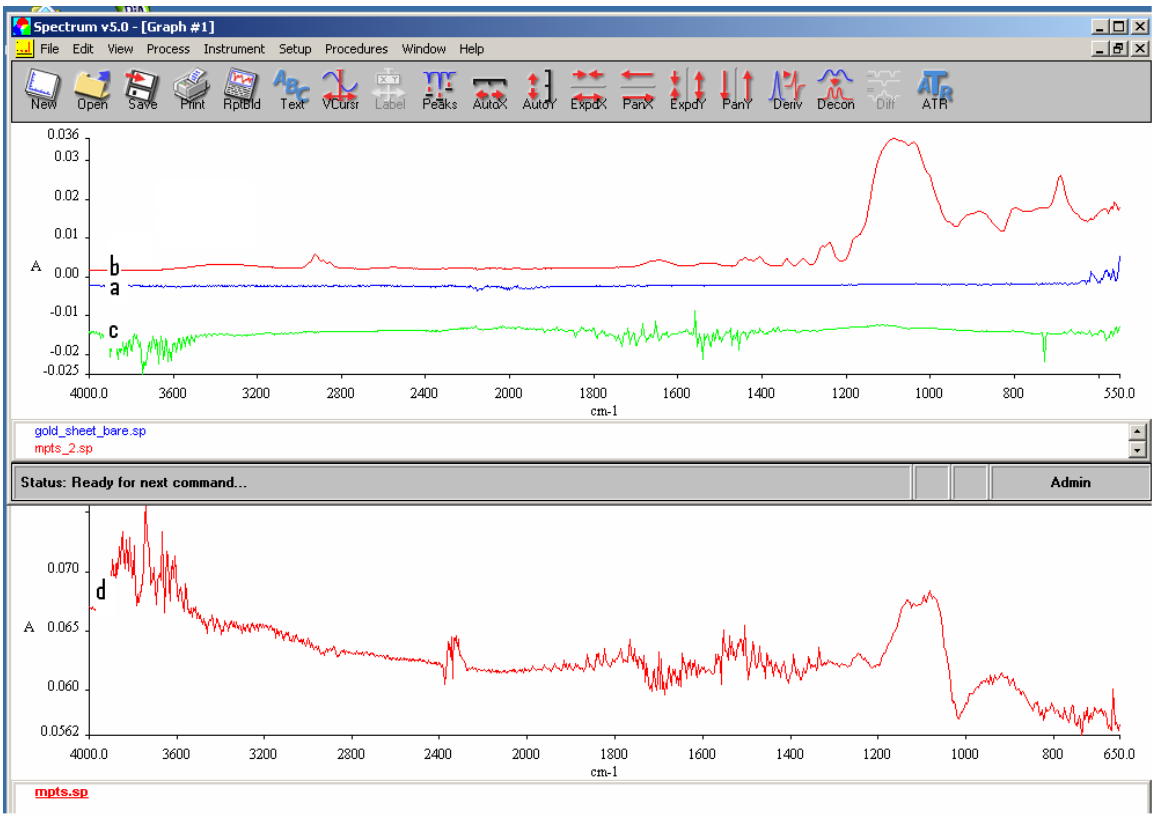

Figure 50: **Plot a shows the bare Au electrode, b after MPTS coating, c following DTNB testing, which is consistent with d representing the standard MPTS IR spectrum.**

Experiment A1-3: To determine the charge and mobility of the colloidal gold nanoparticles, with, and without a MPTS monolayer coating

The colloidal gold shows that it had a slight negative charge since it moved toward the positive electrode in the electrophoresis chamber at a rate of 2cm/hr. When

the particles were coated with MPTS, they did not move, showing that the molecules then had a neutral charge. The MPTS did make the particles slightly larger, but not enough to stop movement through the hydrogel completely.

Discussion

A forced air delivery system could have been employed, but was not in this experiment; gravity and an eyedropper were utilized. In this experiment, we were looking for a binary yes/no result. The representative shape and differential magnitude of the EIS plots eliminate false positives.

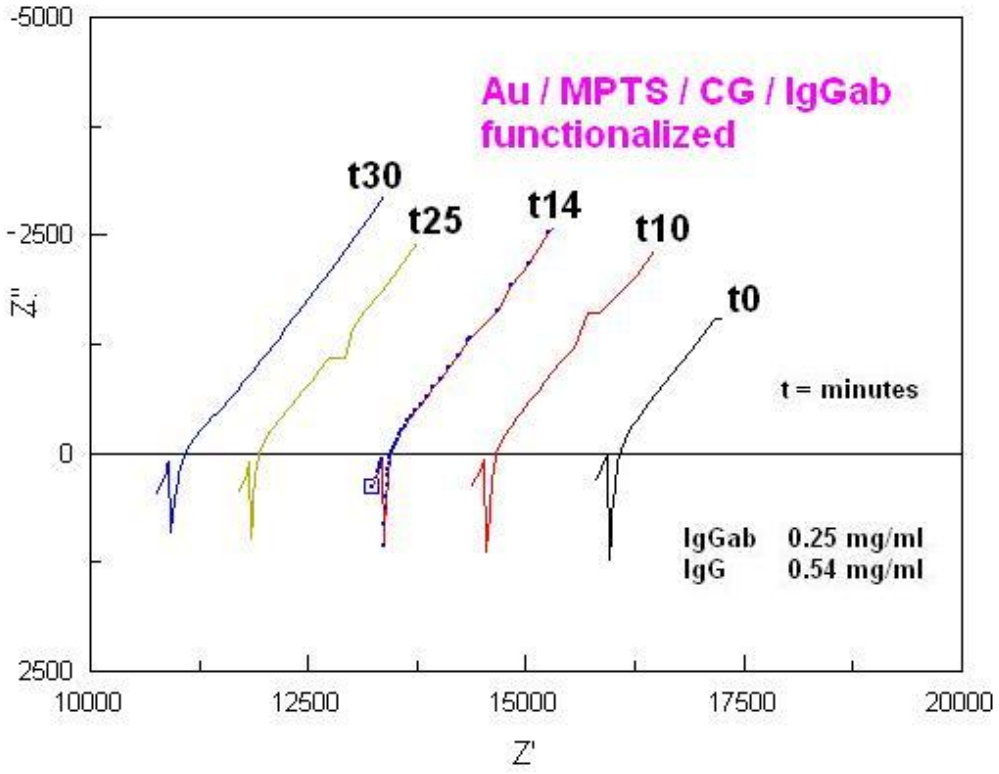

Figure 51: EIS plots for parallel electrode antigen migration through GHA over time

The decrease in Z' over time showed that antibody/antigen conjugation was being detected. The successful results of Aim 1 have proven that my novel GHA hydrogel was a viable medium for the basis of an immunosensor which could be exposed to air in any orientation and capture antigens which can be detected with a specific antibody functionalized electrode. The diffusion rate, added to the conjugate reaction time, took over 30 minutes, so another development would be necessary to obtain more rapid indication of specific antigens being present. This was the goal of Aim 2.

CHAPTER 4

AIM 2: TO DEVELOP A NOVEL LABEL-FREE IMMUNOSENSOR FOR SPECIFIC AIRBORNE ANTIGEN DETECTION … IN A NON-LIQUID MODIFIED HYDROGEL ENVIRONMENT WITH A LINEAR/SERIAL CONFIGURATION

AIM 2: TO DEVELOP A NOVEL LABEL-FREE IMMUNOSENSOR FOR SPECIFIC AIRBORNE ANTIGEN DETECTION USING IMMOBILIZED ANTIBODIES ON A SOL-GEL SELF-ASSEMBLED MONOLAYER ON GOLD NANOPARTICLES IN A NON-LIQUID MODIFIED HYDROGEL ENVIRONMENT WITH A LINEAR/SERIAL CONFIGURATION

Introduction

The main challenge of the sensor measurements in Aim 1 was the length of time of measurements. That time is composed of two parts. One part is the latency time and the other is the biological reaction time. The latter is quite short (fractions of a second), but the latency for the antigens to physically meet with their specific antibodies, is too long in many applications (30 minutes or more.) Therefore, a more efficient electrode configuration needed to be developed.

The impedance characteristics of our parallel bioimmunosensor of Chapter 3 involved mainly those of the double layer electrical characteristics of the surface of the gold substrate electrode. We refer to this configuration as parallel because the ionic currents flow in parallel through the "forest" of the MPTS self-assembled monolayer molecules attached to the gold substrate at one end and has either antibodies (with or without antigens conjugated), or blocking substances such as BSA, or no attachments, or, in the majority, gold nanoparticles with antibodies attached [29]. The overall current

flow is the sum of the individual currents, which can each vary in magnitude as they encounter different *impedances* i.e. the various molecules and conjugates on the end of the MPTS.

Aforementioned, was the challenge of latency time to get antibodies and antigens together. Because of the long time shown in Chapter 3 results, concerning the time of diffusion through the modified hydrogel, this time had to be shortened. The obvious solution is to bring the electrode closer to the outer surface of the hydrogel. However, if the fixed substrate electrode was simply moved to the surface, if would not be long before evaporation would leave it "high and dry" in the air. For this reason, a new type of electrode was needed to be able to float on top of, or just under, the surface of the modified hydrogel, and thus be able to stay at that relative position, while minimizing the distance to the environment antigens, therefore the time of diffusion.

In this chapter, we address a novel configuration of electrodes, or, perhaps more appropriately, ionic conductors, which we call the linear/serial configuration, because the ionic current flowed through these conductors, one after another, in a serial fashion. Each of these conductors was a gold nanoparticle with its own double layer characteristics, i.e. Stern layer, as they each had a separate coating of an MPTS SAM with attached antibodies, and, potentially, antibody/antigen conjugates [33]. With the colloidal gold contained mainly in a confining entity, the significant portion of the ionic current had to travel along the colloidal gold route and encountered antibody/antigen conjugate impedance, when present, all along the conduction path. This greatly amplified the impedance influence on the EIS measurements, increasing the sensitivity of the bioimmunosensor.

When using the single gold electrode, the vast majority of the reactions of interest are in the close proximity of the surface of the electrode. The Stern layer dominates the electrical sensitivity and when the ions in solution are forced to flow through the single small surface layer, detection of changes in the capacitance of the layer is possible because the signal is well above the noise level [35].

A novel approach was taken to amplify the signal by using colloidal gold as the ion conductor replacement to the redox mediator, instead of the prior art use as a backfiller [49]. The colloidal gold particles were also coated with MPTS monolayers and effectively had thousands of Stern layer and surface effect conditions. These were operating in tandem mode as opposed to the single mode of the one gold electrode surface and therefore increase, or amplify, the output signal of the FDU.

Methods

Experiment A2-4: Determination of the conductivity and impedance characteristics of the colloidal gold complex along a confining entity.

Electric current, through ions, needs to be directed along a path of coated gold nanoparticles of the FDC to be effective and obtain useable detection measurements. Therefore, in order to keep the nanoparticles in line, a confining entity was needed. In the parallel embodiment, the gold electrode was the base. In this linear/serial embodiment, to effect the serial arrangement, a thin thread or string-like material was utilized by soaking it with the MPTS coated colloidal gold solution (suspension.) (see Figure 50.) The conductivity and impedance characteristics were then measured over applicable voltage and frequency ranges to provide a baseline for comparison to the

electrical characteristics, after exposure to non-specific and/or specific conjugating antigens. Thereafter, the delta measurements were evaluated to determine if specific or non-specific antigens were present.

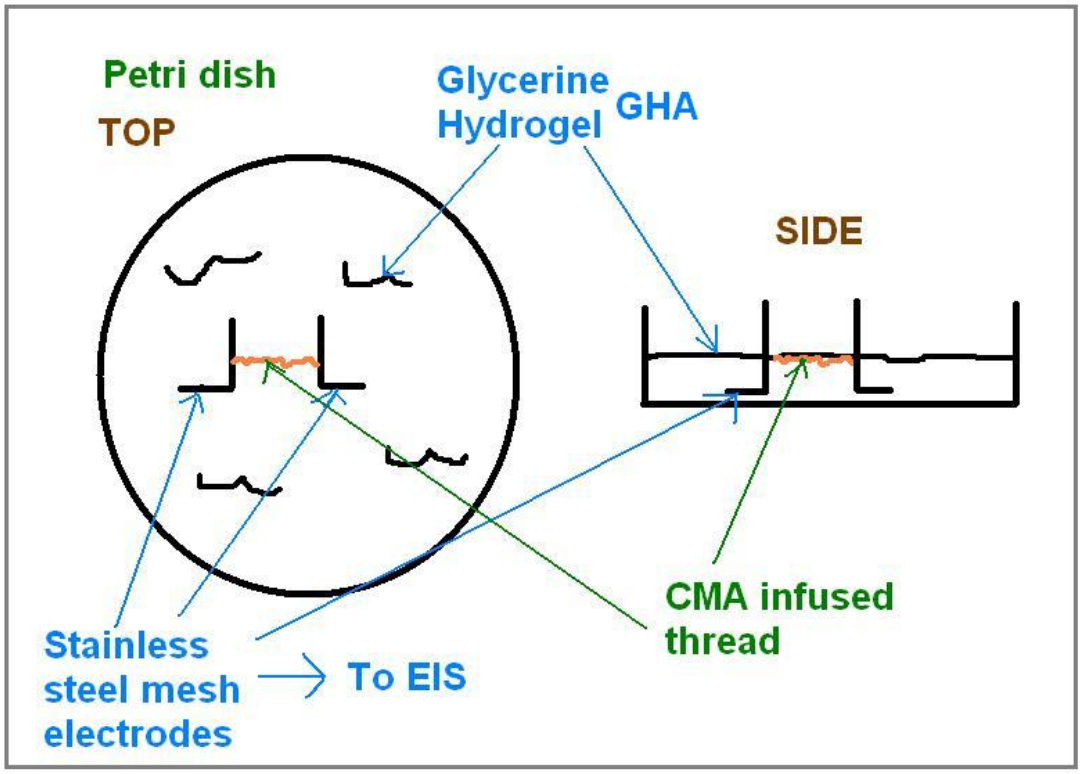

Figure 52: Linear/serial experiment setup with CMA electrode.

Experiment A2-5: Determination of the concentration of a given antibody solution

Antibodies that are produced in animals are commercially available. They can be labeled (tagged) in various ways [39]. Since the production is in the body of the animals, even after external purification, the concentration is generally indicated by the supplier, in a given range. The antibodies were labeled with FITC (fluorescein isothiocyanate.) In

order to determine the exact concentration, a spectrophotometer was used. Once the initial concentrations were determined, the solutions could be diluted to any desired concentrations. The antibody samples measured were Anti-Human IgG FITC antibody produced in goat affinity isolated antibody, buffered aqueous solution. Sigma *F9512* and Anti-Human IgM (μ-chain specific) FITC antibody produced in goat affinity isolated antibody, buffered aqueous solution. Sigma *F5384*.

Experiment A2-6: Determination of the EIS characteristics of a refinement of the confining entity with the introduction of an attached antibody

In the linear/serial embodiment, the thinner the conduction path is, the more the amplification of the detection ability becomes since the antigen-antibody conjugates represent a larger percentage of the cross sectional area of the conduction path. In practicality, the electrical impedance characteristics of the conjugates must be unique (compared to pre-conjugation, and non-specific antigen introduction), detectable, and repeatable for the immunosensor to be specific and sensitive [40].

Measurements were taken with a thin 2.5 cm thread alone, in gel with PBS buffer added (at each stage), with the FDC solution (suspension), and, finally, after exposure to a specific antigen. At an ambient temperature of 22.9 ºC, a cotton-polyester thread 23A (J&P Coats) was strung between electrodes on glycerol-hydrogel (GLYGEL) in a loop. EIS was measured.

One side of the thread loop was then saturated with colloidal gold with an MPTS SAM with IgGab antibodies attached to the top of the SAM layer (CG/MPTS/IgGab).

EIS was measured. PBS buffer was added to that side of the thread loop and EIS was measured. Then, the other side of the thread loop was saturated with CG/MPTS/IgGab and EIS was measured.

To that end of the thread, PBS buffer, with the IgG was added to the solution, and EIS was measured.

Experiment A2-7: Determination of the EIS characteristics of the introduction of specific and non-specific antigens to the FDU (FDE=CG/MPTS/IgGab)

The FDU was separately subjected to specific, and non-specific, antigens in a saline (NaCl) solution, which was used to reconstitute the antigens per Sigma instructions. At an ambient temperature of 20.3 ºC, a reconstituting solution of 150nM NaCl was prepared per supplier specifications for the IgG antigen (Sigma F9512 Anti-Human IgG MSDS FITC antibody produced in goat.) was prepared. Preparations were produced by adding 3 µg IgG into 1ml of 150nM NaCl (heretoforth referred to as solution IgG(1)). Also prepared was a non-specific solution of IgM (Sigma F5384 Anti-Human IgM MSDS (µ-chain specific)-FITC antibody produced in goat) by adding 3 µl if IgM into 1ml of 150nM NaCl. A direct comparison was performed of the resulting EIS characteristics.

Experiment A2-8: To compare successive building of the antibody sensor FDC parts, in order to determine the contribution of the

electrical characteristics of the various coatings of the antibody immobilization scaffolding

The construction of the FDC was analyzed thoroughly by electrical EIS and cyclical voltammetry measurements and at each step and compared to previous steps. This aided in the development of improvements and fine tuning of the complete sensor.

Experiment A2-9: Effects of length of conductor on colloidal gold (CMA), and CMA with antigen IgG.

At an ambient temperature of 19.6 ºC, 8 ml of colloidal gold solution was mixed with 2 ml MPTS solution [hereto forth referred as GM]. GHA gel was prepared as previously described. CG-MPTS and IgGab was prepared and placed in dark for 7 hours [solution mix hereto forth referred to as CMA.] Tests were performed by soaking the lengths of thread strung between the conductors shown with 10 µl of CMA and EIS was measured. Then, 10 µl of IgG was added, and EIS was measured.

Various lengths of thread were soaked with various combinations of GMI and IgG were tested. The table in Figure 51 was applied:

Test thread	Length x cm	GMI x 10 µl	GMI x 10 µl
1	1	1	1
2	1.5	1	1
3	2	1	1
4	2	1.5	1
5	2	2	1
6	2	2	2
7	1.5	1.5	1
8	1.5	1.5	1.5

Figure 53: **Table of lengths of conductors to measuring the impedance (EIS)**

Experiment A2-10: Effects on EIS impedance results over time after the introduction of specific antigens to the FDU.

The reaction of the antibody/antigen conjugate was quite rapid with the thread confinement at the surface of the gel (<5 seconds) though practically, it was about 45 seconds before a measurement could be completed. A thread-like material was saturated with a solution/suspension of capture molecules (10µl), with the capture molecules permeating the pores of the thread-like material that was positioned on the surface of an electrolytic or non-electrolytic gel.

In the parallel embodiment, diffusion was much less of a factor, since the FDC's were immobilized with covalent bonds. As long as the FDC's were confined to the thread, the detection signal was amplified. However, over time, the FDC's diffused into the hydrogel and the signal (electrical characteristics) between the electrodes moved back toward equilibrium, and positive detection of the antigens was impeded. Readings were taken approximately every 2-5 minutes, which is the time required for our measuring equipment to sweep through the EIS frequencies of interest.

Experiment A2-11: Determination of the selectivity of the CG/MPTS/IgGab FDU in a range of concentrations of specific and non-specific antigens

In the first test, IgGab antibodies were attached to MPTS coated colloidal gold nanoparticles (CG/MPTS/IgGab)[CMA], and then exposed to non-specific IgM of medium concentration.

In a second test, low a concentration of non-specific IgM was used as in the previous test.

Finally, the third test was to show that the FDU is capable of operation independent of the order of exposure, by starting with antigens and adding antibodies, then vice versa.

The IgM was diluted 3 µl into 1 ml of 150 mM NaCl for a solution indicated as IgM(1). The IgG(1) was measured by a spectrophotometer to be a concentration of 0.54 mg/ml.

Test 1: Introduction of IgM of Medium Concentration to the CMA FDU

a. Baseline 10 µl of CG/MPTS/IgGab (CMA) solution.

b. Add 10 µl of IgM(0.1)

Test 2: Introduction of IgM of Low & High Concentrations to the CMA FDU

a. Baseline 10 µl of CMA solution.

b. Add 10 µl of IgM(0.01)

Test 3: Effects of Antibody/Antigen Order to the CMA FDU

a. Baseline 10 µl of IgG (1) solution.

b. Add 10 µl of IgGab.

c. Add 10 µl of IgG (1) solution.

d. Add 10 µl of IgGab.

Experiment A2-12: Determination of the sensitivity and detection limits of the "Facilitating Detection Unit" (FDU) of the device

IgGab antibodies were attached to MPTS coated colloidal gold nanoparticles (CG/MPTS/IgGab or CMA), then, exposed to specific IgG of decreasing concentration to the point of non-detection. The pseudo-linear portion of response was then plotted and used for calibration. Effects of non-antigen influence were filtered from the results.

Sensitivity is the amount of sensor output change per measured quantity changes. An ideal sensor has a linear output, and therefore the sensitivity is defined as the ratio between output signal and measured quantity. In practice, a sensor typically approaches linearity in its rated range, which will be determined by this experiment. Literature reports a linear calibration in the range of 8.3–2128 ng/ml and detection limits of 3.3 ng/ml plotted against the logarithm of the antigen concentration [14]. This research is

concerned with detecting the higher levels of concentration that would be toxic to the environment of man, animals, and plants.

IgG was prepared in 5 dilutions of 1:10:100:1000:10000 for the sensitivity experiments.

Experiment A2-13: Determination of the characteristics of air transfer to the FDU

A dry antigen was introduced to the immunosensor. The EIS measurements showed how the diffusion and migration of the rehydrated antigen patterned the movement toward the antibodies for a detectable conjugate action. The FDU was set up as in the previous experiment. An EIS reading was taken with the bare thread only. After introducing 20 µl of CMA to the thread, another EIS reading was taken. A small amount (2 mm^3) of powdered antigen (IgG) was sprinkled on the FDU. EIS readings were taken at 5-10 minute intervals.

Experiment A2-14: Use of differential measurements to eliminate background non-specific interference of contamination

In our case, the immunosensor background interference consisted mainly of non-specific contamination. This affected the output and it was advantageous to have the effect filtered or cancelled out. That left any specific results. In this experiment, two immunosensors were utilized, with differing antibodies attached to the CG/MPTS monolayer.

The construction of the FDC was analyzed thoroughly by electrical EIS and cyclical voltammetry measurements and at each step and compared to previous steps.

EIS was run on:

1. cAu20 (Colloidal 20nm gold nanoparticle) solution
2. cAu20 solution plus a monolayer of MPTS
3. IgGab antibodies attached directly to cAu20
4. IgGab antibodies attached to the ends of a monolayer of MTPS which was attached to cAu20

The gel used consisted of 100 ml of glycerol and 7g of agarose (7%) prepared as previously described, here forth referred to as GLYGEL.

Incubation times of the IgGab in samples 3 & 4 were 2.5 hr.

Results

Experiment A2-1: Verification of the conformation of our FDC's on gold leaf for imaging with an AFM (Atomic Force Microscope)

A scan with an AFM (Atomic Force Microscope) (the Veeco Innova AFM, bought by Bruker AXS) verified the typical size and shape of our FDC's colloidal gold nanoparticle and its MPTS layer. A drop of the CG(Colloidal Gold)/MPTS solution was immobilized by evaporation on gold leaf before the scan. Figure 52 shows the results of the scan. The gold nanoparticle size was approximately 20 nm. Also, consistant with colloidal gold nanoparticles of that size, the shape had become a slight ellipsoid. Smaller gold nanoparticles were generally spheres.

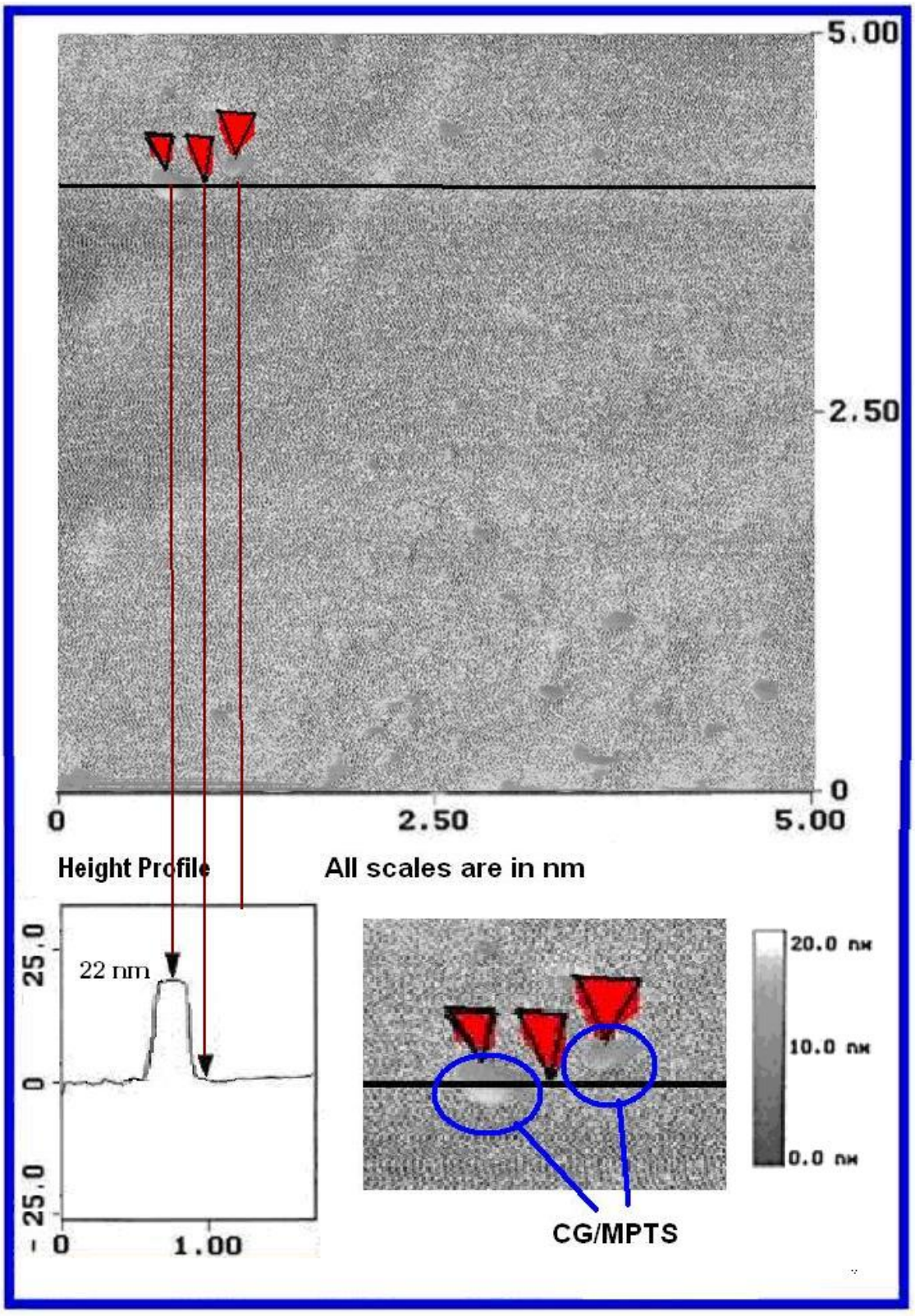

Figure 54: **Constant Force Mode image (5μm x 5μm) from the Atomic Force Microscope (AFM) of the 20 nm colloidal gold nanoparticles with a self-assembled monolayer (MPTS) attached.**

The AFM data shows that the physical assumptions of the colloidal gold and MPTS are consistent with the data values used in the experiments. The conjugates formed when the antigens are introduced would facilitate ion and electron transfer through the GNP's to lower the real impedance value.

Experiment A2-2: To compare conductivity of gel, colloidal gold, and colloidal gold with an MPTS monolayer

A solution (suspension) of colloidal gold, and colloidal gold with an MPTS monolayer was tested electrically, as well as the gel alone, as a baseline.

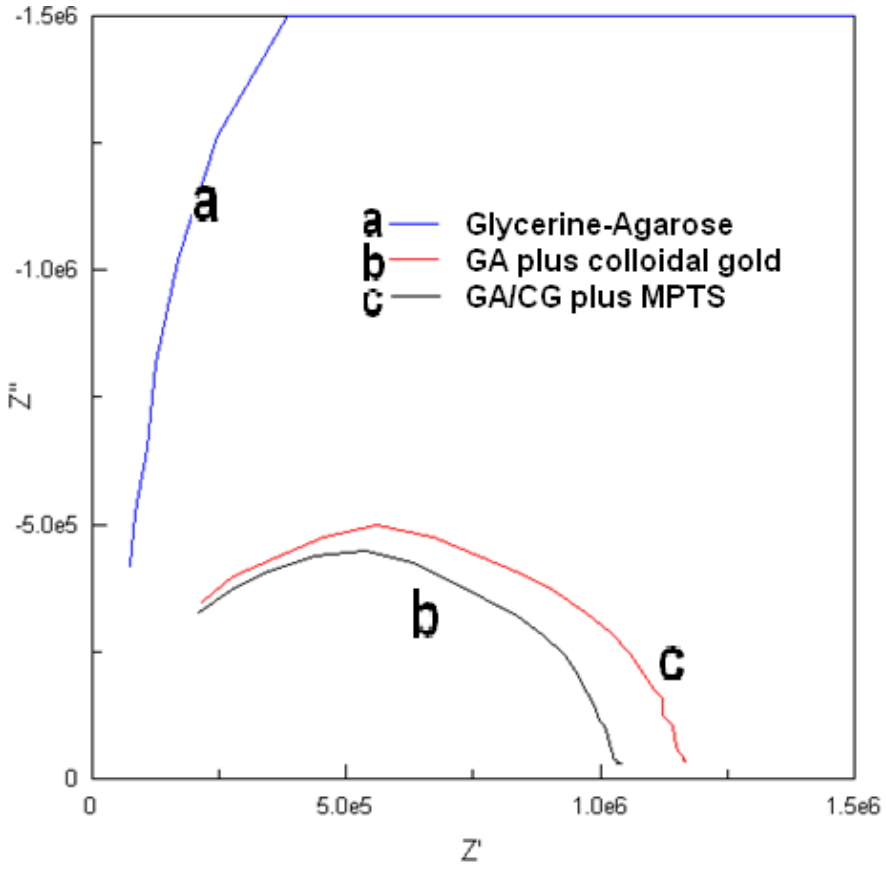

Figure 55: EIS plots of Glycerol-agarose, GA with colloidal gold, and with MPTS

The glycerol-agarose hydrogel was a relatively poor conductor. This was desirable in the situation, because that means that it will have a higher resistance, and therefore, less contribution (bulk resistance) to the overall resistance; this also strengthened the case for the 2-probe EIS system in our project.

Experiment A2-3: To determine the charge and mobility of the colloidal gold nanoparticles, with, and without a MPTS monolayer coating

The colloidal gold, electrophoresis lane, produced a red band that migrated in the gel. The MPTS coated colloidal gold did not seem to migrate at all, over several hours. This proves that the plain colloidal gold was negatively charged (migrated toward the positive electrode.) The CG migrated 1 cm toward the positive electrode in .5 hr, so the migration rate was approximately 2 cm/hr. This explained why the gold nanoparticles stayed in suspension as the negatively charged particles repelled each other.

The MPTS surrounded the colloidal gold, and also clumped the gold nanoparticles together, which caused the deep red color to turn milky pink. These particles became too large to easily move through the gel. The MPTS also added a slight positive charge, neutralizing the negative CG charge, which further inhibited movement toward the positive electrode.

Experiment A2-4: Determination of the conductivity and impedance characteristics of the colloidal gold complex along a confining entity.

At ambient temperature of 21.8 ºC, and using GLYGEL, a small Pyrex dish was ¼ filled with glycerol and heated (melted) and the gel was poured over the glycerol. Two stainless steel mesh electrodes were embedded into the liquid hydrogel, which was allowed to cool and solidify. EIS was measured with a two probe arrangement using the stainless steel mesh electrodes. A 2.5 cm piece of thread was saturated with CG and placed on top of the gel between the bases of each electrode (on the gel above each electrode base, but not touching the metal.) EIS was measured. Then, another 2.5 cm thread was soaked in colloidal gold that had an MPTS SAM (Self Assembling Monolayer) grown on the gold nanoparticles. The previous thread was replaced with this one and EIS was measured. (A bare thread only was tried, but it dried too fast for stable measurements).

The EIS plots for the plain GYLGEL are shown, and with a 2.5 cm thread.

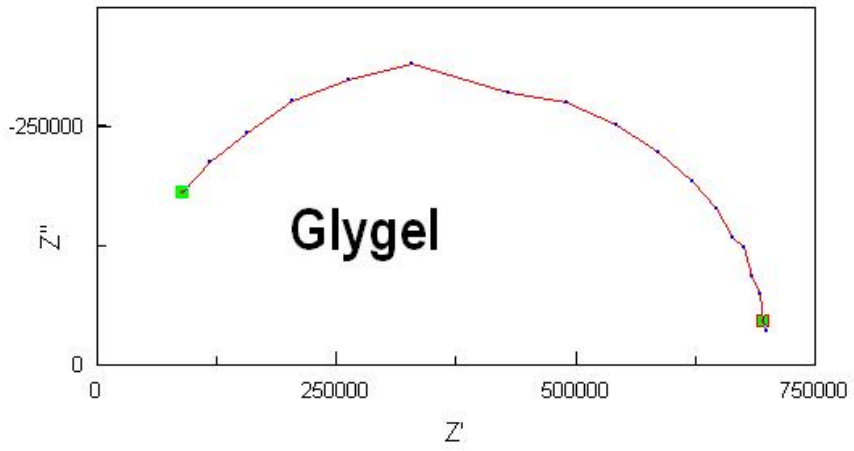

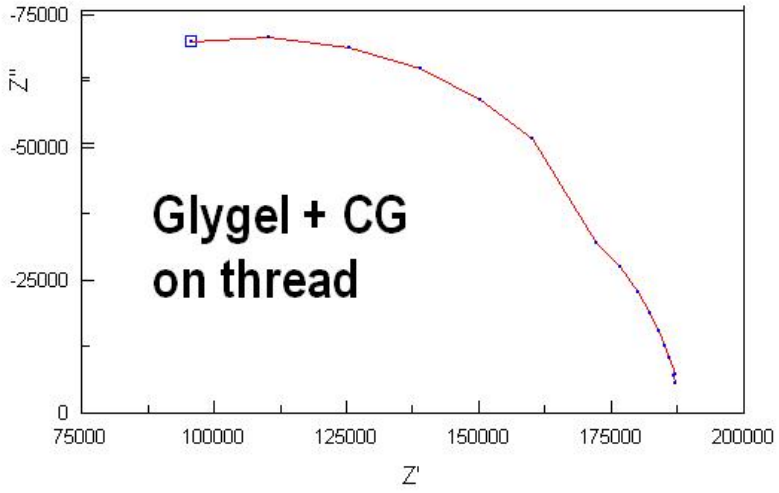

Figure 56: **Formulated Glygel (top) and Glygel with CG on bottom.**

Figure 54 clearly show that the CG increases conductivity of the serial electrode.

Experiment A2-5: Determination of concentration of an antibody solution

The IgGab concentration was determined by a NanoDrop spectrophotometer to be 2.5 mg/ml measuring the peak absorbance at 230 nm. The IgMab concentration was determined by a NanoDrop spectrophotometer to be 4.1 mg/ml.

Experiment A2-6: Determination of the EIS characteristics of a refinement of the confining entity with the introduction of an attached antibody

A conjugate of the IgGab and IgG antigen was formed and significantly decreased the impedance Z as shown in Figure 55. The right three traces are before the antigen IgG was introduced (3 traces over time); the left three traces are after the IgG was introduced.

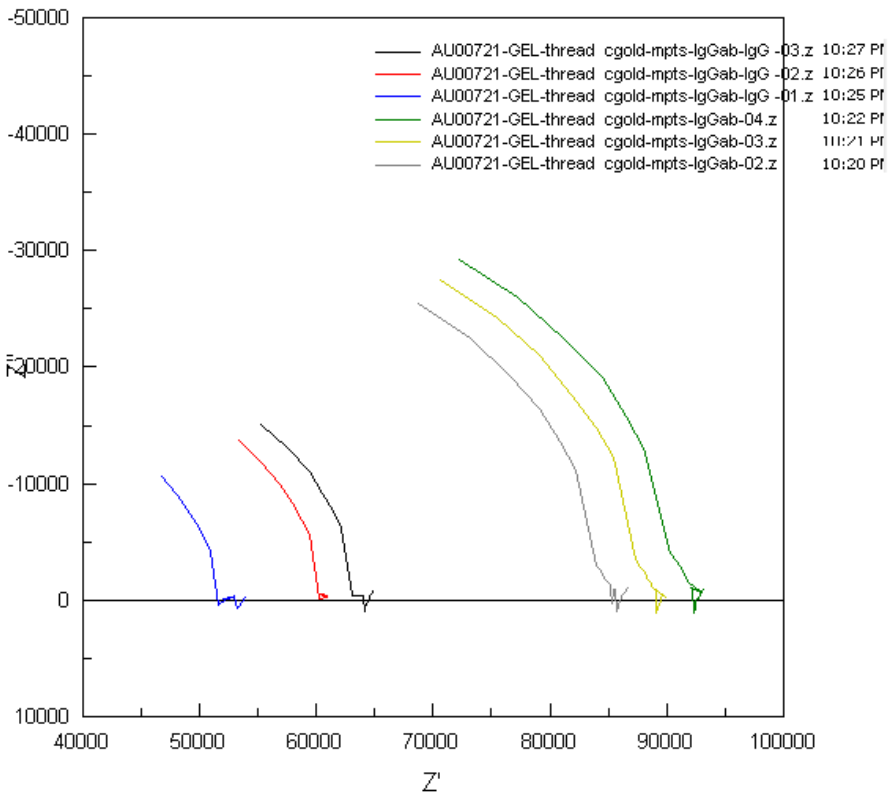

Figure 57: EIS of Serial electrode

Experiment A2-7: Determination of the EIS characteristics of the introduction of specific and non-specific antigens to the FDU (FDE=CG/MPTS/IgGab)

Surrounding the active centers of most oxidoreductases are considerably thick insulating protein shells, which block the electron transfer between the electrodes and the active centers, and cause poor analytical performances of electrochemical bioimmunosensors without electron transfer mediators. However, gold nanoparticles can improve the electron conductivity between the active centers of proteins and electrodes[61]. (see Figure 56 & 57)

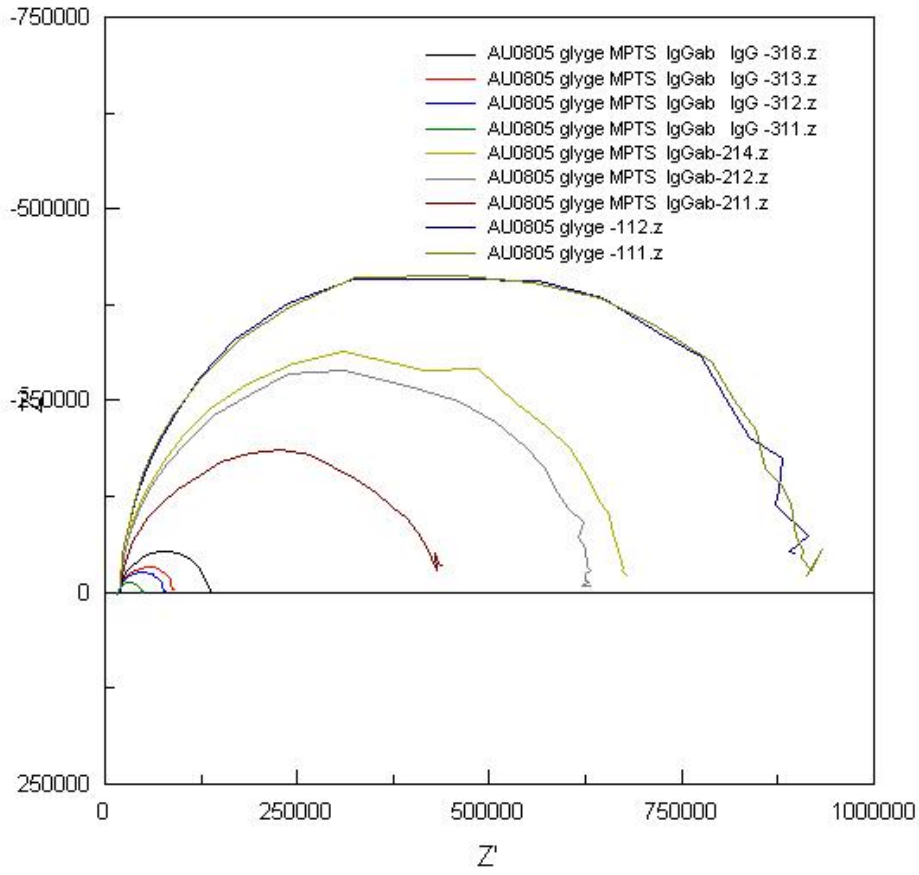

Figure 58: **EIS was measured before and after the introduction of a specific antigen.**

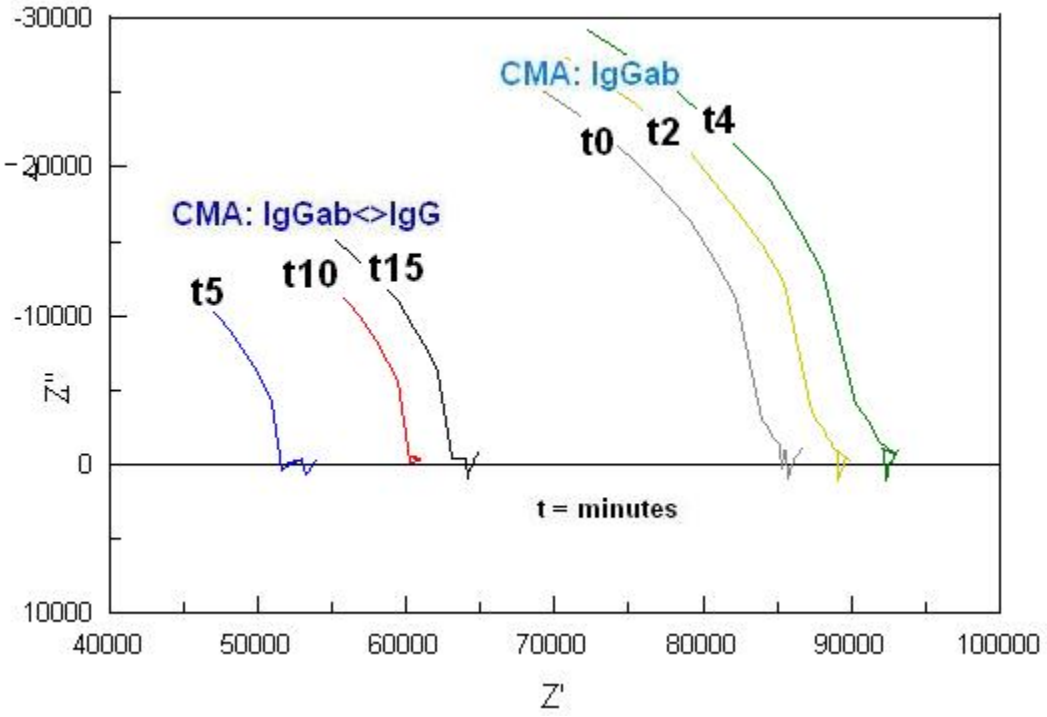

Figure 59: **EIS was measured over time. Antigen was introduced at time t5.**

Experiment A2-8: To compare successive building of the antibody sensor FDC parts, in order to determine the contribution of the electrical characteristics of the various coatings of the antibody immobilization scaffolding

In prior biosensors, the antibodies were immobilized by attaching them, directly or indirectly, to a stationary substrate. In our linear (serial) process, the antibodies were attached to the ends of a self assembling monolayer of MPTS that was covalently attached, by disulfide bonds, to the colloidal gold nanoparticles, themselves; the nanoparticles were free to move about in a confined space, so that the coated particles acted like, and replaced, the need for redox substances. (see plots in Figure 58)

The ions in the solution transferred electrons from particle to particle, so that the serial string of the nanoparticles acted as a conductor of electricity. Each nanoparticle had the same properties of the previously mentioned stationary substrate electrodes, but, since the capture surface for the antigens was spread out in a serial fashion (on the nanoparticles), the antigens did not have to travel to the previously mentioned coated substrate electrode to be detected. Thusly, the presence of a small amount of antigen changed the electrical properties of the sensor sooner, and detection was accomplished more rapidly; since the impedance/conductance was affected by the surfaces charges, the Stern layers surrounding each colloidal gold nanoparticle, the antibody/antigen conjugate had an impedance altering effect anywhere along the ionic current path, rather than just at the previously mentioned coated substrate electrode.

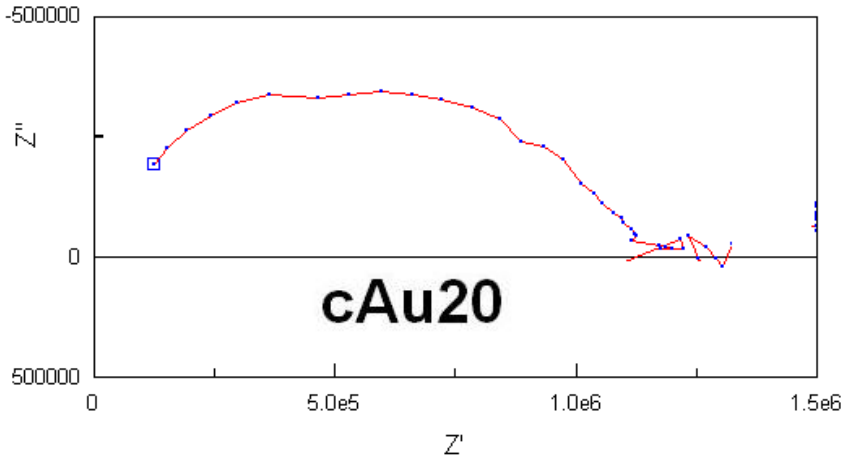

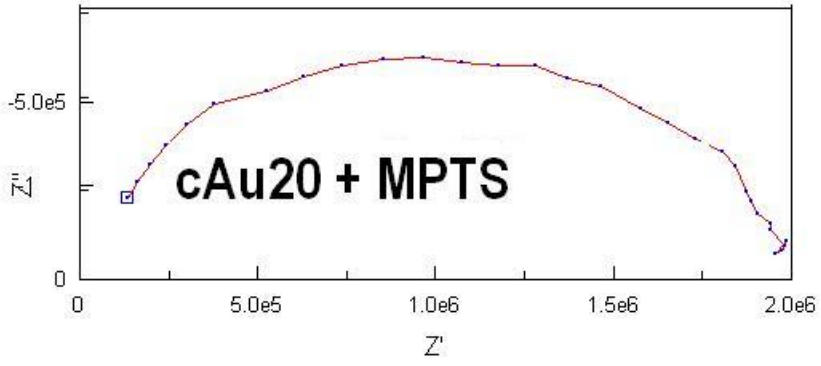

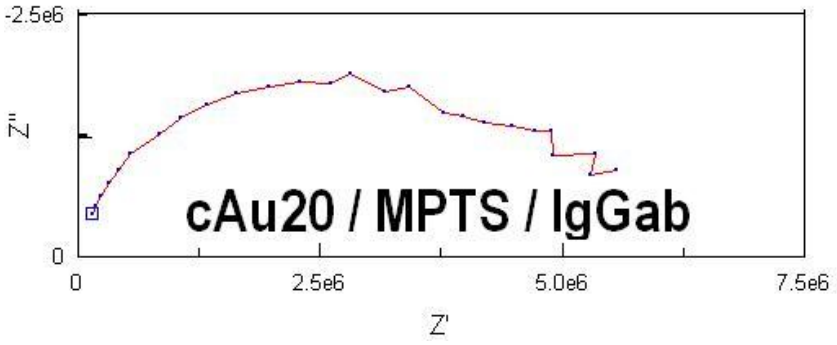

Figure 60: **EIS plots of a progressive building of an FDU.**

Experiment A2-9: Effects of length of conductor on colloidal gold (GMI), and GMI with antigen IgG.

The results showed that there was negligible difference in impedance within the length range.

Experiment A2-10: Effects on EIS impedance results over time after the introduction of specific antigens to the FDU.

As long as the FDC's were confined to the thread, the detection signal was amplified. However, over time, the FDC's diffused into the hydrogel and the signal (electrical characteristics) between the electrodes moved back toward equilibrium, and positive detection of the antigens was impeded. Readings were taken approximately every 2-5 minutes, which was the time required for our measuring equipment to sweep through the EIS frequencies of interest as shown in Figure 59.

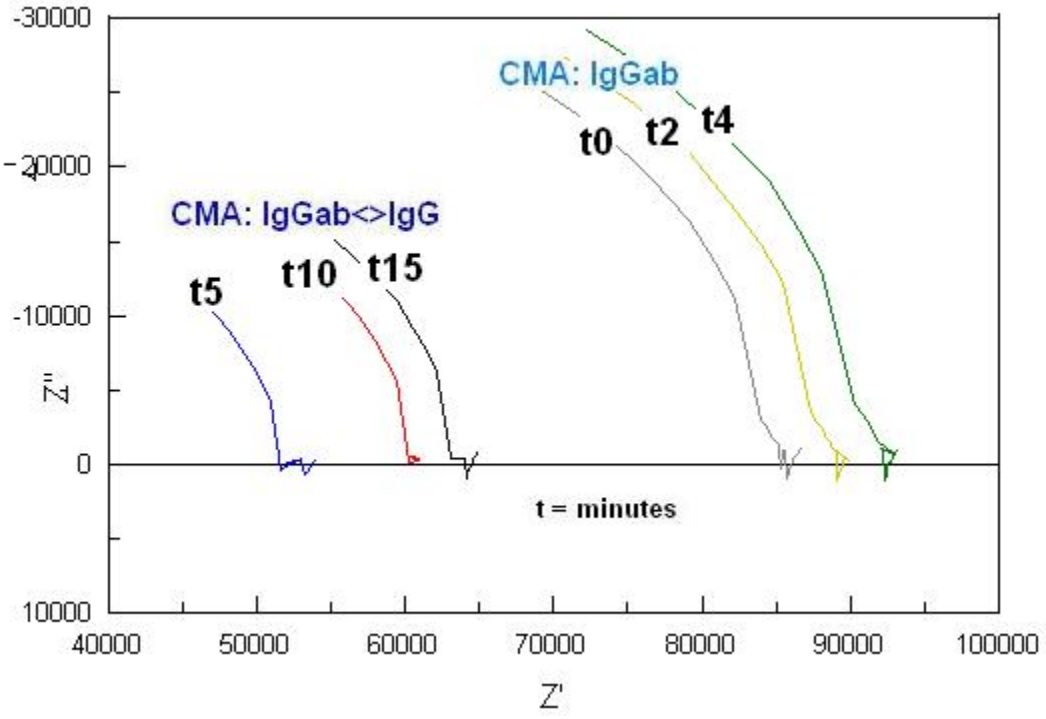

Figure 61: **EIS showing the impedance change over time. The IgG antigen was introduced at t5.**

Experiment A2-11: Determination of the selectivity of the CG/MPTS/IgGab FDU in a range of concentrations of specific and non-specific antigens

IgGab antibodies were attached to MPTS coated colloidal gold nanoparticles (CG/MPTS/IgGab)[call it CMA], and then exposed to non-specific IgM of medium concentration. In a second test, low and high concentrations (these were combined in one test, because they would not significantly alter the measurements of the high concentration because they overwhelmed the low concentration.)

In the third test, a different specific antibody—antigen pair (IgMab—IgM) was measured for their electrical characteristics, showing that a different FDE could produce similar results.

Finally, the fourth test was to show that the FDU is capable of operation independent of the order of exposure, by starting with antigens and adding antibodies, then vice versa.

The concentration of IgM = 5.79 mg/ml as determined by a spectrophotometer (at the peak absorbance at 230 nm), which utilizes the Beer-Lambert law:

$$A=\varepsilon bc \qquad \text{(Eq. 4.1)}$$

where

A absorbance = log10 P0 / P unit less

ε the molar absorbtivity with units of L mol^{-1} cm^{-1}

b the path length of light through the sample in centimeters

c the concentration of the compound in solution, expressed in mol L^{-1}

The tests and results of the EIS measurements were as in Figures 60–62.

Test 1: Introduction of IgM of Medium Concentration to the CMA FDU

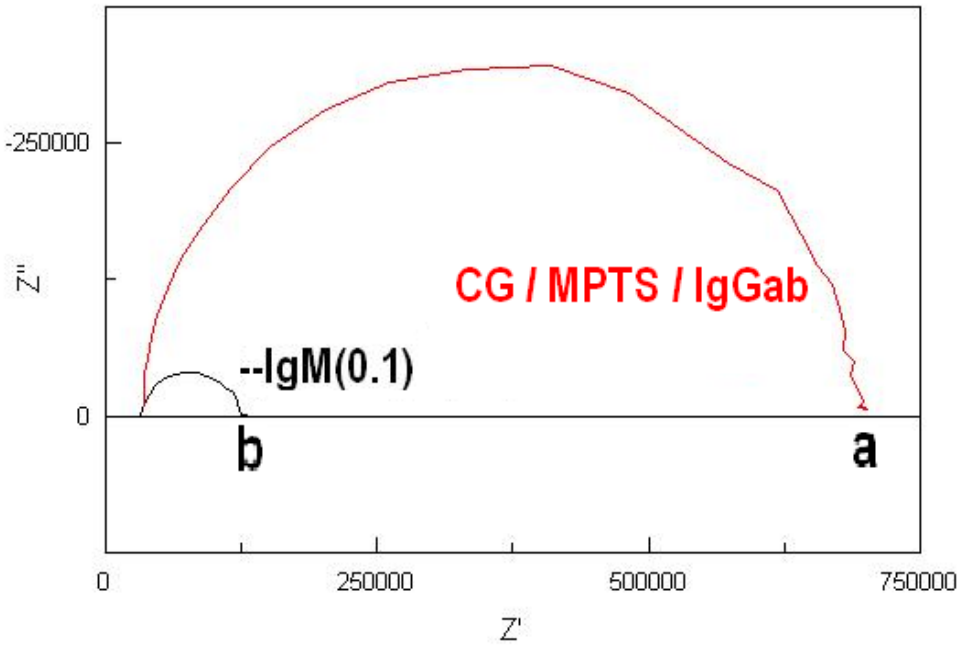

Figure 62: **(a) Baseline 10 µl of CG/MPTS/IgGab (CMA) solution, (b) Add 10 µl of IgM(0.1)**

Test 2: Introduction of IgM of Low Concentration to the CMA FDU

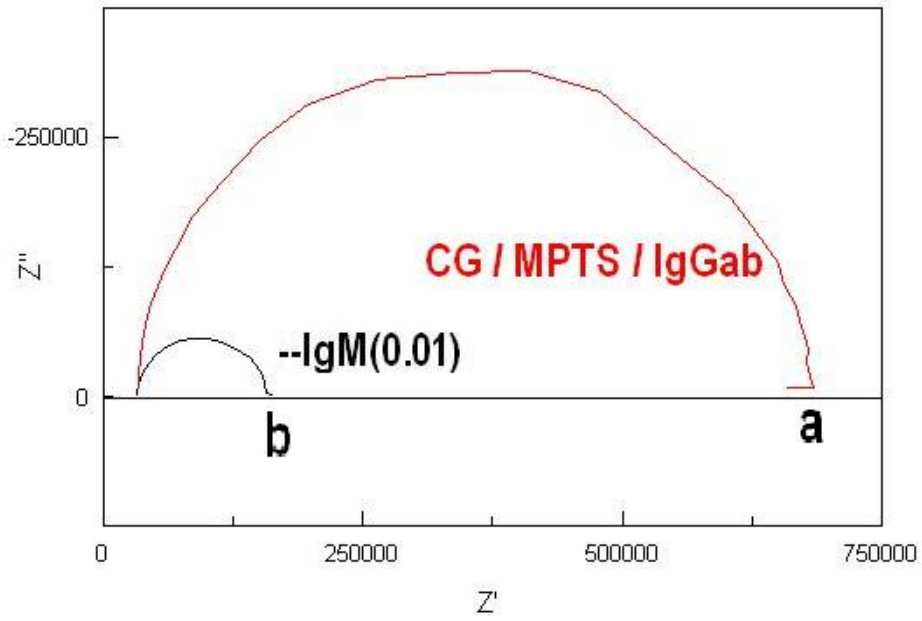

Figure 63: **(a) Baseline 10 µl of CG/MPTS/IgGab (CMA) solution, (b) Add 10 µl of IgM(0.01)**

Test 3: Effects of Antibody/Antigen Order to the CMA FDU

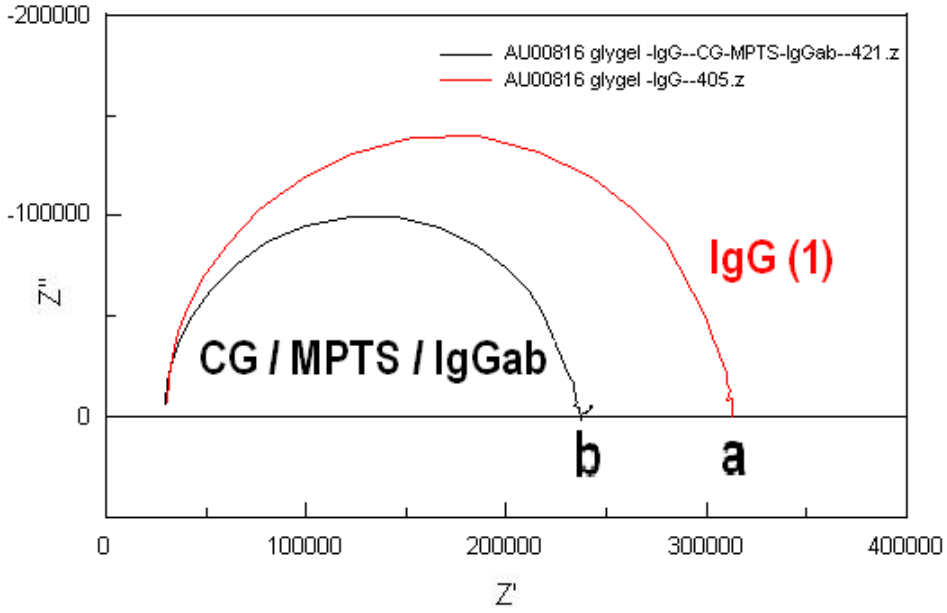

Figure 64: **(a) Baseline 10 µl of IgG, (b) add 10 µl of CG/MPTS/IgGab (CMA) solution**

Experiment A2-12: Determination of the sensitivity and detection limits of the "Facilitating Detection Unit" (FDU) of the device

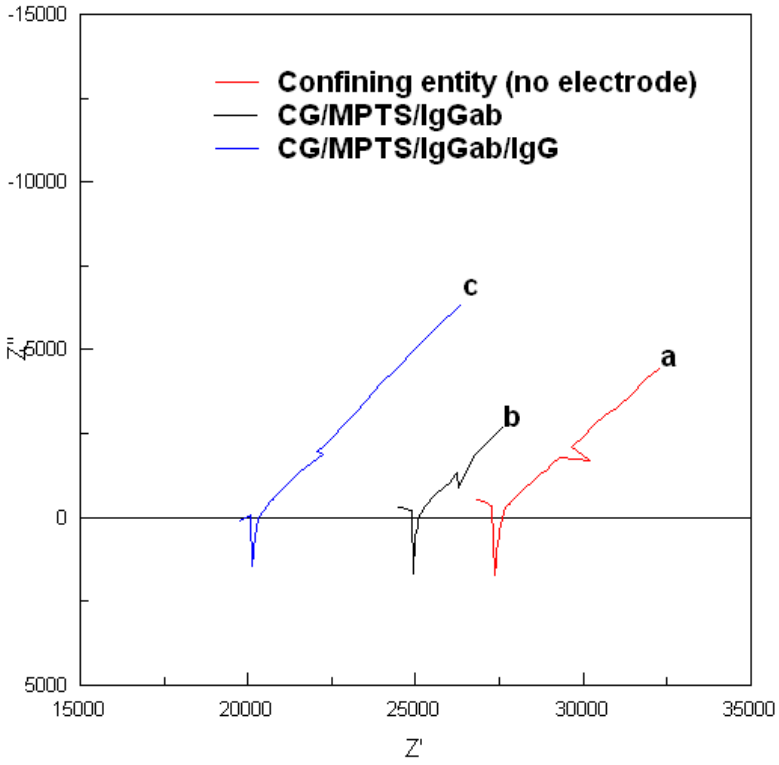

Figure 65: **EIS plots of adding cumulatively, (a) empty confining entity, (b) colloidal gold with MPTS and IgGab, (c) IgG**

Figure 63 shows the contributions to the EIS impedance measurements of the parts of the serial CG electrode. The EIS plots utilizing the serial colloidal gold, MPTS coated, nanoparticles in a confining entity are shown for a range of antigen concentrations in Figures 64-67, with the numerical results in the table in Figure 68. The EIS plots of CG/MPTS/Antibody serial electrode (CMA) were as shown in Figure 67. At t0, there is only the confining entity for the electrode. At t3, the CG/MPTS/IgGab was introduced as the electrode. At t6, the antigen IgG was introduced. Times t6 and t7 showed a small diffusion toward equilibrium. The Z" zero intercept was consistently at a frequency between 3.2KHz and 5.0 KHz.

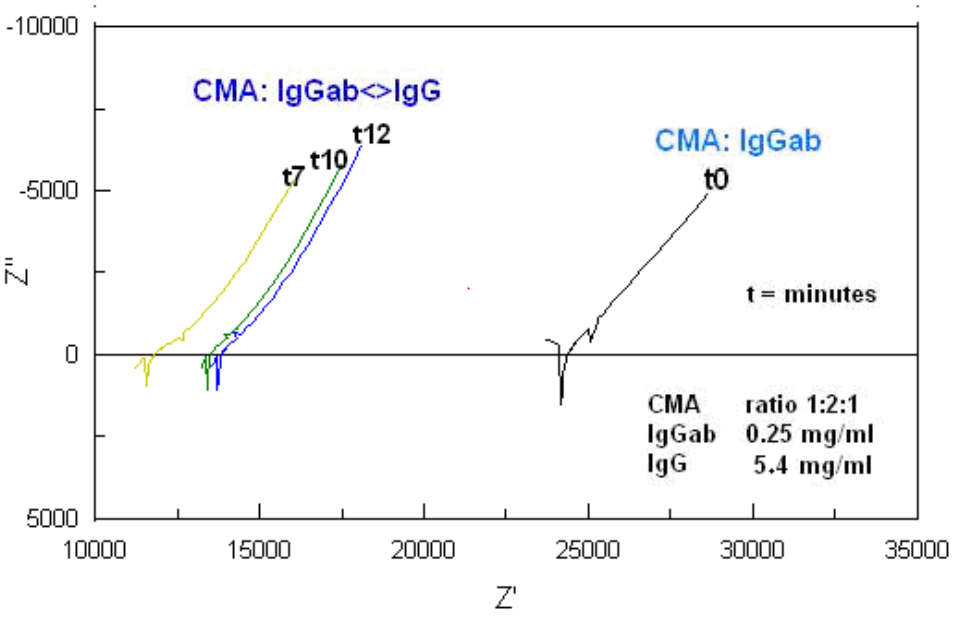

Figure 66: **EIS plots of CG/MPTS/Antibody serial electrode (CMA), Antigen=5.4 mg/ml at times (tn) (Antigen introduced at t7)**

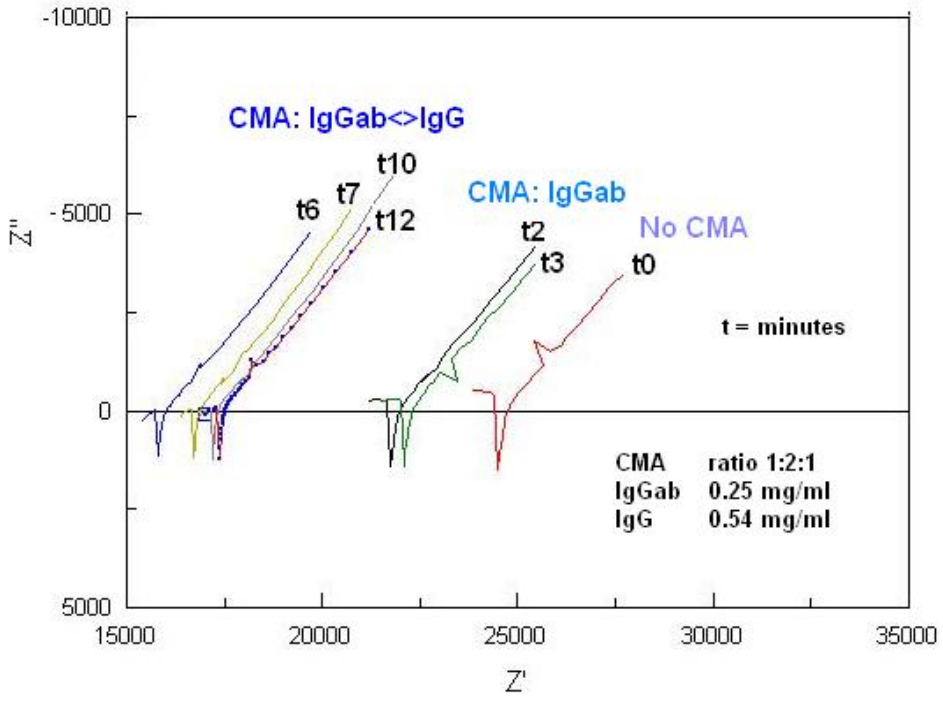

Figure 67: **EIS plots of CG/MPTS/Antibody serial electrode (CMA), Antigen=0.54mg/ml at times (tn) (Antigen introduced at t6)**

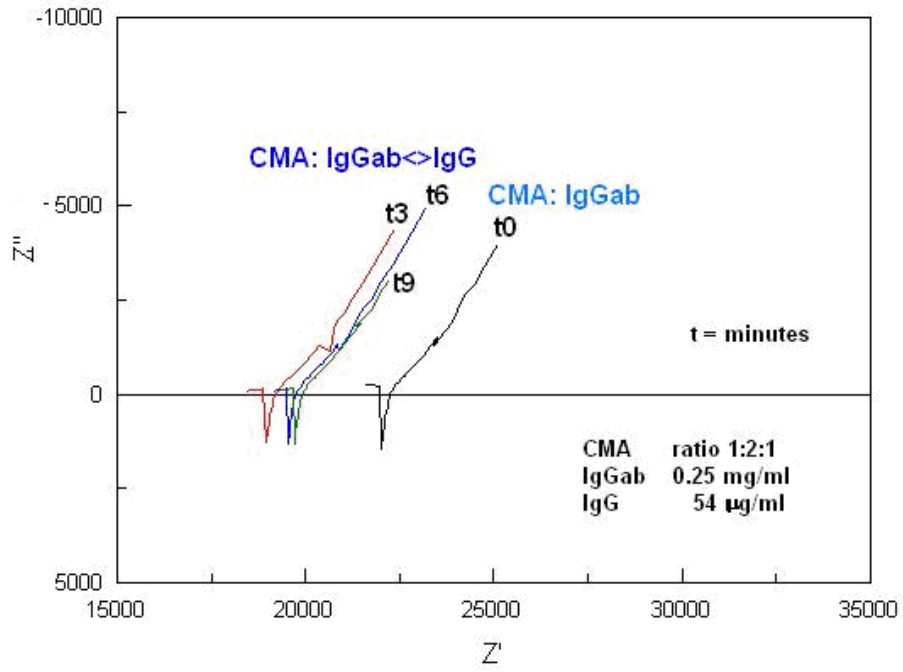

Figure 68: **EIS plots of CG/MPTS/Antibody serial electrode (CMA), Antigen=54µg/ml at times (tn) (Antigen introduced at t3)**

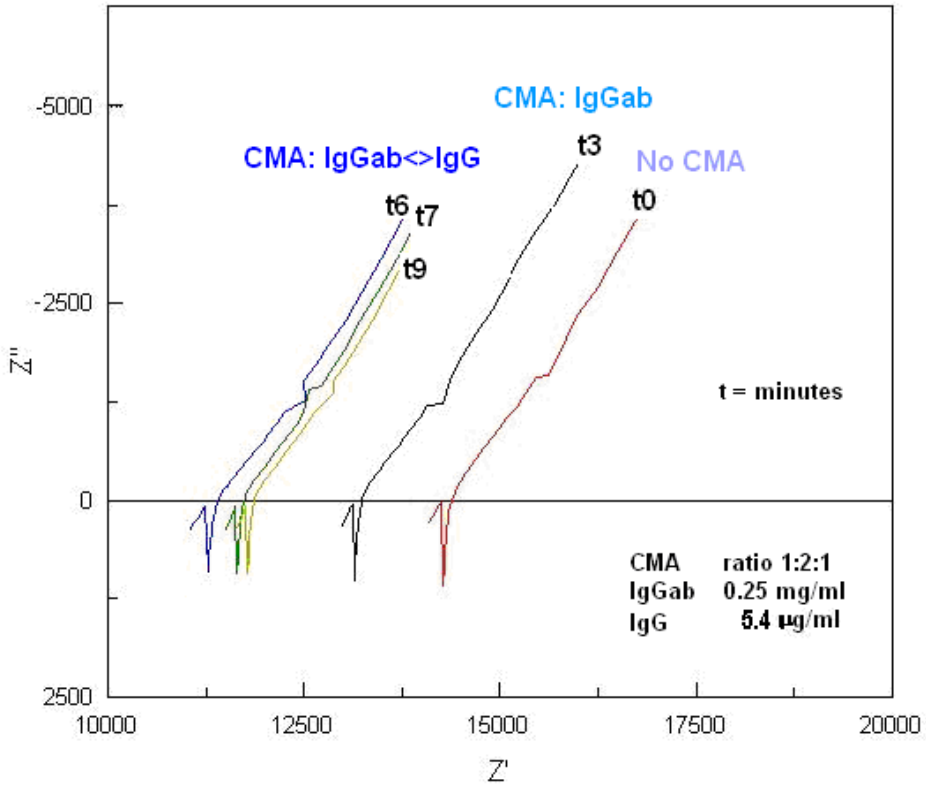

Figure 69: **EIS plots of CG/MPTS/Antibody serial electrode serial electrode (CMA), Antigen=5.4µg/ml at times (tn) (Antigen introduced at t6)**

IgG con	Ohms	lo	hi	Δ lo	Δ hi	Normalized		Log of ratio
µg/ml	CMA	CMA-ant	CMA-ant	CMA-ant	CMA-ant	hi CMA-ant	lo	to ref conc
5.4	13176	11284	11801	1892	1375	1.0380	0.7544	1.0000
54	22040	18991	19709	3049	2331	1.0000	0.7645	2.0000
540	22371	15845	17394	6526	4977	2.1087	1.6082	3.0000
5400	24157	13600	15294	18048	15000	4.3065	3.5792	4.0000

Figure 70: **Table of EIS data for CMA for concentrations of IgG antigen (log of ratio of impedance changes was referenced to IgG 540 ng/ml)**

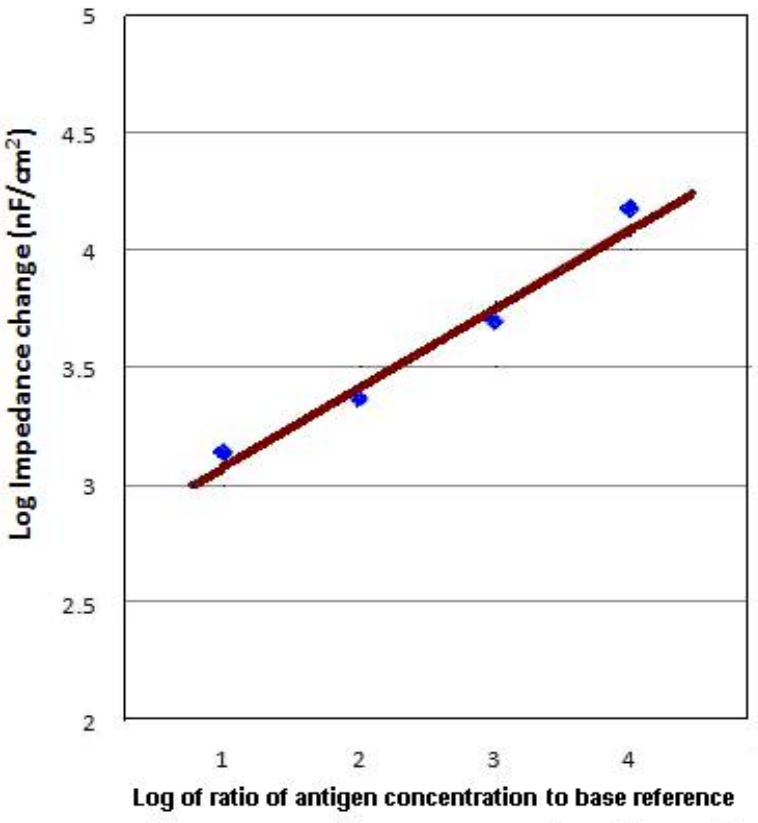

Figure 71: **Log plots of IgG ratio to ref concentration vs. log change in impedance. All measurements were performed in 10 mM PBS (pH 7.4) (referenced to IgG 540 ng/ml)**

The EIS measurements of impedance of the monolayer and colloidal nanogold reveal that as the extension of the monolayer-conjugate attachments were added to the colloidal gold particles, the impedance was decreased. This may have been caused by the alignment of attachments allowing greater ion/electron transfer. The linear regression plot utilizing least squares analysis is shown in Figure 69.

The linear regression equation, with a sensitivity of 0.33 was:

$$\text{Log } \Delta Z' = 0.33 \text{ Log ratio (IgG concentration to ref)} + 2.80 \qquad \text{(Eq. 4.2)}$$

The sensitivity of the linear/serial sensor arrangement was determined by subjecting the sensor with CMA to varying concentrations of specific antigens. Between the lower limits of detection and the saturation point, there existed a pseudo-linear region that was used for calibration of the bioimmunosensor [42]. The CMA with IgGab was measured with EIS in the range of frequencies from 100 kHz to 100 Hz. Multiple readings were taken at active points in the experiment. The initial readings were without CMA, just the confining entity, in this case, polyester thread. The thread was tightly wrapped, around and between, two stainless steel mesh electrodes approximately 1.5 cm apart (see Figure 50). Per results in Experiment 9, the distance, within one standard deviation, did not significantly affect the EIS readings with a given volume of CMA.

The CMA was prepared as described above, with a 1:2:1 ratio of 20nm colloidal gold to MPTS to 0.25 mg/ml IgGab. Each concentration test was performed with 20 μl of CMA and included an EIS reading immediately after introduction to the polyester thread. After the initial drop in real impedance, multiple EIS readings were taken over the next few minutes as the FDU reached equilibrium at a slightly higher real impedance value. This was caused by repulsion of the negative charges of the CMA nanoparticles

and diffusion into the GHA hydrogel [43]. A known concentration of antigen (10 μl of IgG) was then introduced onto the FDU and multiple readings of EIS were taken over several minutes as the real impedance value moved upward toward equilibrium. Given the predominantly cationic or positive surface charge of the IgGab, the anionic or negatively charged antigen IgG conjoined with the antibodies, reduced the distance between molecules, and increased the capacitance of each nanoparticle.

The AC impedance of a capacitor is called capacitive reactance. It decreases with increasing frequency and increases with decreasing plate distance [45]. This result is commonly expressed in polar form, as

$$Z_{capacitor} = \frac{1}{\omega C} e^{-j\frac{\pi}{2}} \qquad \text{(Eq. 4.3)}$$

or, by applying Euler's formula, as

$$Z_{capacitor} = -j\frac{1}{\omega C} = \frac{1}{j\omega C} \qquad \text{(Eq. 4.4)}$$

Capacitance of an entity can be calculated if the geometry of the conductors and the dielectric properties of the insulator between the conductors are known. For example, the capacitance of a parallel-plate capacitor constructed of two parallel plates both of which have area *A* separated by a distance *d* (see Chapter 2).

$$C = \varepsilon_r \varepsilon_0 \frac{A}{d} \qquad \text{(Eq. 4.5)}$$

However, the geometry of the antibody/antigen conjugate is very complex and therefore, we rely upon empirical measurements.

Our EIS detection becomes non-linear below 5.4 μg/ml and above 5.4 mg/ml, this being our linear sensitivity range. Our detection limit was 5 μg/ml, when plotted versus the log of the ratio of antigen concentration referenced to 540 ng/ml.

Experiment A2-13: Determination of the characteristics of air transfer to the FDU

The results showed an initial latency of 0.2 minutes, and then a gradual decrease in impedance over the next 45 minutes.

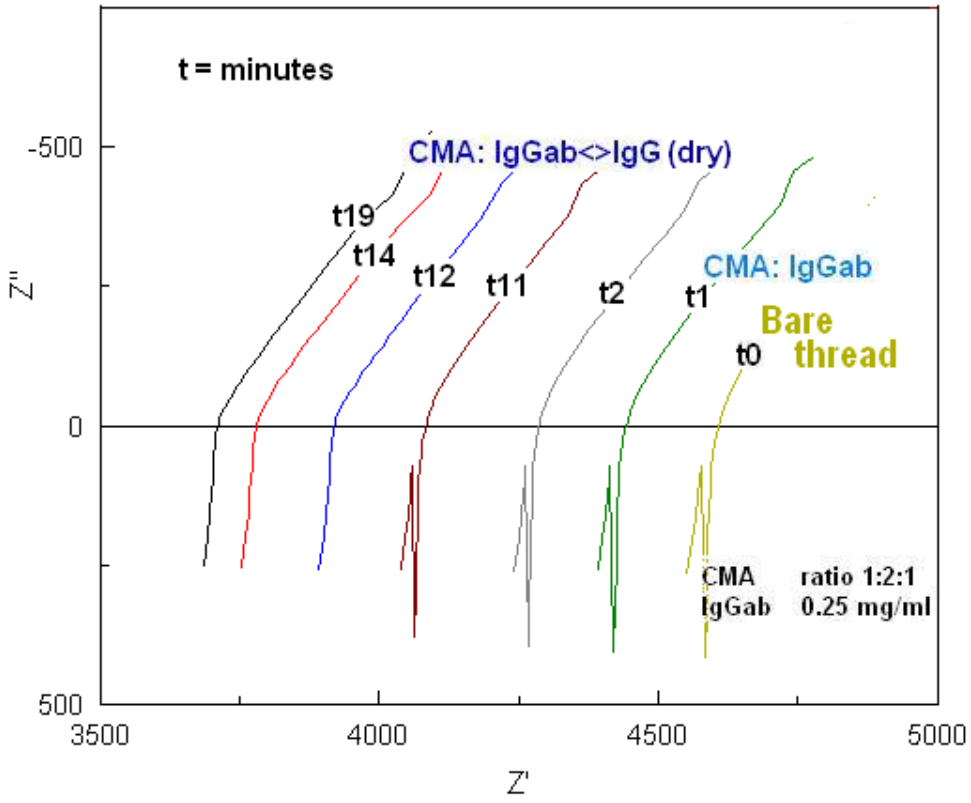

Figure 72: EIS plot over time, CMA:IgGab introduced at time t1, dry IgG antigen from air introduced at time t2.

To prove that the CMA was not producing the decreasing impedance, a test was run with the CMA alone and not adding antigen. The results, in Figure 71, showed that, over time, the impedance contribution was actually an increase in impedance or, in this case, capacitive reactance, as given by the following equation:

$$Xc = 1/\omega C \qquad \text{(Eq. 4.6)}$$

Since the antigen was hydrophilic and became reconstituted and/or hydrolyzed when entering the hydrogel, it is hypothesized in the dissertation that the results of the concentration calibrations in liquid are the same, on a molecular basis, as those would be from starting with dry antigens in air.

To be efficient, a fan or other air flow device would be utilized to expose the FDU to a greater amount of antigen, if present. The cubic volume of air moved per minute by the fan or other device could be calibrated to molecular density, but also a factor would have to be employed to account for any wind, positive or negative, or any other air disturbance in the immediate environment.

The mobility of the antigen through the unique hydrogel would have an effect on the operation of the immunosensor [44], but this would simply establish the latency of detection (see Figure 71). This latency would differ with different sizes of specific antigens, though the percentage of water in the modified hydrogel could be adjusted if desired to increase or decrease latency. The concentration the specific of airborne antigen would have to be determined by assuming a fixed time of migration to the FDE's and beginning the readings immediately upon detection, then the rate of accumulation could be measured by sequential readings and the corresponding molecular concentration could be determined.

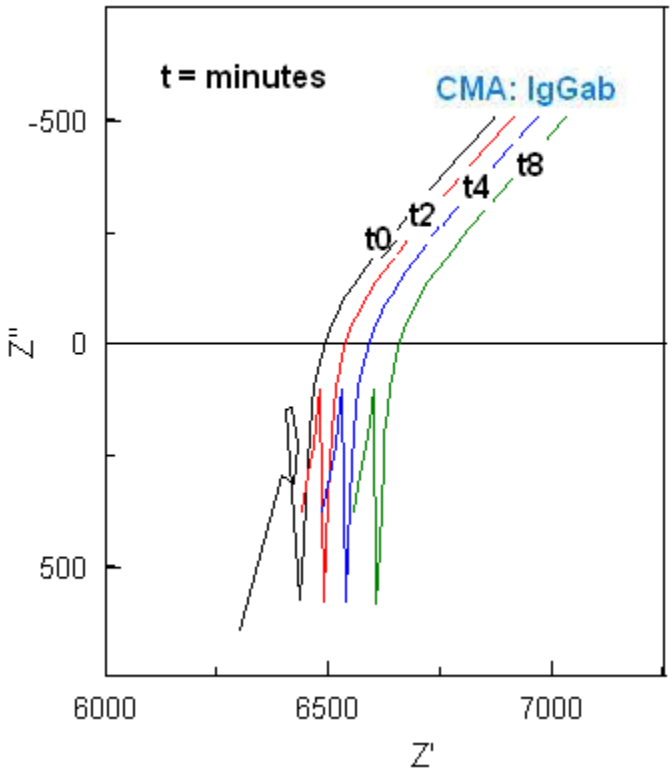

Figure 73: **EIS plot of CMA:IgGab over time with no antigen. All measurements were performed in 10 mM PBS (pH 7.4)**

Experiment A2-14: Use of differential measurements to filter out background interference of non-specific antigens

In this experiment, two immunosensors were utilized to test the same samples to achieve differential interference abatement. One immunosensor had an FDU consisting of CG/MPTS/IgGab, and the other had an FDU consisting of CG/MPTS/IgMab. Because we only had one set of EIS processing equipment available, e.g. the potentiostat, frequency generator, control PC, etc., the immunosensors could not be measured simultaneously, but rather alternately. However, the results are still valid since all significant parameters were kept consistent. Only the FDE's (antibodies) differed

between the immunosensors. One had IgGab FDE's and the other had IgMab FDE's.

First, a baseline reading was taken for control. That was followed by the introduction of a non-specific antigen. Finally, a specific antigen was introduced. This sequence was repeated for both immunosensors and the results showed that by subtracting the changes in Z, at each step in the sequence.

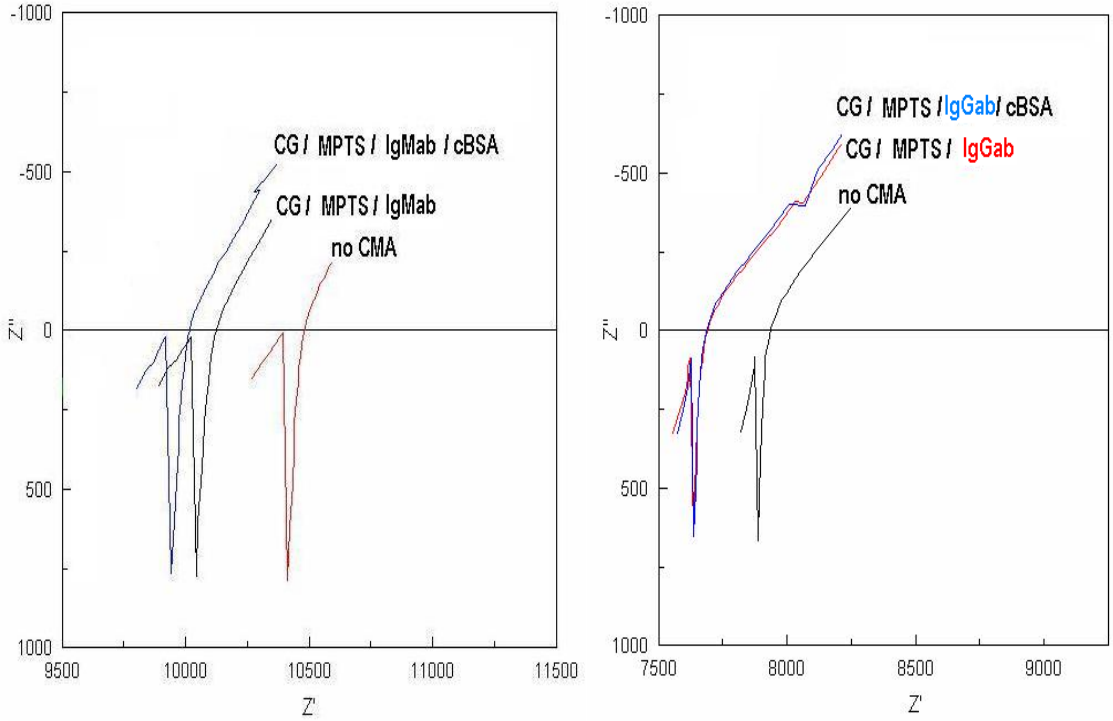

Figure 74: **Differential Signals Non-specific IgM (left), specific IgG (right) with BSA (145mg/ml)**

Figure 73 illustrates a double proof of conjugation detection. As can be seen in the side by side comparisons, when the IgGab is introduced to non-specific antigens, the IgMab reaction is similar. The reaction of the IgMab is greater, however, when *its* specific antigen is encountered, while the IgGab has less change in impedance, Z'. The side by side graphs in Figures 72-74 represent the background control electrode on the left, and the specific IgGab electrode results on the right side. Figure 72 shows a non-

specific (to either electrode) reaction. There was a slight dip in impedance on the left graph, most likely do to multiple paratopes on the IgMab antibodies. Figure 74 shows the specific antigen readings (note different scales- right being a larger change).

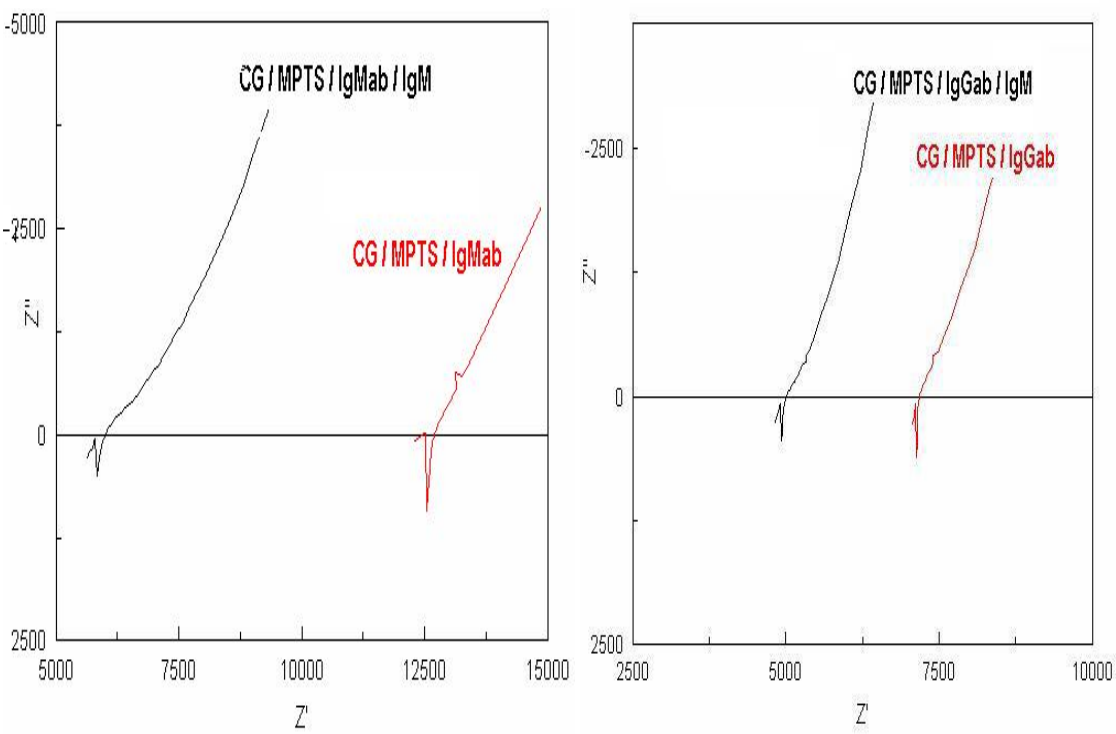

Figure 75: **Differential Signals (left) IgMab/IgM, (right) IgGab/IgM**

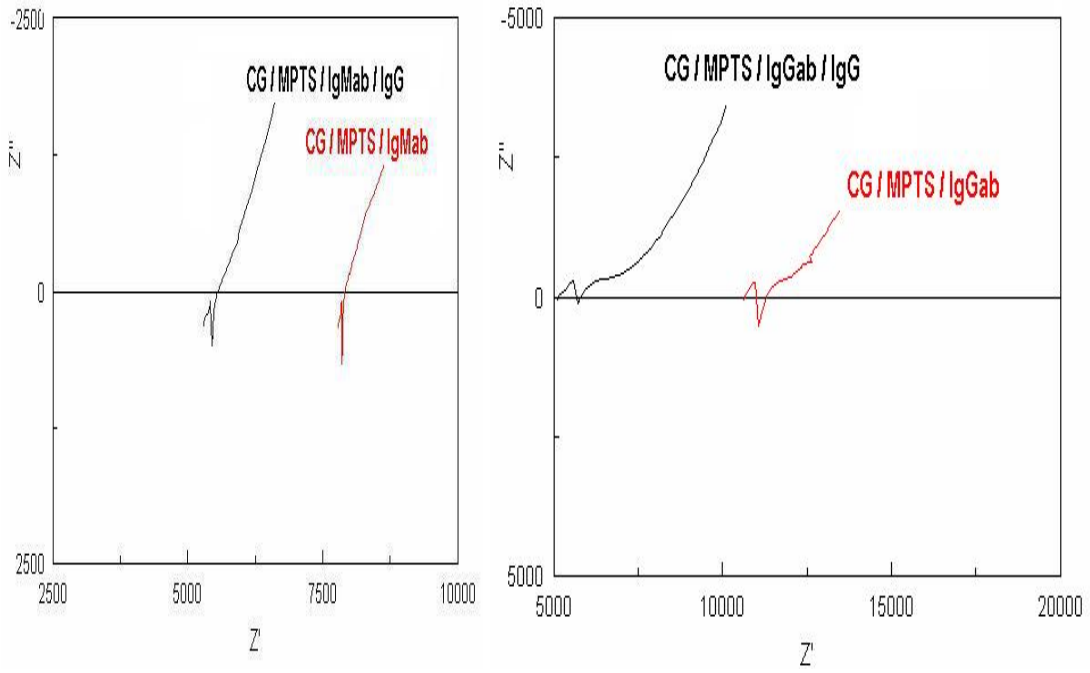

Figure 76: **Differential Signals (left) IgMab/IgG, (right) IgGab/IgG**

Preparation protocol of MPTS Coated Colloidal Gold Nanoparticle Suspension

The preparation work required for the linear/serial configuration was much less than in the parallel configuration. The preparation described in Chapter 3, involving alumina polishing, dangerous piranha solution, and rinsing, did not apply. The colloidal gold nanoparticles did not have to be (or perhaps, could not *even* be) polished, since they were produced through a nano-chemical process, and, in the suspension solution, were never exposed to any type of contamination or corrosion, from the air, that had to be removed. They did not have to be cleaned of organic material, because, again, they were never exposed to any organic material while in the sterile suspension solution. The gold nanoparticles were quite ready to have an MPTS SAM applied by chemisorbing thiols

(RS-H) onto gold surfaces forming Au-SR bonds [46]. The strong, covalent bonds between the SAM and gold nanoparticles were characterized by:

a. High enthalpy: 50 kJ/mol <ΔH< 800 kJ/mol
b. Adsorption which takes place only in the monolayer
c. High activation energy
d. An increase in electron density in the MPTS/gold interface
e. Reversibility only at high temperature

Discussion

When an antigen was introduced to the immunosensor, if the change in Z of the non-specific antibody FDU was greater or about equal to the change in Z of the specific antibody FDU, that was an indication that the specific antigen was not present as in Figure 73. If, on the other hand, the change in Z of the specific antibody FDU was much greater than the change in Z of the non-specific antibody FDU, then the specific antigen was present as in Figures 74 and 75. Therefore, the comparison of the magnitudes of the measurements reliably indicated if the specific antigen was present or not, and eliminated many false positives.

Statistical Analysis

Some of the experiments in this dissertation were only run a small number of times, due to the long length of setup time for fresh preparations, and cost considerations. One such statistical method for analysis with small samples is to use the Wilcoxon

matched pairs signed ranks-test method [63]. This is a non-parametric statistical hypothesis test used to validate results by assessing whether two independent samples of observations have equally large values. The object of the test is to obtain an approximate idea of significance of the differences in results of similar experiments. Wilcoxon general assumptions include:

1.) All observations from two groups are independent of each other.

2.) The responses are ordinal (of the pairs, one is greater or equal to the other).

3.) The distributions of groups X & Y, for the null hypothesis, are equal. That is, the probability of an observation from one population (group X) exceeding an observation from the second population (group Y) equals the probability of an observation from Y exceeding an observation from X.

Under the alternative hypothesis the probability of an observation can be given as:

$$P(X > Y) + 0.5\, P(x=Y) > 0.5 \qquad \text{(Eq. 4.7)}$$

To quantify the effectiveness of the paired rank-test pairing, we:

1.) find the absolute difference |Xa-Xb| for each pair

2.) omit those cases where $|X_a-X_b|=0$ or assign a value of 0.5

3.) rank the remaining absolute differences, from smallest to largest. Give rank 1 to the highest, 2 to the second, etc.

4.) assign to each such rank a "+" sign when $X_a-X_b>0$ and vice versa (ours are all +)

5.) calculate the Spearman's rank correlation coefficient [75]. This will suffice for the quantifier since, with small samples, a normal Gaussian distribution is not meaningful. The Spearman's

rank correlation coefficient will show what we need to know for small samples, so we dispense with the further Wilcoxon calculations, which are more applicable to larger sample sizes.

We applied this matched-pairs signed ranks-test to the experimental results of the sensitivity determination trials as described in Experiment A2-12. Due to the variances of construction from serial electrode to serial electrode, the absolute values of impedance can vary (see Chapter 5), so, therefore, the changes (delta) in impedances were analyzed. The whole purpose of this test was to control for experiment variability. I submit that the factors that could not be controlled, or were quite difficult to control, in the experiment, affected the before and the after measurements equally; therefore they did not affect the differences between before and after. By analyzing only the differences, a paired rank-test controls for some of the sources of scatter [75].

From Figure 69, we use the "Ohms" column as one group and the ohms "lo" column as the other group, with the addition of the reference values. In the tables in Figure 76, the "lo" was the lower impedance, Z" zero crossing value, at a time shortly after the introduction of the antigen, IgG. Readings typically took 1 to 2 minutes to complete. Subsequent readings showed an increase in real impedances as some of the GNP's diffused into the GHA, and took less of an active role in ion/electron transfer through the serial path of the current [48].

IgG con μg/ml >>	5400	540	54	5.4	0.54
CMA impedance	24157	22371	22040	13176	14552
Lo impedance	13600	15845	18991	11284	13519

Differences of CMA & Lo impedances	10557	6526	3049	1892	1033
CMA ranks	1	2	3	5	4
Lo impedance ranks	3	2	1	5	4

Figure 77: **Table of ranks-test input and ranks for concentrations of IgG antigen**

The formula for the Spearman's Rank Correlation Coefficient, R_s [76] is:

$$1-(6\sum_{1}^{n} d^2/(n^3-n)) \qquad \text{(Eq. 4.8)}$$

where d stands for the differences in the ranks

and n is the number of data pairs (5)

Spearman's rank correlation coefficient turns out to be equal to 0.6 which means there is a correlation (linear dependence) between pairs, and the pairings could be effective, but since the standard tables indicate that there is a 0.1 chance of getting above 0.8, the null hypothesis is not rejected. However, introduction of specific antibodies always decreased impedance nearly immediately (within 1 minute.)

Examining the data, the 54 ng/ml run was somewhat of an outlier. Because the trails were run as a group with one batch of antigen, resources did not allow rerunning another batch. The Spearman's rank correlation coefficient becomes 0.8 without that trial

included. Since the concentration of the IgG was being decreased at a given rate, it is reasonable to assume that more trials of the 54 ng/ml would have produced results consistent with the other trails. I would suggest that there was some other contamination or biological problem with the sample.

The data showed that the majority of the results of the sensitivity experiments were essentially similar from experiment to experiment. That is a very important relationship for the data. Though the sample sizes are small due to setup time and expense, a steady decline in impedance differences of CMA & Lo values, in step with the IgG concentration decreases, can be seen on Figure 76. The other results were consistent in a pseudo-linear range (Figure 70), and together they support the thesis of this dissertation.

Colloidal Gold based electrodes

The use of colloidal gold nanoparticles allows the effective surface area of the functionalized electrode to be increased dramatically [49]. In addition, this surface area allows the self-assembled monolayer to be covalently bonded to the gold surface of each nanoparticle in a more efficient way.

When assembling the MPTS SAM on a noble metal substrate electrode, as in my parallel mode electrode, the MPTS tends to form initially as small islands. Eventually the islands grow and combine into larger areas of SAM. Ideally, the coverage will become complete, but the process can terminate prematurely for a number of reasons. One reason is insufficient time to grow the SAM. If the gold substrate is removed from the MPTS before the SAM islands are completely closed together, the coverage will, of

course, have gaps in coverage. This affects the final electrode assembly, as the antibodies and/or colloidal gold nanoparticles, do not have a contact point on the SAM for every location of the gold substrate surface area. This allows the possibilities that antibody Fc areas will directly attach the substrate [52]. This, in and of itself, is not a detrimental occurrence, as these antibodies can combine to for antibody-antigen conjugates, just the same as they would if they were located on the ends of the MPTS molecules. However, the purpose of the MPTS SAM is to keep the antibodies aligned and outward facing. When the antibodies attach directly to the electrode substrate surface, they are free to orient in different orientations; that can cause unpredictable results in impedance measurements as ions and electrons can bypass the conjugates to get to the electrode and alter the double layer capacitance of the Stern layer [51]. Also, just as importantly, the antibody can attach in an orientation that can cause them to block either their own or another or even all of their paratopes, which are needed to attach to the epitopes of the antigens. The value of the crucial double layer capacitance depends on many variables including electrode potential, ionic concentrations and types, and temperature. While these parameters were kept constant or controlled between experiments, there were other factors which could affect electrode performance. These included oxide layers, electrode roughness, and impurity adsorption, among others, so the preparation of the fixed substrate electrode must minimize these by meticulous cleaning, tedious polishing, and controlled storage to prevent corrosion and contamination [50]. The colloidal gold electrode did not suffer from these concerns since they were created from a clean chemical reaction, they were inherently smooth, and they were stored in the colloidal solution. This saved much preparation time, and produced better and more

repeatable results.

On the other hand, if the MPTS is either exposed to the bare gold substrate or the substrate partly or fully covered with a SAM, the MPTS will dimerize and begin to form another SAM attached to the existing SAM [52]. This process extends the distance of the antibodies or antibody functionalized colloidal gold nanoparticles and, therefore, the impedance characteristics of the electrode when making the EIS measurements. This situation is less critical than when the antibodies attach directly to the gold substrate surface directly because, whether the one layer SAM or two layer SAM, or a combination of both, exists, the antibodies attached to the ends of a SAM are, because of the orientation of the SAM, facing outward and able to combine with antigens to form conjugates in a uniform fashion and ideally, with nearly full coverage [66]. However, any contamination of the gold surface can impede the SAM formation and leave a non-ideal, or hole infested, SAM. In addition, these contaminants can also prevent the antibodies from attached to the gold substrate directly, allowing the ions and electrons, in most cases, to flow freely though the holes and overwhelm the antibody-antigen conjugates' contributions to the EIS measurements.

The AC voltage frequency component of EIS is utilized to characterize the time constants of the reactions of interest. The higher frequencies can monitor electron transfer, while the lower frequencies can monitor mass transfer [13]. When the voltage and current are in phase the real resistance can be calculated with Equation 2.2. This is represented by an intercept along the real Z' axis at Z"=0 on the Nyquist plot. As shown in Figure 7 of the Randles equivalent circuit, R_s represents the solution phase resistance, in this case, of the modified hydrogel, that was specifically engineered to have a

negligible value and not significant in the EIS measurements. Z_w, the Warburg impedance, is connected with mass-transfer. C_{dl} is the double layer capacitance, as described previously, while R_{ct} represents the charge-transfer resistance, which is inversely proportional to the rate of electron transfer, and these last two parameters are the most useful for EIS detection purposes in this application [18]. The measured capacitance, *C*, is a series combination of the antibody/antigen binding, C_{bind}, the sensing layer capacitance, C_{sense}, and the capacitance of the colloidal gold nanoparticle with its MPTS sol-gel monolayer, C_{AuMPTS} by the formula:

$$C = \frac{1}{\frac{1}{C_{bind}} + \frac{1}{C_{sense}} + \frac{1}{C_{AuMPTS}}} \qquad \text{(Eq. 4.9)}$$

It should be noted that the effects that most influence the EIS measurements in this dissertation occur very near the surface of the electrode. In a fixed substrate electrode, as has been predominately used in the previous art, there are only one or two such regions (there being one or two electrodes), even if the electrodes are interdigitated. Gold is known to be a poor catalyst as a bulk substrate, but recent studies show that GNP's exhibit excellent catalytic activity [72]. However, with the novel serial colloidal gold electrodes developed in this dissertation, there existed a similar surface effect region around *each* MPTS/ab coated GNP resulting in a multitude of regions, albeit smaller in individual area, contributing to EIS measurements. More importantly, an electric current takes the path of least resistance and, therefore, went through the many GNP's in its path (recall there was no redox couple added, which can detrimentally affect protein binding.) Additionally, as the current passed from GNP to GNP, it passed through <u>two</u> surface

regions on each GNP, going in, then out, doubling the effect. This resulted in an overall amplification of the change in EIS values of impedance.

Using differential type sensors with multiple FDU's can increase the accuracy of the bioimmunosensor by filtering out the background contamination noise. A hydrogel-based immunosensor can be affective in conjunction with a CMA type serial electrode in the FDU, by placing it very near the surface and monitoring the reaction with EIS. The minimal set of frequencies points (Pn) to be tested for EIS are determined by each set of antibody and antibody-antigen conjugates [62]. The parameters Pn are established by data mining the EIS Nyquist plot data to describe important points of frequencies sufficient to describe the curves of interest relating to the antibody and antibody-antigen conjugates of interest. Typically, these would include peaks of the semicircles of Z, and Z' intercepts or other deflection points.

CHAPTER 5

CONCLUSION AND FUTURE DIRECTIONS

Conclusion

EIS is a powerful technology that can be used very effectively to monitor certain biological events, in particular for this dissertation, antibody-antigen conjugation. This can open the way for the detection of a wide range of antigen/pathogens. Integrated into a portable device, novel bioimmunosensors, which are results of this research, could be used to rapidly, and inexpensively (on a mass scale), test populations in third world countries for, as example, tuberculosis. Those infected could be given treatments early in the infection, while sparing those who do not need it.

These novel bioimmunosensors could be readily integrated into a commercial device such as the i-SPEC™ Q 100 (Paradigm Sensors, LLC), handheld EIS analyzer. The FDU‘s are small in size and will fit as a add-on interface head. The EIS data to characterize the various antibody/antigen conjugates can be ascertained be using the techniques in this document. The microprocessor in the handheld device can be programmed to give a visual display of a go/no-go indication when specific antigens are present. Internal memory can store historical data.

Limitations and weaknesses

The major drawback of using impedance methods for bioimmunosensors is the instance of interference from non-specific contamination of the measuring media [36]. This is why the lower limit of detection of the impedance biosensors in a liquid in controlled laboratory conditions with no non-specific antigens, which have been reported in the nM-pM range, is not as critical as the real world experience with many non-specific contaminants. EIS can distinguish the impedance characteristics of a specific

antibody/antigen conjugate by developing an impedance spectrum from alternating current (AC) excitation measurements at a spectrum of frequencies. In an ideal environment, the specific antigens would migrate to the antibodies and conjugate. However, as can be seen from the results of similar experiments, the impedance at time *t0* varies from electrode to electrode with values between 7500 -12500Ω/cm^2. For this reason, the rapid change in impedance exhibited upon specific conjugation is used to indicate the presence of the specific antigen.

Due to the variances of construction from serial electrode to serial electrode, the absolute values of impedance varied. For instance, the distribution of the GNP's will differ when absorbed into the confining entity- in that case, the thread. Secondly, the attachment of the thread to the two stainless steel mesh electrodes can affect overall electrode impedance depending upon the diffusion of the GNP's to the junction of the thread and mesh. This is the reason that change in impedance was used rather than absolute values.

The orientation of the IgG can affect results [51]. The Fab region vs. the Fc region of the antibody, which attaches to the MPTS, may be already buried in the MPTS, and then it is likely that it is not fully exposed. There are also S-S bonds in the Fab region and these may be the ones that get complexed to the layer, so in the end there is probably a mixture of "right side up" and "right side down" orientations of the original IgG.

However, non-specific agents can also alter impedance by blocking epitopes and paratopes thus preventing some conjugation, weakly attaching to the antibodies, contributing electrostatic charges, inhibiting electron or ion flow, etc. Reaction to non-

specific contaminates has been a common concern involving bioimmunosensors deployed in random environments [37][38]. Various methods have been incorporated to try to mitigate this problem. One common approach has been to block binding with non-specific entities by attaching BSA to the ends of the SAM's. Another approach has been to embed the antibody (probe) into a composite film interspersed with a protein resistant species such as those containing ethylene-glycol moieties [66].

In this dissertation, a more direct approach was taken – differential measurements. Experiment 14 employed multiple electrodes, identical in construction, except for the FDE. This ensured that the electrode with the antibody of interest in the FDE had a greater drop in impedance, when the specific antigen was introduced, than the other electrode with the non-specific FDE. This phenomenon can be seen in the results of Figures 72-74.

The techniques used in the dissertation can produce very accurate results, but they do rely on apriori knowledge. Each individual application needs to gather the applicable data with the specific antigens, and store that data. The sample sizes were limited due to the long length of setup time for fresh preparations and cost considerations. Also, in order to experiment with dangerous pathogens, a bio-safe laboratory would be required, to which I did not have access.

The two Aims of this dissertation have been successfully accomplished by the development of a novel modified hydrogel for antibody/antigen conjugate detection which does not dry out rapidly, maintains biological activity, and is easy to use. In addition, that uniquely modified hydrogel was utilized in the fabrication of a novel bioimmunosensor electrode based upon colloidal gold nanoparticles coated with a self-

assembling monolayer of MPTS with specific (for the antigen) antibodies attached at the surface of the MPTS monolayer[62]. This configuration was used to show proof of concept to capture samples from the air or a liquid, making it a multi-functional device. The object was not to develop an instrument, but to develop a method to allow that accomplishment, and that was fulfilled. With unlimited resources and time, I would develop an immunosensor device with a processor that would utilize feedback from the FDU to control and alter parameters of the biological process, such as pH and temperature, to increase the efficiency during times of detection, but save energy and sensor life at other times.

Further Research

A novel DC bias technique could be very promising to be able to control the impedance to linearize the calibration of the sensor. That is, by using feedback from calculations of a microprocessor, and a digital to analog converter, a DC bias could be applied to the electrodes to force the reaction toward an EIS output that would adjust it to a linear output for a given AC frequency.

In the future, larger sample sizes could be collected and a bio-safe laboratory (at least level 2) could be utilized. Further research could also investigate techniques to form and operate an array of sensors with multiple antibodies in the array. In addition, control by electrical bias may be able to control pH and separate antigen conjugates to facilitate reuse of electrodes. Another innovation could employ environmentally sensitive hydrogels which are also known as 'Smart Gels' or 'Intelligent Gels' which have the

ability to sense changes of temperature, pH, and/or the concentration of metabolite, and release their load as result of such a change.

REFERENCES

[1] Terry, L.A., White, S.F. and Tigwell, L.J., The application of biosensors to fresh produce and the wider food industry, *J. Agric. Food Chem.* 53 (2005) pp. 1309–1316.

[2] Newman, J. D., Tigwell, L. J., Turner, A. P. F.,Warner, P. J., "Biosensors: A clearer view. 8th World Congress on Biosensors," Granada, Spain, (2004) May 24-26.

[3] Hu, S.Q., Wu, Z.Y., Zhou, Y.M., Cao, Z.X., Shen, G.L. and Yu, R.Q., Capacitive immunosensor for transferrin based on an o-aminobenzenthiol oligomer layer, *Anal. Chim. Acta* 458 (2002) pp. 297–304.

[4] Gracheva, S., Livingstone, C. and Davis, J., Development of a disposable potentiometric sensor for the near patient testing of plasma thiol concentrations, *Anal. Chem.* 76 (2004) pp. 3833–3836.

[5] Patolsky, F., Lichtenstein, A. and Willner, I., Amplified microgravimetric quartz-crystal-microbalance assay of DNA using oligonucleotide-functionalized liposomes or biotinylated liposomes, *J. Am. Chem. Soc*. 122 (2000) pp. 418–419.

[6] Kawaguchi, T., Shankaran, D.R., Kim, S.J., Matsumoto, K., Toko, K. and Miura, N., Surface plasmon resonance immunosensor using Au nanoparticle for detection of TNT, *Sens. Actuat*. B 133 (2008) pp. 467–472.

[7] Yakhno, T., Sanin, A., Pelyushenko, A., Kazakov, V., Shaposhnikova, Chernov, O., A., Yakhno, V., Vacca, C., Falcione, F. and Johnson, B., Uncoated quartz resonator as a universal biosensor, *Biosens. Bioelectron.* 22 (2007) pp. 2127–2131.

[8] Yang, L., Li, Y. and Erf, G.F., Interdigitated array microelectrode-based electrochemical impedance immunosensor for detection of Escherichia coli O157:H7, *Anal. Chem*. 76 (2004) pp. 1107–1113.

[9] Katz, E., Willner, I., *Electroanalysis* 15 (2003) p 917.

[10] Croucher, P., JAR professional pilot studies, Lulu, Morrisville, NC, (2004) ISBN 0968192823, 9780968192825.

[11] Macdonald, J.R., Impedance Spectroscopy, Wiley-Interscience, (1987) New York, N.Y.

[12] Bockris, J.O'M., Reddy, A.K.N., Gamboa-Aldeco, M., "Modern Electrochemistry", Second Edition, Fundamentals of Electrodics, (2000) Vol. 2A, Kluwer Acad., p. 1425.

[13] Polcyznski, M., Seitz, M. A., Hirthe, R., and Hoeller, T., "Use of AC Electrical Impedance Techniques for Monitoring Microstructural Changes in Electronic Materials", Proc. of the 1991 Internatl. Sym. on Microelectronics, Orlando, FL, (1991) Oct. 21-23, p. 431-435.

[14] Wu, Z-S, et. al., "A novel capacitive immunosensor based on gold colloid monolayers associated with a sol-gel matrix", *Analytica Chimica Acta* 528, (2005) pp. 235-242.

[15] Tang, D, Yuan, R, Chai, Y. "Ultrasensitive electrochemical immunosensor for clinical immunoassay using thionine-doped magnetic gold nanospheres as labels and horseradish peroxidase as enhancer", *Analytical chemistry*. (2008) March 80(5) p 1582.

[16] Tang, D.; Yuan, R.; Chai, Y. *Electroanalysis* /(2006) 18, pp 259-266.

[17] Shen, G, Wang, F., et. Al. " Electrochemical immunoassay of carcinoembryonic antigen based on a lead sulfide nanoparticle label", (2008) *Nanotechnology* 19 435501.

[18] Pethig, R., Dielectric and electronic properties of biological materials, (1979) Wiley Interscience, New York.

[19] Chen, H., Heng, C.K., Puiu, P.D., Zhou, X.D., Lee, A.C., Lim, T.M. and Tan, S.N., *Anal. Chim. Acta* 554 (2005) p. 52.

[20] Pei, R.J., Cheng, Z.L., Wang, E.K. and Yang, X.R., Amplification of antigen–antibody interactions based on biotin labeled protein–streptavidin network complex using impedance spectroscopy, *Biosensors & Bioelectronics*. 16 (2001) pp. 355–361.

[21] Sanders, W., Anderson, M.R., Potential Driven Deposition of Poly(diallyldimethylammonium chloride) onto the Surface of 3-Mercaptopropionic Acid Monolayers Assembled on Gold, *Langmuir* (2008) Oct 24, pp 12766-12770.

[22] Sanders, W., Anderson, M.R., Characterization of Carboxylic Acid-Terminated Self-Assembled Monolayers by Electrochemical Impedance Spectroscopy and Scanning Electrochemical Microscopy, *Langmuir* (2008) Mar 11, pp 6133-6139.

[23] Retrieved from the Internet http://en.wikipedia.org/wiki/Geiger_counter, May 23, 2011.

[24] Dequarie, M., Degrand, C., and Limoges, B., An electrochemical metalloimmunoassay based on a colloidal gold label, *Anal. Chem*., (2000) p 5521.

[25] Chena, J., Tangb, J., Yanb, F., Ju, H., A gold nanoparticles/sol–gel composite architecture for encapsulation of immunoconjugate for reagentless electrochemical immunoassay, *Biomaterials*, 27 (2006) pp 2313–2321.

[26] Chen, H.; Jiang, J. H.; Huang, Y.; Deng, T.; Li, J. S.; Shen, G. L.; Yu, R. Q., An electrochemical impedance immunosensor with signal amplification based on Au-colloid labeled antibody complex, *Sens. Actuators*, B (2006) 117, pp 211-218.

[27] Tang, Hao and Chen, Jinhua and Nie, Lihua and Kuang, Yafei and Yao, Shouzhuo A label-free electrochemical immunoassay for carcinoembryonic antigen (CEA) based on gold nanoparticles (AuNPs) and nonconductive polymer film. *Biosensors & Bioelectronics*, 22 (6). (2007) pp. 1061-1067. ISSN 0956-5663.

[28] Zhu, N., Gao, H., Gu, Y., Xu, Q., He, P., Fang, Y., PAMAM dendrimer-enhanced DNA biosensors based on electrochemical impedance spectroscopy, *Analyst*. (2009) May;134(5) pp 860-6.

[29] Wang, M., Wang, L., Wang, G., Ji, X., Bai, Y., Li, T., et al., Application of impedance spectroscopy for monitoring colloid Au-enhanced antibody immobilization and antibody–antigen reactions. *Biosensors & Bioelectronics* (2004);19 pp 575-582.

[30] Radi, A, Muñoz-Berbel, X., Lates, V., Marty, J., Label-free impedimetric immunosensor for sensitive detection of ochratoxin A, *Biosensors & Bioelectronics* 24(7) (2009) p 1888.

[31] Georganopoulou, D.G., et al., Nanoparticle-based detection in cerebral spinal fluid of a soluble pathogenic biomarker for Alzheimer's disease, *Proc. Natl. Acad. Sci*. U. S. A. 102 (2005), pp 2273–2276.

[32] IBM, http://www.zurich.ibm.com/~bmi/REVFIG1.TIF

[33] Childs, E. C., The space charge in the Gouy layer between two plane, parallel non-conducting particles. *Trans. E'araday Soc*. (1957) 50 pp 1356-62.

[34] Randles, J.B., Kinetics of rapid electrode reactions, *Disc. Faraday Soc.* 1 (1947) p.11–19.

[35] Fletcher, S., The new theory of electron transfer. Thermodynamic potential profiles in the inverted and superverted regions. *Journal of solid state electrochemistr*y (2007) 12 pp 765-770.

[36] Ehrhart J.C., Bennetau B., Renaud L., Madrange J.P., Thomas L., Morisot J., Brosseau A., Allano S., Tauc P. & Tran P.L. A new immunosensor for breast cancer cell detection using antibody-coated long alkylsilane self-assembled

monolayers in a parallel plate flow chamber. *Biosens.Bioelectron* (2008) Nov 15;24(3) pp 467-74.

[37] Pradeep, T., Mitra, S., Sreekumaran Nair A., and, Mukhopadhyay R., Dynamics of Alkyl Chains in Monolayer-Protected Au and Ag Clusters and Silver Thiolates: A Comprehensive Quasielastic Neutron Scattering Investigation, The Journal of Physical Chemistry B (2004) 108 (22) pp 7012-7020.

[38] Zhong X, et.al., Glucose biosensor based on self-assembled gold nanoparticles and double-layer 2d-network (3-mercaptopropyl)-trimethoxysilane polymer onto gold substrate, *Sensors and Actuators* B (2005) 104 pp 191–198.

[39] Hsu, S.M., Raine, L., Fanger, H., Use of avidin-biotin-peroxidase complex (ABC) in immunoperoxidase techniques: A Comparison between ABC and Unlabeled Antibody (PAP), *Journal of histochemistry and cytochemistry*, (1981) - VOl. 29. No. i. pp. 580-581.

[40] Morgan, H., Sun, T., Holmes, D., Gawad, S. and Green, N.G., Single cell dielectric spectroscopy, *J. Phys. D: Appl. Phys*. 40 (2007) pp 61–70.

[41] Flynn, N.T., et al., Long-Term Stability of Self-Assembled Monolayers in Biological Media, *Langmuir*, (2003) 19 (26), pp 10909–10915.

[42] Hirthe, R.W., Adikes, R.P., Bohacheck, M.M., Koehler, C,J, III, Tomlinson. D,F,, Seitz, M.A., *Impedance Spectroscopy (Is) Methods And Systems For Characterizing Fuel*, United States Patent Application 20080172187. (2008).

[43] Piwonski, I., Grobelny, J., Cichomski, M., Celichowski, G., Rogowski, J., Investigation of 3-mercaptopropyltrimethoxysilane self-assembled monolayers on Au(111) surface, *Applied Surface Science*, Volume 242, Issues 1-2, 31 March (2005) pp 147-153.

[44] Wang, J., Pamidi, P.V.A., Zanette, D.R., Self-assembled silica gel networks, (1998) *J. Am. Chem. Soc.*

[45] Swietlow, A; Skoog, M; Johansson, G. *Electroanalysis* (1992) 4, p 921.

[46] Innocenzi, P., Zub, Y., Kessler, V.G., Sol-Gel Methods for Materials Processing, NATO Science for Peace and Security Series C: Environmental Security, (2008) Springer Netherlands.

[47] Aswal, D. K.; Lenfant, S.; Guerin, D.; Yakhmi, J. V.; Vuillaume, D., Tunnel current in self assembled monolayers of 3-mercaptopropyltrimethoxysilane, *Small* (2005), 1, p 725.

[48] Turkevich, J., Stevenson, P. Hillier. C., J., A study of the nucleation and growth processes in the synthesis of colloidal gold, Discuss. Faraday. Soc. (1951) 11 pp 55-75.

[49] An, H., Yuan, R., Tang, D., Chai, Y. and Li, N, Dual-Amplification of Antigen–Antibody Interactions via Backfilling Gold Nanoparticles on (3-Mercaptopropyl) Trimethoxysilane Sol-Gel Functionalized Interface. *Electroanalysis*, (2007) 19 pp 479–486.

[50] Lee, J., Takhistov, P., Direct Detection of the Biological Toxin in Acidic Environment by Electrochemical Impedimetric Immunosensor, *Sensors*, Vol. 10, No. 12. 13 December (2010) pp 11414-11427.

[51] Jia, J., Wang, B., Wu, A., Cheng, G., Li, Z., Dong, S., A Method to Construct a Third-Generation Horseradish Peroxidase Biosensor: Self-Assembling Gold Nanoparticles to Three-Dimensional Sol-Gel Network, *Anal. Chem*. (2002) 74 pp 2217–2223.

[52] Doron A., Katz E., Willner I., Organization of Au colloids as monolayer films onto ITO glass surfaces: Application of the metal colloid films as based interfaces to construct redox-active monolayers, *Langmuir* 11 (1995) pp 1313–1317.

[53] Williams, D.H., Stephens, E., and Zhou, M., Ligand binding energy and catalytic efficiency from improved packing within receptors and enzymes. *Journal of Molecular Biology*, May (2003) 329(2) pp 389-399.

[54] Grandbois, B., Rief, Clausen-Schaumann, and Gaub.
How strong is a covalent bond? *Science*, March (1999) 283(5408) pp 1727-30.

[55] Li,Y, Li, H, Smith,H, Mariuzza,R, *Biochemistry*, (2000) 39 p 6296

[56] Schiffman, G., MD, http://www.medicinenet.com/tuberculosis/article.htm, (2011) .June.

[57] New York City website, http://www.nyc.gov/html/doh/html/cd/cdant.shtml, (2011) .June.

[58] Hudault, S., Guignot, J., Servin, A.L., Escherichia coli strains colonising the gastrointestinal tract protect germfree mice against Salmonella typhimurium infection, *Gut 49*, July (2001) 1 pp 47–55.

[59] Erosa, M.S., Holl, W.H., Horst, J., Sorption of selenium species onto weakly basic anion exchangers:I. *Equilibrium studies, Reactive & Functional Polymers*, April (2009) 69 pp 576–585.

[60] Wang, L., Wang, E., A novel hydrogen peroxide sensor based on horseradish peroxidase immobilized on colloidal Au modified ITO electrode, *Electrochemistry Communications,* (2004) *6* pp 225–229.

[61] Brown, K.R., Fox, A.P., Natan, M.J., Morphology-Dependent Electrochemistry of Cytochrome c at Au Colloid-Modified SnO_2 Electrodes, *J. Am. Chem. Soc*., (1996) 118 pp 1154-1157.

[62] Mazzari et al., *BIOSENSOR*, Provisional U.S. Patent Application No.: 61/466,886, Filing Date: (2011) March 23, U.S. Patent Application No.: 13/196,653, Filing Date: (2011) August 2.

[63] Wilcoxon, F., Individual Comparisons by Ranking Methods, *Biometrics Bulletin*, Vol. 1, No. 6. (Dec 1945) pp. 80-83.

[64] Li, Y., Schluesenerb, H.J., Xua, S., Gold nanoparticle-based biosensors, *Gold Bulletin*, Volume 43 No 1 (2010) pp 20-41.

[65] Suni, I.I., Impedance methods for electrochemical sensors using nanomaterials, *Trends in Analytical Chemistry*, Vol. 27, No. 7 (2008) pp 604-611.

[66] Qian, X., Metallo, S.J., Choi, I.S., Wu, H., Liang, M.N., Whitesides, G.M., Arrays of self-assembled monolayers for studying inhibition of Bacterial Adhesion, *Anal. Chem*. 74 (2002) pp 1805-1810.

[67] Nicholson, R. S., Shain I., Theory of Stationary Electrode Polarography. Single Scan and Cyclic Methods Applied to Reversible, Irreversible, and Kinetic Systems, *Anal. Chem*. (1964) 36 (4) pp 706–723.

[68] Xiao, Y., Patolsky, F., Katz E., Hainfeld, J.F., Willner, I., Plugging into Enzymes: Nanowiring of Redox Enzymes by a Gold Nanoparticle, *Science* (2003) 299 pp 1877-1880.

[69] He, L., Musick, M.D., Nicewarner, S.R., Salinas, F.G., Benkovic, S.J., Natan, M.J., Keating, C.D., Colloidal Au-Enhanced Surface Plasmon Resonance for Ultrasensitive Detection of DNA Hybridization, *Journal of the American Chemical Society* (2000) 122 pp 9071-9077.

[70] Liu, T., Tang, J., Meimei, H., Jiang, L., Surface modification of nanogold particles in DNA detection with quartz crystal microbalance, *Chinese Science Bulletin*, (2003) 313 pp 873-875.

[71] Andreescu, S., Luck, L.A., Studies of the Binding and Signaling of Surface-immobilized , *Anal Biochem* (2008), 375 p 282.

[72] Jena, B.K., Raj, C.R., Electrochemical Biosensor Based on Integrated Assembly of Dehydrogenase Enzymes and Gold Nanoparticles, *Anal. Chem.* (2006) 78 pp 6332-6339.

[73] Lee, T.M-H., Over-the-Counter Biosensors: Past, Present, and Future, *Sensors*, (2008) 8 pp 5535-5559.

[74] Oyama, M., Recent Nanoarchitectures in Metal Nanoparticle-modified Electrodes for Electroanalysis, *Analytical Sciences*, (2010) 26 pp 1-12.

[75] Motulsky, H., Analyzing Data with GraphPad Prism, (1999) GraphPad Software, Inc. pp 59-62.

[76] Spearman's_Rank_Correlation_Coefficient, retreived from http://en.wikipedia.org/wiki/Spearman's_rank_correlation_coefficient (2011).